Search for electroweak production of supersymmetric particles infinal states with two or three leptons at √s=13 TeV with theATLAS detector

doi: 10.1140/epjc/s10052-018-6423-7

Eur. Phys. J. C (2018) 78:995
https://doi.org/10.1140/epjc/s10052-018-6423-7

THE EUROPEAN PHYSICAL JOURNAL C

Regular Article - Experimental Physics

Search for electroweak production of supersymmetric particles in final states with two or three leptons at $\sqrt{s} = 13$ TeV with the ATLAS detector

ATLAS Collaboration[⋆]

CERN, 1211 Geneva 23, Switzerland

Received: 8 March 2018 / Accepted: 7 November 2018 / Published online: 5 December 2018

Abstract A search for the electroweak production of charginos, neutralinos and sleptons decaying into final states involving two or three electrons or muons is presented. The analysis is based on 36.1 fb^{-1} of $\sqrt{s} = 13$ TeV proton–proton collisions recorded by the ATLAS detector at the Large Hadron Collider. Several scenarios based on simplified models are considered. These include the associated production of the next-to-lightest neutralino and the lightest chargino, followed by their decays into final states with leptons and the lightest neutralino via either sleptons or Standard Model gauge bosons; direct production of chargino pairs, which in turn decay into leptons and the lightest neutralino via intermediate sleptons; and slepton pair production, where each slepton decays directly into the lightest neutralino and a lepton. No significant deviations from the Standard Model expectation are observed and stringent limits at 95% confidence level are placed on the masses of relevant supersymmetric particles in each of these scenarios. For a massless lightest neutralino, masses up to 580 GeV are excluded for the associated production of the next-to-lightest neutralino and the lightest chargino, assuming gauge-boson mediated decays, whereas for slepton-pair production masses up to 500 GeV are excluded assuming three generations of mass-degenerate sleptons.

1 Introduction

Supersymmetry (SUSY) [1–7] is one of the most studied extensions of the Standard Model (SM). In its minimal realization (the Minimal Supersymmetric Standard Model, or MSSM) [8,9], it predicts new fermionic (bosonic) partners of the fundamental SM bosons (fermions) and an additional Higgs doublet. These new SUSY particles, or sparticles, can provide an elegant solution to the gauge hierarchy problem [10–13]. In R-parity-conserving models [14], sparticles can only be produced in pairs and the lightest supersymmetric particle (LSP) is stable. This is typically assumed to be the $\tilde{\chi}_1^0$ neutralino,[1] which can then provide a natural candidate for dark matter [15,16]. If produced in proton–proton collisions, a neutralino LSP would escape detection and lead to an excess of events with large missing transverse momentum above the expectations from SM processes, a characteristic that is exploited to search for SUSY signals in analyses presented in this paper.

The production cross-sections of SUSY particles at the Large Hadron Collider (LHC) [17] depend both on the type of interaction involved and on the masses of the sparticles. The coloured sparticles (squarks and gluinos) are produced in strong interactions with significantly larger production cross-sections than non-coloured sparticles of equal masses, such as the charginos ($\tilde{\chi}_i^{\pm}$, $i = 1, 2$) and neutralinos ($\tilde{\chi}_j^0$, $j = 1, 2, 3, 4$) and the sleptons ($\tilde{\ell}$ and $\tilde{\nu}$). The direct production of charginos and neutralinos or slepton pairs can dominate SUSY production at the LHC if the masses of the gluinos and the squarks are significantly larger. With searches performed by the ATLAS [18] and CMS [19] experiments during LHC Run 2, the exclusion limits on coloured sparticle masses extend up to approximately 2 TeV [20–22], making electroweak production an increasingly important probe for SUSY signals at the LHC.

This paper presents a set of searches for the electroweak production of charginos, neutralinos and sleptons decaying into final states with two or three electrons or muons using 36.1 fb^{-1} of proton–proton collision data delivered by the LHC at a centre-of-mass energy of $\sqrt{s} = 13$ TeV. The results build on studies performed during LHC Run 1 at $\sqrt{s} = 7$ TeV and 8 TeV by the ATLAS Collaboration [23–25]. Analogous

⋆e-mail: atlas.publications@cern.ch

[1] The SUSY partners of the Higgs field (known as higgsinos) and of the electroweak gauge fields (the bino for the U(1) gauge field and winos for the W fields) mix to form the mass eigenstates known as charginos and neutralinos.

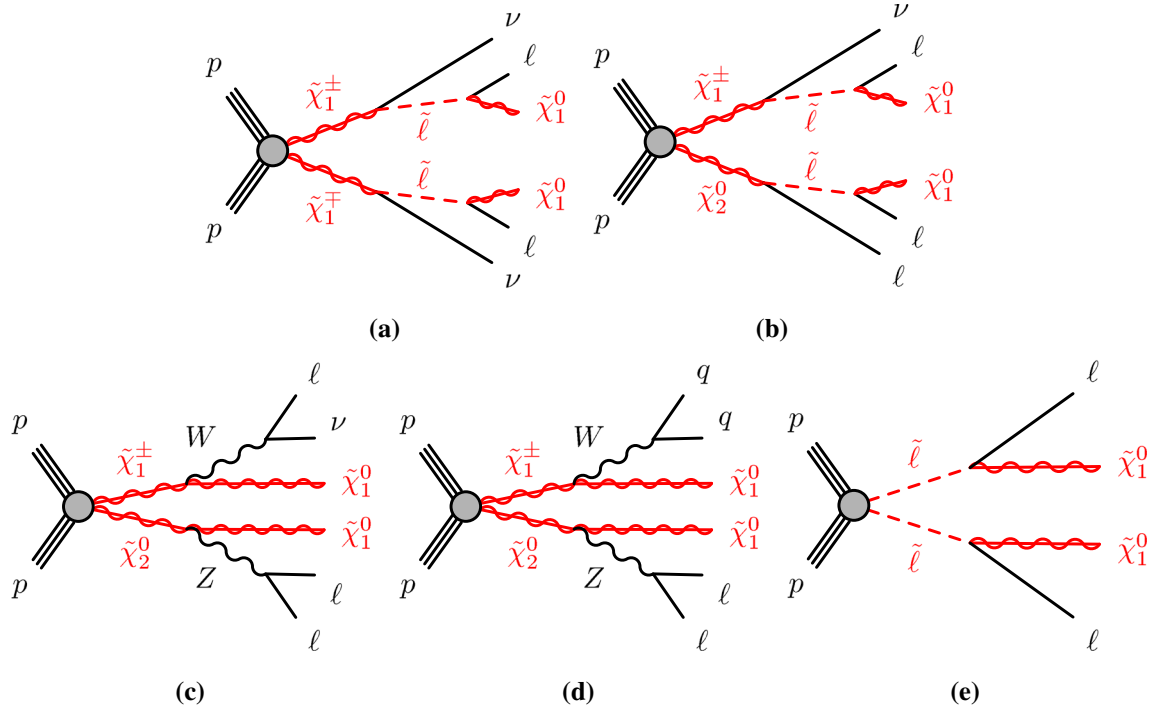

Fig. 1 Diagrams of physics scenarios studied in this paper: **a** $\tilde{\chi}_1^+\tilde{\chi}_1^-$ production with $\tilde{\ell}$-mediated decays into final states with two leptons, **b** $\tilde{\chi}_1^\pm\tilde{\chi}_2^0$ production with $\tilde{\ell}$-mediated decays into final states with three leptons, **c** $\tilde{\chi}_1^\pm\tilde{\chi}_2^0$ production with decays via leptonically decaying W and Z bosons into final states with three leptons, **d** $\tilde{\chi}_1^\pm\tilde{\chi}_2^0$ production with decays via a hadronically decaying W boson and a leptonically decaying Z boson into final states with two leptons and two jets, and **e** slepton pair production with decays into final states with two leptons

studies by the CMS Collaboration are presented in Refs. [26–29].

After descriptions of the SUSY scenarios considered (Sect. 2), the experimental apparatus (Sect. 3), the simulated samples (Sect. 4) and the event reconstruction (Sect. 5), the analysis search strategy is discussed in Sect. 6. This is followed by Sect. 7, which describes the estimation of SM contributions to the measured yields in the signal regions, and by Sect. 8, which discusses systematic uncertainties affecting the searches. Results are presented in Sect. 9, together with the statistical tests used to interpret them in the context of relevant SUSY benchmark scenarios. Section 10 summarizes the main conclusions.

2 SUSY scenarios and search strategy

This paper presents searches for the direct pair-production of $\tilde{\chi}_1^+\tilde{\chi}_1^-$, $\tilde{\chi}_1^\pm\tilde{\chi}_2^0$ and $\tilde{\ell}\tilde{\ell}$ particles, in final states with exactly two or three electrons and muons, two $\tilde{\chi}_1^0$ particles, and possibly additional jets or neutrinos. Simplified models [30], in which the masses of the relevant sparticles are the only free parameters, are used for interpretation and to guide the design of the searches. The pure wino $\tilde{\chi}_1^\pm$ and $\tilde{\chi}_2^0$ are taken to be mass-degenerate, and so are the scalar partners of the left-handed charged leptons and neutrinos ($\tilde{e}_\mathrm{L}$, $\tilde{\mu}_\mathrm{L}$, $\tilde{\tau}_\mathrm{L}$ and $\tilde{\nu}$). Intermediate slepton masses, when relevant, are chosen to be midway between the mass of the heavier chargino and neutralino and that of the lightest neutralino, which is pure bino, and equal branching ratios for the three slepton flavours are assumed. The analysis sensitivity is not expected to depend strongly on the slepton mass hypothesis for a broad range of slepton masses, while it degrades as the slepton mass approaches that of the heavier chargino and neutralino, leading to lower p_T values for the leptons produced in the heavy chargino and neutralino decays [25]. Lepton flavour is conserved in all models. Diagrams of processes considered are shown in Fig. 1. For models exploring $\tilde{\chi}_1^+\tilde{\chi}_1^-$ production, it is assumed that the sleptons are also light and thus accessible in the sparticle decay chains, as illustrated in Fig. 1a. Two different classes of models are considered for $\tilde{\chi}_1^\pm\tilde{\chi}_2^0$ production: in one case, the $\tilde{\chi}_1^\pm$ chargino and $\tilde{\chi}_2^0$ neutralino can decay into final-state SM particles and a $\tilde{\chi}_1^0$ neutralino via an intermediate $\tilde{\ell}_\mathrm{L}$ or $\tilde{\nu}_\mathrm{L}$, with a branching ratio of 50% to each (Fig. 1b); in the other case the $\tilde{\chi}_1^\pm$ chargino and $\tilde{\chi}_2^0$ neutralino decays proceed via SM gauge bosons (W or Z). For the gauge-boson-mediated decays, two distinct final states are considered: three-lepton (where lepton refers to an electron or muon) events where both the W and Z bosons decay

leptonically (Fig. 1c) or events with two opposite-sign leptons and two jets where the W boson decays hadronically and the Z boson decays leptonically (Fig. 1d). In models with direct $\tilde{\ell}\tilde{\ell}$ production, each slepton decays into a lepton and a $\tilde{\chi}_1^0$ with a 100% branching ratio (Fig. 1e), and $\tilde{e}_{\mathrm{L}}$, $\tilde{e}_{\mathrm{R}}$, $\tilde{\mu}_{\mathrm{L}}$, $\tilde{\mu}_{\mathrm{R}}$, $\tilde{\tau}_{\mathrm{L}}$ and $\tilde{\tau}_{\mathrm{R}}$ are assumed to be mass-degenerate.

Events are recorded using triggers requiring the presence of at least two leptons and assigned to one of three mutually exclusive analysis channels depending on the lepton and jet multiplicity. The 2ℓ + 0 jets channel targets chargino- and slepton-pair production, the 2ℓ + jets channel targets chargino-neutralino production with gauge-boson-mediated decays, and the 3ℓ channel targets chargino-neutralino production with slepton- or gauge-boson-mediated decays. For each channel, a set of signal regions (SR), defined in Sect. 6, use requirements on $E_{\mathrm{T}}^{\mathrm{miss}}$ and other kinematic quantities, which are optimized for different SUSY models and sparticle masses. The analyses employ "inclusive" SRs to quantify significance without assuming a particular signal model and to exclude regions of SUSY model parameter space, as well as sets of orthogonal "exclusive" SRs that are considered simultaneously during limit-setting to improve the exclusion sensitivity.

3 ATLAS detector

The ATLAS experiment [18] is a multi-purpose particle detector with a forward-backward symmetric cylindrical geometry and nearly 4π coverage in solid angle.[2] The interaction point is surrounded by an inner detector (ID), a calorimeter system, and a muon spectrometer.

The ID provides precision tracking of charged particles for pseudorapidities $|\eta| < 2.5$ and is surrounded by a superconducting solenoid providing a 2 T axial magnetic field. The ID consists of silicon pixel and microstrip detectors inside a transition radiation tracker. One significant upgrade for the $\sqrt{s} = 13$ TeV running period is the installation of the insertable B-layer [31], an additional pixel layer close to the interaction point which provides high-resolution hits at small radius to improve the tracking performance.

In the pseudorapidity region $|\eta| < 3.2$, high-granularity lead/liquid-argon (LAr) electromagnetic (EM) sampling calorimeters are used. A steel/scintillator tile calorimeter measures hadron energies for $|\eta| < 1.7$. The endcap and forward regions, spanning $1.5 < |\eta| < 4.9$, are instrumented with LAr calorimeters, for both the EM and hadronic measurements.

The muon spectrometer consists of three large superconducting toroids with eight coils each, and a system of trigger and precision-tracking chambers, which provide triggering and tracking capabilities in the ranges $|\eta| < 2.4$ and $|\eta| < 2.7$, respectively.

A two-level trigger system is used to select events [32]. The first-level trigger is implemented in hardware and uses a subset of the detector information. This is followed by the software-based high-level trigger, which runs offline reconstruction and calibration software, reducing the event rate to about 1 kHz.

4 Data and simulated event samples

This analysis uses proton–proton collision data delivered by the LHC at $\sqrt{s} = 13$ TeV in 2015 and 2016. After fulfilling data-quality requirements, the data sample amounts to an integrated luminosity of 36.1 fb^{-1}. This value is derived using a methodology similar to that detailed in Ref. [33], from a calibration of the luminosity scale using x–y beam-separation scans performed in August 2015 and May 2016.

Various samples of Monte Carlo (MC) simulated events are used to model the SUSY signal and help in the estimation of the SM backgrounds. The samples include an ATLAS detector simulation [34], based on GEANT4 [35], or a fast simulation [34] that uses a parameterization of the calorimeter response [36] and GEANT4 for the other parts of the detector. The simulated events are reconstructed in the same manner as the data.

Diboson processes were simulated with the SHERPA v2.2.1 event generator [37,38] and normalized using next-to-leading-order (NLO) cross-sections [39,40]. The matrix elements containing all diagrams with four electroweak vertices with additional hard parton emissions were calculated with COMIX [41] and virtual QCD corrections were calculated with OPENLOOPS [42]. Matrix element calculations were merged with the SHERPA parton shower [43] using the ME+PS@NLO prescription [44]. The NNPDF3.0 NNLO parton distribution function (PDF) set [45] was used in conjunction with dedicated parton shower tuning developed by the SHERPA authors. The fully leptonic channels were calculated at NLO in the strong coupling constant with up to one additional parton for 4ℓ and $2\ell + 2\nu$, at NLO with no additional parton for $3\ell + \nu$, and at leading order (LO) with up to three additional partons. Processes with one of the bosons decaying hadronically and the other leptonically were calculated with up to one additional parton at NLO and up to three additional partons at LO.

[2] ATLAS uses a right-handed coordinate system with its origin at the nominal interaction point (IP) in the centre of the detector and the z-axis along the beam direction. The x-axis points from the IP to the centre of the LHC ring, and the y-axis points upward. Cylindrical coordinates (r, ϕ) are used in the transverse plane, ϕ being the azimuthal angle around the beam direction. The pseudorapidity is defined in terms of the polar angle θ as $\eta = -\ln\tan(\theta/2)$. Angular distance is measured in units of $\Delta R \equiv \sqrt{(\Delta\eta)^2 + (\Delta\phi)^2}$. The transverse momentum, p_{T}, and energy, E_{T}, are defined with respect to the beam axis (x–y plane).

Diboson processes with six electroweak vertices, such as same-sign W boson production in association with two jets, $W^{\pm}W^{\pm}jj$, and triboson processes were simulated as above with SHERPA v2.2.1 using the NNPDF3.0 PDF set. Diboson processes with six vertices were calculated at LO with up to one additional parton. Fully leptonic triboson processes (WWW, WWZ, WZZ and ZZZ) were calculated at LO with up to two additional partons and at NLO for the inclusive processes and normalized using NLO cross-sections.

Events containing Z bosons and associated jets (Z/γ^* + jets, also referred to as Z + jets in the following) were also produced using the SHERPA v2.2.1 generator with massive b/c-quarks to improve the treatment of the associated production of Z bosons with jets containing b- and c-hadrons [46]. Matrix elements were calculated with up to two additional partons at NLO and up to four additional partons at LO, using COMIX, OPENLOOPS, and SHERPA parton shower with ME+PS@NLO in a way similar to that described above. A global K-factor was used to normalize the Z + jets events to the next-to-next-to-leading-order (NNLO) QCD cross-sections [47].

For the production of $t\bar{t}$ and single top quarks in the Wt channel, the POWHEG-BOX v2 [48,49] generator with the CT10 PDF set [50] was used, as discussed in Ref. [51]. The top quark mass was set at 172.5 GeV for all MC samples involving top quark production. The $t\bar{t}$ events were normalized using the NNLO+next-to-next-to-leading-logarithm (NNLL) QCD [52] cross-section, while the cross-section for single-top-quark events was calculated at NLO+NNLL [53].

Samples of $t\bar{t}V$ (with $V = W$ and Z, including non-resonant Z/γ^* contributions) and $t\bar{t}WW$ production were generated at LO with MADGRAPH5_aMC@NLO v2.2.2 [54] interfaced to PYTHIA 8.186 [55] for parton showering, hadronisation and the description of the underlying event, with up to two ($t\bar{t}W$), one ($t\bar{t}Z$) or no ($t\bar{t}WW$) extra partons included in the matrix element, as described in Ref. [56]. MADGRAPH was also used to simulate the tZ, $t\bar{t}t\bar{t}$ and $t\bar{t}t$ processes. A set of tuned parameters called the A14 tune [57] was used together with the NNPDF2.3LO PDF set [58]. The $t\bar{t}W$, $t\bar{t}Z$, $t\bar{t}WW$ and $t\bar{t}t\bar{t}$ events were normalized using their NLO cross-section [56] while the generator cross-section was used for tZ and $t\bar{t}t$.

Higgs boson production processes (including gluon–gluon fusion, associated VH production and vector-boson fusion) were generated using POWHEG-BOX v2 [59] and PYTHIA 8.186 and normalized using cross-sections calculated at NNLO with soft gluon emission effects added at NNLL accuracy [60], whilst $t\bar{t}H$ events were produced using MADGRAPH5_aMC@NLO 2.3.2 + Herwig++ [61] and normalized using the NLO cross-section [56]. All samples assume a Higgs boson mass of 125 GeV.

The SUSY signal processes were generated from LO matrix elements with up to two extra partons, using the MADGRAPH v2.2.3 generator interfaced to PYTHIA 8.186 with the A14 tune for the modelling of the SUSY decay chain, parton showering, hadronization and the description of the underlying event. Parton luminosities were provided by the NNPDF2.3LO PDF set. Jet–parton matching was realized following the CKKW-L prescription [62], with a matching scale set to one quarter of the pair-produced superpartner mass. Signal cross-sections were calculated at NLO, with soft gluon emission effects added at next-to-leading-logarithm (NLL) accuracy [63–67]. The nominal cross-section and its uncertainty were taken from an envelope of cross-section predictions using different PDF sets and factorization and renormalization scales, as described in Ref. [68]. The cross-section for $\tilde{\chi}_1^+\tilde{\chi}_1^-$ production, each with a mass of 600 GeV, is 9.50 ± 0.91 fb, while the cross-section for $\tilde{\chi}_1^{\pm}\tilde{\chi}_2^0$ production, each with a mass of 800 GeV, is 4.76 ± 0.56 fb.

In all MC samples, except those produced by SHERPA, the EVTGEN v1.2.0 program [69] was used to model the properties of b- and c-hadron decays. To simulate the effects of additional pp collisions per bunch crossing (pile-up), additional interactions were generated using the soft QCD processes of PYTHIA 8.186 with the A2 tune [70] and the MSTW2008LO PDF set [71], and overlaid onto the simulated hard-scatter event. The Monte Carlo samples were reweighted so that the distribution of the number of pile-up interactions matches the distribution in data.

5 Event reconstruction and preselection

Events used in the analysis were recorded during stable data-taking conditions and must have a reconstructed primary vertex [72] with at least two associated tracks with $p_{\mathrm{T}} > 400$ MeV. The primary vertex of an event is identified as the vertex with the highest Σp_{T}^2 of associated tracks.

Two identification criteria are defined for the objects used in these analyses, referred to as "baseline" and "signal" (with the signal objects being a subset of the baseline ones). The former are defined to disambiguate between overlapping physics objects and to perform data-driven estimations of non-prompt leptonic backgrounds (discussed in Sect. 7) while the latter are used to construct kinematic and multiplicity discriminating variables needed for the event selection.

Baseline electrons are reconstructed from isolated electromagnetic calorimeter energy deposits matched to ID tracks and are required to have $|\eta| < 2.47$, $p_{\mathrm{T}} > 10$ GeV, and to pass a loose likelihood-based identification requirement [73,74]. The likelihood input variables include measurements of calorimeter shower shapes and track properties from the ID.

Baseline muons are reconstructed in the region $|\eta| < 2.7$ from muon spectrometer tracks matching ID tracks. All

muons must have $p_{\mathrm{T}} > 10$ GeV and must pass the "medium identification" requirements defined in Ref. [75], based on selection of the number of hits and curvature measurements in the ID and muon spectrometer systems.

Jets are reconstructed with the anti-k_t algorithm [76] as implemented in the FastJet package [77], with radius parameter $R = 0.4$, using three-dimensional energy clusters in the calorimeter [78] as input. Baseline jets must have $p_{\mathrm{T}} > 20$ GeV and $|\eta| < 4.5$ and signal jets have the tighter requirement of $|\eta| < 2.4$. Jet energies are calibrated as described in Refs. [79,80]. In order to reduce the effects of pile-up, jets with $p_{\mathrm{T}} < 60$ GeV and $|\eta| < 2.4$ must have a significant fraction of their associated tracks compatible with originating from the primary vertex, as defined by the jet vertex tagger [81]. Furthermore, for all jets the expected average energy contribution from pile-up is subtracted according to the jet area [81,82]. Events are discarded if they contain any jet that is judged by basic quality criteria to be detector noise or non-collision background.

Identification of jets containing b-hadrons (b-jets), so called b-tagging, is performed with the MV2c10 algorithm, a multivariate discriminant making use of track impact parameters and reconstructed secondary vertices [83,84]. A requirement is chosen corresponding to a 77% average efficiency obtained for b-jets in simulated $t\bar{t}$ events. The corresponding rejection factors against jets originating from c-quarks, from τ-leptons, and from light quarks and gluons in the same sample at this working point are 6, 22 and 134, respectively.

Baseline photon candidates are required to meet the "tight" selection criteria of Ref. [85] and satisfy $p_{\mathrm{T}} > 25$ GeV and $|\eta| < 2.37$, but excluding the transition region $1.37 < |\eta| < 1.52$, where the calorimeter performance is degraded.

After object identification, an "object-removal procedure" is performed on all baseline objects to remove possible double-counting in the reconstruction:

1. Any electron sharing an ID track with a muon is removed.
2. If a b-tagged jet (identified using the 85% efficiency working point of the MV2c10 algorithm) is within $\Delta R = 0.2$ of an electron candidate, the electron is rejected, as it is likely to be from a semileptonic b-hadron decay; if the jet within $\Delta R = 0.2$ of the electron is not b-tagged, the jet itself is discarded, as it likely originates from an electron-induced shower.
3. Electrons within $\Delta R = 0.4$ of a remaining jet candidate are discarded, to further suppress electrons from semileptonic decays of b- and c-hadrons.
4. Jets with a nearby muon that carries a significant fraction of the transverse momentum of the jet ($p_{\mathrm{T}}^{\mu} > 0.7 \sum p_{\mathrm{T}}^{\text{jet tracks}}$, where p_{T}^{μ} and $p_{\mathrm{T}}^{\text{jet tracks}}$ are the transverse momenta of the muon and the tracks associated with the jet, respectively) are discarded either if the candidate muon is within $\Delta R = 0.2$ of the jet or if the muon is matched to a track associated with the jet. Only jets with fewer than three associated tracks can be discarded in this step.
5. Muons within $\Delta R = 0.4$ of a remaining jet candidate are discarded to suppress muons from semileptonic decays of b- and c-hadrons.

Signal electrons must satisfy a "medium" likelihood-based identification requirement [73] and the track associated with the electron must have a significance of the transverse impact parameter relative to the reconstructed primary vertex, d_0, of $|d_0|/\sigma(d_0) < 5$, with $\sigma(d_0)$ being the uncertainty in d_0. In addition, the longitudinal impact parameter (again relative to the reconstructed primary vertex), z_0, must satisfy $|z_0 \sin\theta| < 0.5$ mm. Similarly, signal muons must satisfy the requirements of $|d_0|/\sigma(d_0) < 3$, $|z_0 \sin\theta| < 0.5$ mm, and additionally have $|\eta| < 2.4$. Isolation requirements are also applied to both the signal electrons and muons to reduce the contributions of "fake" or non-prompt leptons, which originate from misidentified hadrons, photons conversions, and hadron decays. These p_{T}- and η-dependent requirements use track- and calorimeter-based information and have efficiencies in $Z \to e^+e^-$ and $Z \to \mu^+\mu^-$ events that rise from 95% at 25 GeV to 99% at 60 GeV.

The missing transverse momentum $\mathbf{p}_{\mathrm{T}}^{\mathrm{miss}}$, with magnitude $E_{\mathrm{T}}^{\mathrm{miss}}$, is the negative vector sum of the transverse momenta of all identified physics objects (electrons, photons, muons, jets) and an additional soft term. The soft term is constructed from all tracks that are not associated with any physics object and that are associated with the primary vertex, to suppress contributions from pile-up interactions. The $E_{\mathrm{T}}^{\mathrm{miss}}$ value is adjusted for the calibration of the jets and the other identified physics objects above [86].

Events considered in the analysis must pass a trigger selection requiring either two electrons, two muons or an electron plus a muon. The trigger-level thresholds on the p_{T} value of the leptons involved in the trigger decision are in the range 8–22 GeV and are looser than those applied offline to ensure that trigger efficiencies are constant in the relevant phase space.

Events containing a photon and jets are used to estimate the Z + jets background in events with two leptons and jets. These events are selected with a set of prescaled single-photon triggers with p_{T} thresholds in the range 35–100 GeV and an unprescaled single-photon trigger with threshold $p_{\mathrm{T}} = 140$ GeV. Signal photons in this control sample must have $p_{\mathrm{T}} > 37$ GeV to be in the efficiency plateau of the lowest-threshold single-photon trigger, fall outside the barrel-endcap transition region defined by $1.37 < |\eta| < 1.52$, and pass "tight" selection criteria described in Ref. [87],

as well as p_{T}- and η-dependent requirements on both track- and calorimeter-based isolation.

Simulated events are corrected to account for small differences in the signal lepton trigger, reconstruction, identification, isolation, as well as b-tagging efficiencies between data and MC simulation.

6 Signal regions

In order to search for the electroweak production of supersymmetric particles, three different search channels that target different SUSY processes are defined:

- 2ℓ+ 0 jets channel: targets $\tilde{\chi}_1^+\tilde{\chi}_1^-$ and $\tilde{\ell}\tilde{\ell}$ production (shown in Fig. 1a, e) in signal regions with a jet veto and defined using the "stransverse mass" variable, m_{T2} [88,89], and the dilepton invariant mass $m_{\ell\ell}$;
- 2ℓ+ jets channel: targets $\tilde{\chi}_1^\pm\tilde{\chi}_2^0$ production with decays via gauge bosons (shown in Fig. 1d) into two same-flavour opposite-sign (SFOS) leptons (from the Z boson) and at least two jets (from the W boson);
- 3ℓ channel: targets $\tilde{\chi}_1^\pm\tilde{\chi}_2^0$ production with decays via intermediate $\tilde{\ell}$ or gauge bosons into three-lepton final states (shown in Fig. 1b, c).

In each channel, inclusive and/or exclusive signal regions (SRs) are defined that require exactly two or three signal leptons, with vetos on any additional baseline leptons. In the 2ℓ + 0 jets channel only, this additional baseline lepton veto is applied before considering overlap-removal. The leading and sub-leading leptons are required to have $p_{\mathrm{T}} > 25$ GeV and 20 GeV respectively; however, in the 2ℓ + jets and 3ℓ channels, tighter lepton p_{T} requirements are applied to the sub-leading leptons.

6.1 Signal regions for 2ℓ + 0 jets channel

In the 2ℓ + 0 jets channel the leptons are required to be of opposite sign and events are separated into "same flavour" (SF) events (corresponding to dielectron, e^+e^-, and dimuon, $\mu^+\mu^-$, events) and "different flavour" (DF) events (electron–muon, $e^\pm\mu^\mp$). This division is driven by the different background compositions in the two classes of events. All events used in the SRs are required to have a dilepton invariant mass $m_{\ell\ell} > 40$ GeV and not contain any b-tagged jets with $p_{\mathrm{T}} > 20$ GeV or non-b-tagged jets with $p_{\mathrm{T}} > 60$ GeV.

After this preselection, exclusive signal regions are used to maximize exclusion sensitivity across the simplified model parameter space for $\tilde{\chi}_1^+\tilde{\chi}_1^-$ and $\tilde{\ell}\tilde{\ell}$ production. In the SF regions a two-dimensional binning in m_{T2} and $m_{\ell\ell}$ is used as high-$m_{\ell\ell}$ requirements provide strong suppression of the Z + jets background, whereas in the DF regions, where the Z + jets background is negligible, a one-dimensional binning in m_{T2} is sufficient. The stransverse mass m_{T2} is defined as:

$$m_{\mathrm{T2}} = \min_{\mathbf{q}_{\mathrm{T}}}\left[\max\left(m_{\mathrm{T}}(\mathbf{p}_{\mathrm{T}}^{\ell 1}, \mathbf{q}_{\mathrm{T}}), m_{\mathrm{T}}(\mathbf{p}_{\mathrm{T}}^{\ell 2}, \mathbf{p}_{\mathrm{T}}^{\mathrm{miss}} - \mathbf{q}_{\mathrm{T}})\right)\right],$$

where $\mathbf{p}_{\mathrm{T}}^{\ell 1}$ and $\mathbf{p}_{\mathrm{T}}^{\ell 2}$ are the transverse momentum vectors of the two leptons, and $\mathbf{q}_{\mathrm{T}}$ is a transverse momentum vector that minimizes the larger of $m_{\mathrm{T}}(\mathbf{p}_{\mathrm{T}}^{\ell 1}, \mathbf{q}_{\mathrm{T}})$ and $m_{\mathrm{T}}(\mathbf{p}_{\mathrm{T}}^{\ell 2}, \mathbf{p}_{\mathrm{T}}^{\mathrm{miss}} - \mathbf{q}_{\mathrm{T}})$, where:

$$m_{\mathrm{T}}(\mathbf{p}_{\mathrm{T}}, \mathbf{q}_{\mathrm{T}}) = \sqrt{2(p_{\mathrm{T}}q_{\mathrm{T}} - \mathbf{p}_{\mathrm{T}}\cdot\mathbf{q}_{\mathrm{T}})}.$$

For SM backgrounds of $t\bar{t}$ and WW production in which the missing transverse momentum and the pair of selected leptons originate from two $W \to \ell\nu$ decays and all momenta are accurately measured, the m_{T2} value must be less than the W boson mass m_W, and requiring the m_{T2} value to significantly exceed m_W thus strongly suppresses these backgrounds while retaining high efficiency for many SUSY signals.

When producing model-dependent exclusion limits in the $\tilde{\chi}_1^+\tilde{\chi}_1^-$ simplified models, all signal regions are statistically combined, whereas only the same-flavour regions are used when probing $\tilde{\ell}\tilde{\ell}$ production. In addition, a set of inclusive signal regions are also defined, and these are used to provide a more model-independent test for an excess of events. The definitions of both the exclusive and inclusive signal regions are provided in Table 1.

6.2 Signal regions for 2ℓ + jets channel

In the 2ℓ + jets channel, two inclusive signal regions differing only in the $E_{\mathrm{T}}^{\mathrm{miss}}$ requirement, denoted SR2-int and SR2-high, are used to target intermediate and large mass splittings between the $\tilde{\chi}_1^\pm/\tilde{\chi}_2^0$ chargino/neutralino and the $\tilde{\chi}_1^0$ neutralino. In addition to the preselection used in the 2ℓ + 0 jets channel, with the exception of the veto requirement on non-b-tagged jets, the sub-leading lepton is also required to have $p_{\mathrm{T}} > 25$ GeV and events must have at least two jets, with the leading two jets satisfying $p_{\mathrm{T}} > 30$ GeV. The b-jet veto is applied in the same way as in the 2ℓ + 0 jets channel. Several kinematic requirements are applied to select two leptons consistent with an on-shell Z boson and two jets consistent with a W boson. A tight requirement of $m_{\mathrm{T2}} > 100$ GeV is used to suppress the $t\bar{t}$ and WW backgrounds and $E_{\mathrm{T}}^{\mathrm{miss}} > 150$ (250) GeV is required for SR2-int (SR2-high).

An additional region in the 2ℓ + jets channel, denoted SR2-low, is optimized for the region of parameter space where the mass splitting between the $\tilde{\chi}_1^\pm/\tilde{\chi}_2^0$ and the $\tilde{\chi}_1^0$ is similar to the Z boson mass and the signal becomes kinematically similar to the diboson (VV) backgrounds. It is split into two orthogonal subregions for performing background estimation and validation, and these are merged when presenting the results in Sect. 9. SR2-low-2J requires exactly

Table 1 The definitions of the exclusive and inclusive signal regions for the 2ℓ + 0 jets channel. Relevant kinematic variables are defined in the text. The bins labelled "DF"or "SF" refer to signal regions with different-flavour or same-flavour lepton pair combinations, respectively

m_{T2} [GeV]	$m_{\ell\ell}$ [GeV]	SF bin	DF bin
2ℓ+ 0 jets exclusive signal region definitions			
100–150	111–150	SR2-SF-a	-
	150–200	SR2-SF-b	-
	200–300	SR2-SF-c	-
	> 300	SR2-SF-d	-
	> 111	-	SR2-DF-a
150–200	111–150	SR2-SF-e	-
	150–200	SR2-SF-f	-
	200–300	SR2-SF-g	-
	> 300	SR2-SF-h	-
	> 111	-	SR2-DF-b
200–300	111–150	SR2-SF-i	-
	150–200	SR2-SF-j	-
	200–300	SR2-SF-k	-
	> 300	SR2-SF-l	-
	> 111	-	SR2-DF-c
> 300	> 111	SR2-SF-m	SR2-DF-d
2ℓ+ 0 jets inclusive signal region definitions			
> 100	> 111	SR2-SF-loose	–
> 130	> 300	SR2-SF-tight	–
> 100	> 111	–	SR2-DF-100
> 150	> 111	–	SR2-DF-150
> 200	> 111	–	SR2-DF-200
> 300	> 111	–	SR2-DF-300

two jets, with $p_{\mathrm{T}} > 30$ GeV, that are both assumed to originate from the W boson, while SR2-low-3J requires 3–5 signal jets (with the leading two jets satisfying $p_{\mathrm{T}} > 30$ GeV) and assumes the $\tilde{\chi}_1^{\pm}\tilde{\chi}_2^0$ system recoils against initial-state-radiation (ISR) jet(s). In the latter case, the two jets originating from the W boson are selected to be those closest in $\Delta\phi$ to the $Z(\rightarrow \ell\ell) + E_{\mathrm{T}}^{\mathrm{miss}}$ system. This is different from SR2-int and SR2-high, where the two jets with the highest p_{T} in the event are used to define the W boson candidate. The rest of the jets that are not associated with the W boson are collectively defined as ISR jets. All regions use variables, including angular distances and the W and Z boson transverse momenta, to select the signal topologies of interest. The definitions of the signal regions in the 2ℓ + jets channel are summarized in Table 2.

6.3 Signal regions for 3ℓ channel

The 3ℓ channel targets $\tilde{\chi}_1^{\pm}\tilde{\chi}_2^0$ production and uses kinematic variables such as $E_{\mathrm{T}}^{\mathrm{miss}}$ and the transverse mass m_{T}, which were used in the Run 1 analysis [24]. Events are required to have exactly three signal leptons and no additional baseline leptons, as well as zero b-tagged jets with $p_{\mathrm{T}} > 20$ GeV. In addition, two of the leptons must form an SFOS pair (as expected in $\tilde{\chi}_2^0 \rightarrow \ell^+\ell^-\tilde{\chi}_1^0$ decays). To resolve ambiguities when multiple SFOS pairings are present, the transverse mass is calculated using the unpaired lepton and $\mathbf{p}_{\mathrm{T}}^{\mathrm{miss}}$ for each possible SFOS pairing, and the lepton that yields the minimum transverse mass is assigned to the W boson. This transverse mass value is denoted by $m_{\mathrm{T}}^{\mathrm{min}}$, and is used alongside $E_{\mathrm{T}}^{\mathrm{miss}}$, jet multiplicity (in the gauge-boson-mediated scenario) and other relevant kinematic variables to define exclusive signal regions that have sensitivity to $\tilde{\ell}$-mediated and gauge-boson-mediated decays. The definitions of these exclusive regions are provided in Table 3. The bins denoted "slep-a,b,c,d,e" target $\tilde{\ell}$-mediated decays and consequently have a veto on SFOS pairs with an invariant mass consistent with the Z boson (this suppresses the WZ background). The invariant mass of the SFOS pair, $m_{\ell\ell}$, the magnitude of the missing transverse momentum, $E_{\mathrm{T}}^{\mathrm{miss}}$, and the p_{T} value of the third leading lepton, $p_{\mathrm{T}}^{\ell_3}$, are used to define the SR bins. Conversely, the bins denoted "WZ-0Ja,b,c" and "WZ-1Ja,b,c" target gauge-boson-mediated decays and thus require the SFOS pair to have an invariant mass consistent with an on-shell Z boson. The 0-jet and $\geq$ 1-jet channels are considered separately and the regions are binned in $m_{\mathrm{T}}^{\mathrm{min}}$ and $E_{\mathrm{T}}^{\mathrm{miss}}$.

7 Background estimation and validation

The SM backgrounds can be classified into irreducible backgrounds with prompt leptons and genuine $E_{\mathrm{T}}^{\mathrm{miss}}$ from neutrinos, and reducible backgrounds that contain one or more "fake" or non-prompt (FNP) leptons or where experimental effects (e.g., detector mismeasurement of jets or leptons or imperfect removal of object double-counting) lead to significant "fake" $E_{\mathrm{T}}^{\mathrm{miss}}$. A summary of the background estimation techniques used in each channel is provided in Table 4. In the 2ℓ + 0 jets and 3ℓ channels only, the dominant backgrounds are estimated from MC simulation and normalized in dedicated control regions (CRs) that are included, together with the SRs, in simultaneous likelihood fits to data, as described further in Sect. 9. In addition, all channels employ validation regions (VRs) with kinematic requirements that are similar to the SRs but with smaller expected signal-to-background ratios, which are used to validate the background estimation methodology. In the 2ℓ + jets channel, the MC modelling of diboson processes is studied in dedicated VRs and found to accurately reproduce data.

For the 2ℓ + 0 jets channel the dominant backgrounds are irreducible processes from SM diboson production (WW, WZ, and ZZ) and dileptonic $t\bar{t}$ and Wt events. MC simulation is used to predict kinematic distributions for these

Table 2 Signal region definitions used for the 2ℓ + jets channel. Relevant kinematic variables are defined in the text. The symbols W and Z correspond to the reconstructed W and Z bosons in the final state. The Z boson is always reconstructed from the two leptons, whereas the W boson is reconstructed from the two jets leading in p_{T} for SR2-int, SR2-high and the 2-jets channel of SR2-low, whilst for the 3–5 jets channel of SR2-low it is reconstructed from the two jets which are closest in $\Delta\phi$ to the $Z\,(\rightarrow \ell\ell) + E_{\mathrm{T}}^{\mathrm{miss}}$ system. The $\Delta R_{(jj)}$ and m_{jj} variables are calculated using the two jets assigned to the W boson. ISR refers to the vectorial sum of the initial-state-radiation jets in the event (i.e. those not used in the reconstruction of the W boson) and jet1 and jet3 refer to the leading and third leading jet respectively. The variable $n_{\text{non-}b\text{-tagged jets}}$ refers to the number of jets with $p_{\mathrm{T}} > 30$ GeV that do not satisfy the b-tagging criteria

	SR2-int	SR2-high	SR2-low-2J	SR2-low-3J
2ℓ + jets signal region definitions				
$n_{\text{non-}b\text{-tagged jets}}$	≥ 2	≥ 2	2	3–5
$m_{\ell\ell}$ [GeV]	81–101	81–101	81–101	86–96
m_{jj} [GeV]	70–100	70–100	70–90	70–90
$E_{\mathrm{T}}^{\mathrm{miss}}$ [GeV]	> 150	> 250	> 100	> 100
p_{T}^{Z} [GeV]	> 80	> 80	> 60	> 40
p_{T}^{W} [GeV]	> 100	> 100		
m_{T2} [GeV]	> 100	> 100		
$\Delta R_{(jj)}$	< 1.5	< 1.5		< 2.2
$\Delta R_{(\ell\ell)}$	< 1.8	< 1.8		
$\Delta\phi_{(\mathbf{p}_{\mathrm{T}}^{\mathrm{miss}},Z)}$			< 0.8	
$\Delta\phi_{(\mathbf{p}_{\mathrm{T}}^{\mathrm{miss}},W)}$	0.5–3.0	0.5–3.0	> 1.5	< 2.2
$E_{\mathrm{T}}^{\mathrm{miss}}/p_{\mathrm{T}}^{Z}$			0.6–1.6	
$E_{\mathrm{T}}^{\mathrm{miss}}/p_{\mathrm{T}}^{W}$			< 0.8	
$\Delta\phi_{(\mathbf{p}_{\mathrm{T}}^{\mathrm{miss}},\mathrm{ISR})}$				> 2.4
$\Delta\phi_{(\mathbf{p}_{\mathrm{T}}^{\mathrm{miss}},\mathrm{jet1})}$				> 2.6
$E_{\mathrm{T}}^{\mathrm{miss}}/p_{\mathrm{T}}^{\mathrm{ISR}}$				0.4–0.8
$\lvert\eta(Z)\rvert$				< 1.6
$p_{\mathrm{T}}^{\mathrm{jet3}}$ [GeV]				> 30

Table 3 Summary of the exclusive signal regions used in the 3ℓ channel. Relevant kinematic variables are defined in the text. The bins labelled "slep" target slepton-mediated decays whereas those labelled "WZ" target gauge-boson-mediated decays. The variable $n_{\text{non-}b\text{-tagged jets}}$ refers to the number of jets with $p_{\mathrm{T}} > 20$ GeV that do not satisfy the b-tagging criteria. Values of $p_{\mathrm{T}}^{\ell_3}$ refer to the p_{T} of the third leading lepton and $p_{\mathrm{T}}^{\mathrm{jet1}}$ denotes the p_{T} of the leading jet

m_{SFOS} [GeV]	$E_{\mathrm{T}}^{\mathrm{miss}}$ [GeV]	$p_{\mathrm{T}}^{\ell_3}$ [GeV]	$n_{\text{non-}b\text{-tagged jets}}$	$m_{\mathrm{T}}^{\mathrm{min}}$ [GeV]	$p_{\mathrm{T}}^{\ell\ell\ell}$ [GeV]	$p_{\mathrm{T}}^{\mathrm{jet1}}$ [GeV]	Bins
3ℓ exclusive signal region definitions							
≤ 81.2	> 130	20–30		> 110			SR3-slep-a
	> 130	> 30		> 110			SR3-slep-b
≥ 101.2	> 130	20–50		> 110			SR3-slep-c
	> 130	50–80		> 110			SR3-slep-d
	> 130	> 80		> 110			SR3-slep-e
81.2–101.2	60-120		0	> 110			SR3-WZ-0Ja
	120–170		0	> 110			SR3-WZ-0Jb
	> 170		0	> 110			SR3-WZ-0Jc
81.2–101.2	120–200		≥ 1	> 110	< 120	> 70	SR3-WZ-1Ja
	> 200		≥ 1	110–160			SR3-WZ-1Jb
	> 200	> 35	≥ 1	> 160			SR3-WZ-1Jc

Table 4 Summary of the estimation methods used in each search channel. Backgrounds denoted CR have a dedicated control region that is included in a simultaneous likelihood fit to data to extract a data-driven normalization factor that is used to scale the MC prediction. The γ + jet template method is used in the 2ℓ + jets channel to provide a data-driven estimate of the Z + jets background. Finally, MC stands for pure Monte Carlo estimation

Channel	2ℓ + 0 jets	2ℓ + jets	3ℓ
Background estimation summary			
Fake/non-prompt leptons	Matrix method	Matrix method	Fake-factor method
$t\bar{t} + Wt$	CR	MC	Fake-factor method
VV	CR	MC	CR (WZ-only)
Z + jets	MC	γ + jet template	Fake-factor method
Higgs/VVV/top + V	MC	MC	MC

Table 5 Control region and validation region definitions for the 2ℓ + 0 jets channel. The DF and SF labels refer to different-flavour or same-flavour lepton pair combinations, respectively. The p_{T} thresholds placed on the requirements for b-tagged and non-b-tagged jets correspond to 20 GeV and 60 GeV, respectively

Region	CR2-VV-SF	CR2-VV-DF	CR2-Top	VR2-VV-SF (DF)	VR2-Top
2ℓ + 0 jets control and validation region definitions					
Lepton flavour	SF	DF	DF	SF (DF)	DF
$n_{\text{non-}b\text{-tagged jets}}$	0	0	0	0	0
$n_{b\text{-tagged jets}}$	0	0	≥ 1	0	≥ 1
$\lvert m_{\ell\ell} - m_Z \rvert$ [GeV]	< 20	–	–	> 20 (–)	–
m_{T2} [GeV]	> 130	50–75	75–100	75–100	> 100

backgrounds, but the $t\bar{t}$ and diboson backgrounds are then normalized to data in dedicated control regions. For the diboson backgrounds, SF and DF events are treated separately and two control regions are defined. The first one (CR2-VV-SF) selects SFOS lepton pairs with an invariant mass consistent with the Z boson mass and has a tight requirement of $m_{\mathrm{T2}} > 130$ GeV to reduce the Z + jets contamination. This region is dominated by ZZ events, with subdominant contributions from WZ and WW events. The DF diboson control region (CR2-VV-DF) selects events with a different flavour opposite sign pair and further requires $50 < m_{\mathrm{T2}} < 75$ GeV. This region is dominated by WW events, with a subdominant contribution from WZ events. The $t\bar{t}$ control region (CR2-Top) uses DF events with at least one b-tagged jet to obtain a high-purity sample of $t\bar{t}$ events. The control region definitions are summarized in Table 5. The Z + jets and Higgs boson contributions are expected to be small in the 2ℓ + 0 jets channel and are estimated directly from MC simulation.

The three control regions are included in a simultaneous profile likelihood fit to the observed data which provides data-driven normalization factors for these backgrounds, as described in Sect. 9. The results are propagated to the signal regions, and to dedicated VRs that are defined in Table 5. The normalization factors returned by the fit for the $t\bar{t}$, VV-DF and VV-SF backgrounds are 0.95 ± 0.03, 1.06 ± 0.18 and 0.96 ± 0.11, respectively. Figure 2a, b show the $E_{\mathrm{T}}^{\mathrm{miss}}$ and m_{T2} distributions, respectively, for data and the estimated backgrounds in VR2-VV-SF with these normalization factors applied.

In the 2ℓ + jets channel, the largest background contribution is also from SM diboson production. In addition, Z + jets events can enter the SRs due to fake $E_{\mathrm{T}}^{\mathrm{miss}}$ from jet or lepton mismeasurements or genuine $E_{\mathrm{T}}^{\mathrm{miss}}$ from neutrinos in semileptonic decays of b- or c-hadrons. These effects are difficult to model in MC simulation, so instead γ+jets events in data are used to extract the $E_{\mathrm{T}}^{\mathrm{miss}}$ shape in Z+jets events, which have a similar topology and $E_{\mathrm{T}}^{\mathrm{miss}}$ resolution. Similar methods have been employed in searches for SUSY in events with two leptons, jets, and large $E_{\mathrm{T}}^{\mathrm{miss}}$ in ATLAS [90] and CMS [91,92]. The $E_{\mathrm{T}}^{\mathrm{miss}}$ shape is extracted from a data control sample of γ+jets events using a set of single-photon triggers and weighting each event by the trigger prescale factor. Corrections to account for differences in the γ and Z boson p_{T} distributions, as well as different momentum resolutions for electrons, muons and photons, are applied. Backgrounds of $W\gamma$ and $Z\gamma$ production, which contain a photon and genuine $E_{\mathrm{T}}^{\mathrm{miss}}$ from neutrinos, are subtracted using MC samples that are normalized to data in a $V\gamma$ control region containing a selected lepton and photon. For each SR separately, the $E_{\mathrm{T}}^{\mathrm{miss}}$ shape is then normalized to data in a corresponding control region with $E_{\mathrm{T}}^{\mathrm{miss}} < 100$ GeV but all other requirements the same as in the SR. To model quantities that depend on the individual lepton momenta, an $m_{\ell\ell}$ value is assigned to each γ+jets event by sampling from $m_{\ell\ell}$

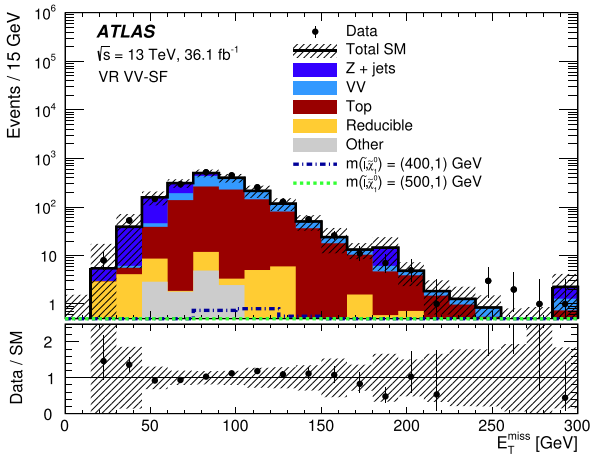

(a) $E_{\mathrm{T}}^{\mathrm{miss}}$ distribution in VR2-VV-SF

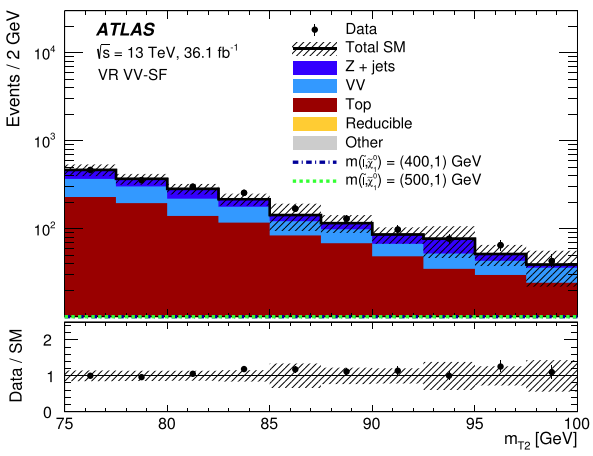

(b) m_{T2} distribution in VR2-VV-SF

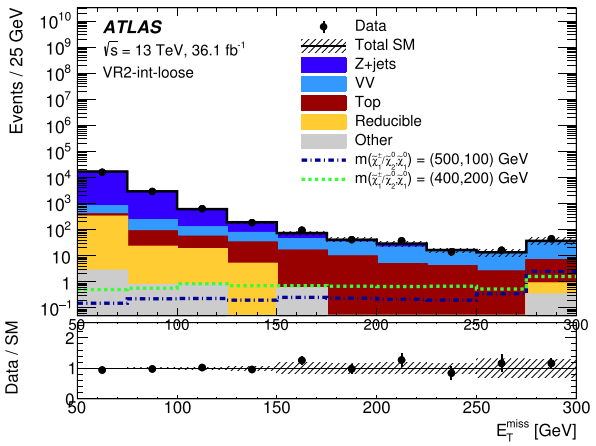

(c) $E_{\mathrm{T}}^{\mathrm{miss}}$ distribution in VR2-int-loose

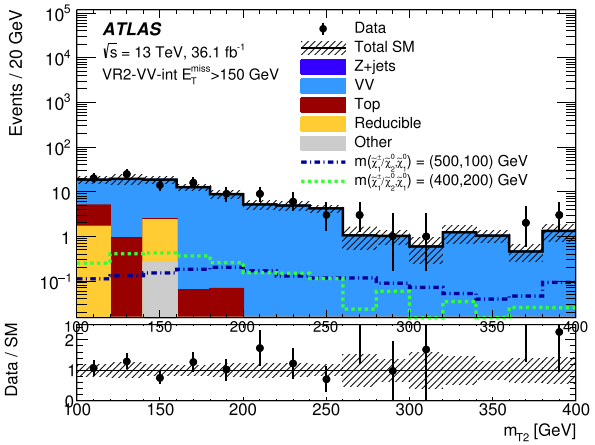

(d) m_{T2} distribution in VR2-VV-int.

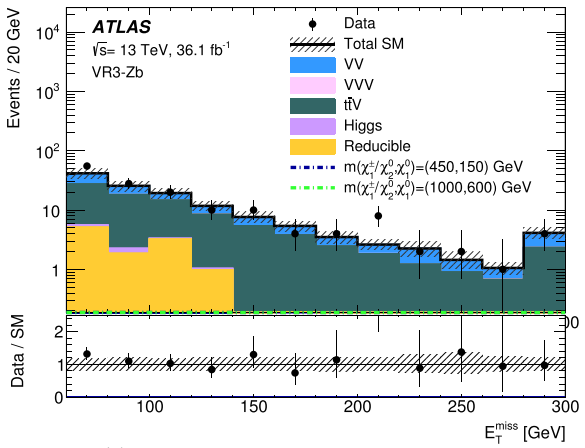

(e) $E_{\mathrm{T}}^{\mathrm{miss}}$ distribution in VR3-Zb

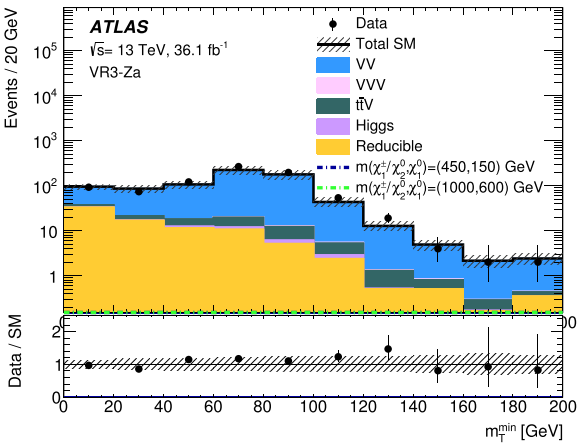

(f) m_T^{min} distribution in VR3-Za

Fig. 2 Distributions of $E_{\mathrm{T}}^{\mathrm{miss}}$, m_T^{min}, and m_{T2} for data and the estimated SM backgrounds in the (top) 2ℓ + 0 jets channel, (middle) 2ℓ + jets channel, and (bottom) 3ℓ channel. Simulated signal models are overlaid for comparison. For the $2\ell + 0$ jets (3ℓ) channel, the normalization factors extracted from the corresponding CRs are used to rescale the $t\bar{t}$ and VV (WZ) backgrounds. For the 2ℓ + 0 jets channel the "top" background includes $t\bar{t}$ and Wt, the "other" backgrounds include Higgs bosons, $t\bar{t}V$ and VVV and the "reducible" category corresponds to the data-driven matrix method estimate. For the 2ℓ + jets channel, the "top" background includes $t\bar{t}$, Wt and $t\bar{t}V$, the "other" backgrounds include Higgs bosons and VVV, the "reducible" category corresponds to the data-driven matrix method estimate, and the Z + jets contribution is evaluated with the data-driven γ + jet template method. For the 3ℓ channel, the "reducible" category corresponds to the data-driven fake-factor estimate. The uncertainty band includes all systematic and statistical sources and the final bin in each histogram also contains the events in the overflow bin

Table 6 Validation region definitions used for the 2ℓ + jets channel. Symbols and abbreviations are analogous to those in Table 2

	VR2-int(high)	VR2-low-2J(3J)	VR2-VV-int	VR2-VV-low
2ℓ + jets validation region definitions				
Loose selection				
$n_{\text{non-}b\text{-tagged jets}}$	≥ 2	2 (3–5)	1	1
$E_{\mathrm{T}}^{\mathrm{miss}}$ [GeV]	> 150 (> 250)	> 100	> 150	> 150
$m_{\ell\ell}$ [GeV]	81–101	81–101 (86–96)		81–101
m_{jj} [GeV]	$\notin$ [60, 100]	$\notin$ [60, 100]		
p_{T}^{Z} [GeV]	> 80	> 60 (> 40)		
p_{T}^{W} [GeV]	> 100			
$\lvert\eta(Z)\rvert$		(< 1.6)		
$p_{\mathrm{T}}^{\mathrm{jet3}}$ [GeV]		(> 30)		
$\Delta\phi_{(\mathbf{p}_{\mathrm{T}}^{\mathrm{miss}},\mathrm{jet})}$			> 0.4	> 0.4
m_{T2} [GeV]			> 100	
$\Delta R_{(\ell\ell)}$				< 0.2
Tight selection				
$\Delta R_{(jj)}$	< 1.5	(< 2.2)		
$\Delta\phi_{(\mathbf{p}_{\mathrm{T}}^{\mathrm{miss}},W)}$	0.5–3.0	> 1.5 (< 2.2)		
$\Delta\phi_{(\mathbf{p}_{\mathrm{T}}^{\mathrm{miss}},Z)}$		< 0.8 ($-$)		
$E_{\mathrm{T}}^{\mathrm{miss}}/p_{\mathrm{T}}^{W}$		< 0.8 ($-$)		
$E_{\mathrm{T}}^{\mathrm{miss}}/p_{\mathrm{T}}^{Z}$		0.6–1.6 ($-$)		
$E_{\mathrm{T}}^{\mathrm{miss}}/p_{\mathrm{T}}^{\mathrm{ISR}}$		(0.4–0.8)		
$\Delta\phi_{(\mathbf{p}_{\mathrm{T}}^{\mathrm{miss}},\mathrm{ISR})}$		(> 2.4)		
$\Delta\phi_{(\mathbf{p}_{\mathrm{T}}^{\mathrm{miss}},\mathrm{jet1})}$		(> 2.6)		
m_{T2} [GeV]	> 100			
$\Delta R_{(\ell\ell)}$	< 1.8			

Table 7 Control and validation region definitions used in the 3ℓ channel. The m_{SFOS} quantity is the mass of the same-flavour opposite-sign lepton pair and $m_{\ell\ell\ell}$ is the trilepton invariant mass. Other symbols and abbreviations are analogous to those in Table 3

	$p_{\mathrm{T}}^{\ell_3}$ [GeV]	$m_{\ell\ell\ell}$ [GeV]	m_{SFOS} [GeV]	$E_{\mathrm{T}}^{\mathrm{miss}}$ [GeV]	$m_{\mathrm{T}}^{\mathrm{min}}$ [GeV]	$n_{\text{non-}b\text{-tagged jets}}$	$n_{b\text{-tagged jets}}$
3ℓ control and validation region definitions							
CR3-WZ-inc	> 20	–	81.2–101.2	> 120	< 110	–	0
CR3-WZ-0j	> 20	–	81.2–101.2	> 60	< 110	0	0
CR3-WZ-1j	> 20	–	81.2–101.2	> 120	< 110	> 0	0
VR3-Za	> 30	$\notin$ [81.2, 101.2]	81.2–101.2	40–60	–	–	–
VR3-Zb	> 30	$\notin$ [81.2, 101.2]	81.2–101.2	>60	–	–	> 0
VR3-offZa	> 30	$\notin$ [81.2, 101.2]	$\notin$ [81.2, 101.2]	40–60	–	–	–
VR3-offZb	> 20	$\notin$ [81.2, 101.2]	$\notin$ [81.2, 101.2]	> 40	–	–	> 0
VR3-Za-0J	> 20	$\notin$ [81.2, 101.2]	81.2–101.2	40–60	–	0	0
VR3-Za-1J	> 20	$\notin$ [81.2, 101.2]	81.2–101.2	40–60	–	> 0	0

distributions (parameterized as functions of boson p_{T} and $E_{\mathrm{T},\parallel}^{\mathrm{miss}}$, the component of $E_{\mathrm{T}}^{\mathrm{miss}}$ that is parallel to the boson's transverse momentum vector) extracted from a Z+jets MC sample. With this $m_{\ell\ell}$ value assigned to the photon, each γ+jets event is boosted to the rest frame of the hypothetical Z boson and the photon is split into two pseudo-leptons, assuming isotropic decays in the rest frame.

To validate the method, two sets of validation regions, "tight" and "loose", are defined for each SR. The definitions of these regions are provided in Table 6. The selections in the "tight" regions are identical to the SR selections with the exception of the dijet mass m_{jj} requirement, which is replaced by the requirement ($m_{jj} < 60$ GeV or $m_{jj} > 100$ GeV) to suppress signal. These "tight" regions are used to

Table 8 Background-only fit results for SR2-SF-a to SR2-SF-g in the $2\ell + 0$ jets channel. All systematic and statistical uncertainties are included in the fit. The "other" backgrounds include all processes producing a Higgs boson, VVV or $t\bar{t}V$. A "–" symbol indicates that the background contribution is negligible

SR2-	SF-a	SF-b	SF-c	SF-d	SF-e	SF-f	SF-g
Observed	56	28	19	13	10	6	6
Total SM	47 ± 12	25 ± 5	25 ± 4	14 ± 7	5.2 ± 1.4	1.9 ± 1.2	3.8 ± 1.9
$t\bar{t}$	10 ± 4	7.4 ± 3.5	7.3 ± 3.0	2.7 ± 1.7	–	–	$0.11^{+0.21}_{-0.11}$
Wt	1.0 ± 1.0	1.3 ± 0.7	1.6 ± 0.6	1.1 ± 1.1	–	–	–
VV	21 ± 4	11.3 ± 2.9	12.6 ± 2.4	3.9 ± 2.4	4.4 ± 1.3	1.8 ± 1.2	2.8 ± 1.6
FNP	$2.1^{+2.9}_{-2.1}$	$0.0^{+0.4}_{-0.0}$	$0.0^{+0.5}_{-0.0}$	5 ± 4	$0.0^{+0.1}_{-0.0}$	$0.00^{+0.01}_{-0.00}$	0.9 ± 0.4
Z + jets	13 ± 9	4.7 ± 2.6	3.3 ± 3.2	$1.2^{+1.7}_{-1.2}$	0.7 ± 0.6	$0.02^{+0.21}_{-0.02}$	–
Other	0.18 ± 0.08	0.12 ± 0.05	0.11 ± 0.04	0.09 ± 0.05	0.05 ± 0.03	0.03 ± 0.01	0.05 ± 0.02

Table 9 Background-only fit results for SR2-SF-h to SR2-SF-m in the $2\ell + 0$ jets channel. All systematic and statistical uncertainties are included in the fit. The "other" backgrounds include all processes producing a Higgs boson, VVV and $t\bar{t}V$. A "–" symbol indicates that the background contribution is negligible

SR2-	SF-h	SF-i	SF-j	SF-k	SF-l	SF-m
Observed	0	1	3	2	2	7
Total SM	3.1 ± 1.0	1.9 ± 0.9	1.6 ± 0.5	1.5 ± 0.6	1.8 ± 0.8	2.6 ± 0.9
$t\bar{t}$	–	–	–	–	–	–
Wt	–	–	–	–	–	–
VV	3.0 ± 1.0	1.5 ± 0.8	1.6 ± 0.5	1.4 ± 0.6	1.7 ± 0.8	2.6 ± 0.9
FNP	$0.00^{+0.02}_{-0.00}$	$0.0^{+0.1}_{-0.0}$	$0.00^{+0.01}_{-0.00}$	$0.00^{+0.01}_{-0.00}$	$0.00^{+0.02}_{-0.00}$	$0.00^{+0.01}_{-0.00}$
Z + jets	$0.02^{+0.11}_{-0.02}$	0.42 ± 0.20	–	$0.02^{+0.20}_{-0.02}$	–	$0.02^{+0.06}_{-0.02}$
Other	0.03 ± 0.01	0.03 ± 0.02	–	0.04 ± 0.02	0.02 ± 0.01	0.02 ± 0.02

Table 10 Background-only fit results for SR2-DF-a to SR2-DF-d in the $2\ell + 0$ jets channel. All systematic and statistical uncertainties are included in the fit. The "other" backgrounds include all processes producing a Higgs boson, VVV or $t\bar{t}V$. A "–" symbol indicates that the background contribution is negligible

SR2-	DF-a	DF-b	DF-c	DF-d
Observed	67	5	4	2
Total SM	57 ± 7	9.6 ± 1.9	$1.5^{+1.7}_{-1.5}$	0.6 ± 0.6
$t\bar{t}$	24 ± 8	–	–	–
Wt	4.5 ± 1.0	–	–	–
VV	26 ± 6	8.8 ± 1.8	$1.5^{+1.7}_{-1.5}$	0.6 ± 0.6
FNP	1.75 ± 0.18	0.57 ± 0.23	$0.00^{+0.01}_{-0.00}$	$0.00^{+0.01}_{-0.00}$
Z + jets	–	–	–	–
Other	0.40 ± 0.09	0.17 ± 0.07	0.07 ± 0.07	0.02 ± 0.02

verify the expectation from the γ+jets method that the residual Z+jets background after applying the SR selections is very small. The "loose" validation regions are instead defined by removing several other kinematic requirements used in the SR definition (m_{T2}, all $\Delta\phi$ and ΔR quantities, and the ratios of E_T^{miss} to W p_T, Z p_T, and p_T of the system of ISR jets). These samples have enough Z+jets events to perform comparisons of kinematic distributions, which validate the normalization and kinematic modelling of the Z+jets background. The data distributions are consistent with the expected background in these validation regions, as shown in Fig. 2c for the E_T^{miss} distribution in VR2-int-loose.

Once the signal region requirements are applied, the dominant background in the 2ℓ + jets channel is the diboson background. This is taken from MC simulation, but the modelling is verified in two dedicated validation regions, one for signal regions with low mass-splitting (VR2-VV-low) and one for the intermediate and high-mass signal regions (VR2-VV-int). Requiring high E_T^{miss} and exactly one signal jet (compared to at least two jets in the SRs) suppresses the $t\bar{t}$ background and enhances the purity of diboson events containing an ISR jet, in which each boson decays leptonically. Figure 2d shows the m_{T2} distribution in VR2-VV-int for data and the expected backgrounds.

Table 11 Background-only fit results for the inclusive signal regions in the $2\ell + 0$ jets channel. All systematic and statistical uncertainties are included in the fit. The "other" backgrounds include all processes producing a Higgs boson, VVV and $t\bar{t}V$. A "–" symbol indicates that the background contribution is negligible

SR2-	SF-loose	SF-tight	DF-100	DF-150	DF-200	DF-300
Observed	153	9	78	11	6	2
Total SM	133 ± 22	9.8 ± 2.9	68 ± 7	11.5 ± 3.1	2.1 ± 1.9	0.6 ± 0.6
$t\bar{t}$	27 ± 11	–	24 ± 8	–	–	–
Wt	5.0 ± 2.2	–	4.5 ± 1.0	–	–	–
VV	70 ± 11	9.6 ± 3.0	37 ± 8	10.8 ± 3.0	2.0 ± 1.9	0.6 ± 0.6
FNP	6 ± 4	0.0 ± 0.0	2.17 ± 0.29	0.42 ± 0.23	$0.00^{+0.01}_{-0.00}$	$0.00^{+0.01}_{-0.00}$
Z + jets	23 ± 14	$0.09^{+0.34}_{-0.09}$	–	–	–	–
Other	0.79 ± 0.23	0.09 ± 0.01	0.67 ± 0.16	0.26 ± 0.08	0.09 ± 0.07	0.02 ± 0.02

Table 12 SM background results in the 2ℓ + jets SRs. All systematic and statistical uncertainties are included. The "top" background includes all processes producing one or more top quarks and the "other" backgrounds include all processes producing a Higgs boson or VVV. A "–" symbol indicates that the background contribution is negligible

SR2-	Int	High	Low (combined)
Observed	2	0	11
Total SM	$4.1^{+2.6}_{-1.8}$	$1.6^{+1.6}_{-1.1}$	$4.2^{+3.4}_{-1.6}$
VV	4.0 ± 1.8	1.6 ± 1.1	1.7 ± 1.0
Top	0.15 ± 0.11	0.04 ± 0.03	0.8 ± 0.4
FNP	$0.0^{+0.2}_{-0.0}$	$0.0^{+0.1}_{-0.0}$	$0.7^{+1.8}_{-0.7}$
Z+jets	$0.0^{+1.8}_{-0.0}$	$0.0^{+1.2}_{-0.0}$	$1.0^{+2.7}_{-1.0}$
Other	–	–	–

For both the $2\ell + 0$ jets and 2ℓ + jets channels, reducible backgrounds with one or two FNP leptons arise from multijet, W + jets and single-top-quark production events. For both analyses, the FNP lepton background is estimated from data using the matrix method (MM) [93]. This method uses two types of lepton identification criteria: "signal", corresponding to leptons passing the full analysis selection, and "baseline", corresponding to candidate electrons and muons as defined in Sect. 5. Probabilities for real leptons satisfying the baseline selection to also satisfy the signal selection are measured as a function of p_{T} and η in dedicated regions enriched in Z boson processes; similar probabilities for FNP leptons are measured in events dominated by leptons from heavy flavour decays and photon conversions. The method uses the number of observed events containing baseline–baseline, baseline–signal, signal–baseline and signal–signal

Table 13 Background-only fits for SR3-WZ-0Ja to SR3-WZ-0Jc and SR3-WZ-1Ja to SR3-WZ-1Jc in the 3ℓ channel. All systematic and statistical uncertainties are included in the fit

SR3-	WZ-0Ja	WZ-0Jb	WZ-0Jc	WZ-1Ja	WZ-1Jb	WZ-1Jc
Observed	21	1	2	1	3	4
Total SM	21.7 ± 2.9	2.7 ± 0.5	1.56 ± 0.33	2.2 ± 0.5	1.82 ± 0.26	1.26 ± 0.34
WZ	19.5 ± 2.9	2.5 ± 0.5	1.33 ± 0.31	1.8 ± 0.5	1.49 ± 0.22	0.92 ± 0.28
ZZ	0.81 ± 0.23	0.06 ± 0.03	0.05 ± 0.01	0.05 ± 0.02	0.02 ± 0.01	–
VVV	0.31 ± 0.07	0.13 ± 0.04	0.13 ± 0.03	0.11 ± 0.02	0.12 ± 0.03	0.23 ± 0.05
$t\bar{t}V$	0.04 ± 0.02	0.01 ± 0.01	0.01 ± 0.01	0.14 ± 0.04	0.12 ± 0.02	0.08 ± 0.02
Higgs	–	–	–	0.01 ± 0.00	–	–
FNP	1.1 ± 0.5	0.02 ± 0.01	0.04 ± 0.02	0.11 ± 0.06	0.07 ± 0.04	0.01 ± 0.00

Table 14 Background-only fits for SR3-slep-a to SR3-slep-e in the 3ℓ channel. All systematic and statistical uncertainties are included in the fit

SR3-	slep-a	slep-b	slep-c	slep-d	slep-e
Observed	4	3	9	0	0
Total SM	2.2 ± 0.8	2.8 ± 0.4	5.4 ± 0.9	1.4 ± 0.4	1.14 ± 0.23
WZ	1.1 ± 0.4	1.98 ± 0.31	3.9 ± 0.7	0.91 ± 0.26	0.76 ± 0.17
ZZ	0.02 ± 0.01	0.01 ± 0.01	0.13 ± 0.03	0.06 ± 0.02	0.03 ± 0.01
VVV	0.26 ± 0.08	0.34 ± 0.05	0.72 ± 0.12	0.36 ± 0.10	0.25 ± 0.05
$t\bar{t}V$	0.07 ± 0.03	0.09 ± 0.02	0.20 ± 0.04	0.07 ± 0.02	0.02 ± 0.01
Higgs	0.01 ± 0.00	0.01 ± 0.01	0.03 ± 0.02	0.01 ± 0.00	–
FNP	0.80 ± 0.46	0.36 ± 0.18	0.48 ± 0.25	–	0.08 ± 0.04

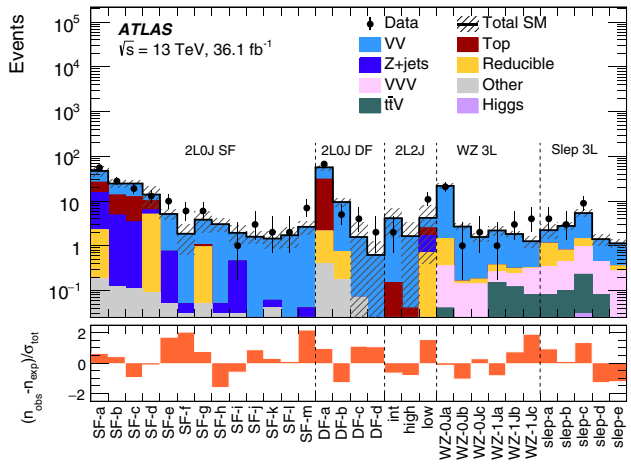

Fig. 3 The observed and expected SM background yields in the signal regions considered in the 2ℓ + 0 jets, 2ℓ + jets and 3ℓ channels. The statistical uncertainties in the background prediction are included in the uncertainty band, together with the experimental and theoretical uncertainties. The bottom plot shows the difference in standard deviations between the observed and expected yields. Here n_{obs} and n_{exp} are the observed data and expected background yields, respectively, $\sigma_{\text{tot}} = \sqrt{n_{\text{bkg}} + \sigma_{\text{bkg}}^2}$, and σ_{exp} is the total background uncertainty

lepton pairs in a given SR to extract data-driven estimates for the FNP lepton background in the CRs, VRs, and SRs for each analysis.

For the 3ℓ channel, the irreducible background is dominated by SM WZ diboson processes. As in the 2ℓ + 0 jets channel, the shape of this background is taken from MC simulation but normalized to data in a dedicated control region. The signal regions shown in Table 3 include a set of exclusive regions inclusive in jet multiplicity which target $\tilde{\ell}$-mediated decays, and a set of exclusive regions separated into 0-jet and $\geq$ 1 jet categories which target gauge-boson-mediated decays. To reflect this, three control regions are defined in order to extract the normalization of the WZ background: an inclusive region (CR3-WZ-inc) and two exclusive control regions (CR3-WZ-0j and CR3-WZ-1j). The results of the background estimations are validated in a set of dedicated validation regions. This includes two validation regions that are binned in jet multiplicity (VR3-Za-0J and VR3-Za-1J), and a set of inclusive validation regions (VR3-Za, VR3-Zb, VR3-offZa and VR3-offZb) targeting different regions of phase space considered in the analysis (i.e. within and outside the Z boson mass window, high and low $E_{\text{T}}^{\text{miss}}$, and vetoing events with a trilepton invariant mass within the Z boson mass window). The definitions of the control and validation regions used in the 3ℓ analysis are shown in Table 7. The normalization factors extracted from the fit for inclusive WZ events, WZ events with zero jets, and WZ events with at least one jet are 0.97 ± 0.06, 1.08 ± 0.06 and 0.94 ± 0.07, respectively. Other small background sources such as VVV, tV and Higgs boson production processes contributing to the irreducible background are taken from MC simulation.

In addition to processes contributing to the reducible backgrounds in the 2ℓ channels, the reducible backgrounds in the 3ℓ channel also include Z+jets, $t\bar{t}$, WW and in general any physics process leading to less than three prompt and isolated leptons. The reducible backgrounds in the 3ℓ channel are estimated using a data-driven fake-factor (FF) method [94]. This method uses two sets of lepton identification criteria: the tight, or "ID", criteria corresponding to the signal lepton selection used in the analysis and the orthogonal loose, or "anti-ID", criteria which are designed to yield an enrichment in FNP leptons. In particular, for the anti-ID leptons the isolation and identification requirements applied to signal leptons are reversed. The Z + jets background events in the signal, control and validation regions are estimated using lepton p_{T}-dependent fake factors, defined as the ratio of the numbers of ID to anti-ID leptons in an FNP-dominated region. These fake factors are then applied to events passing selection requirements identical to those in the signal, control or validation region in question but where one of the ID leptons is replaced by an anti-ID lepton. The "top-like" contamination, which includes $t\bar{t}$, Wt, and WW, is subtracted from these anti-ID regions along with contributions from any remaining MC processes, to avoid double-counting. The top-like reducible background contributions are then estimated differently: data-to-MC scale factors derived with DF opposite-sign events are applied to simulated SF events. Figure 2e, f show the $E_{\text{T}}^{\text{miss}}$ distribution in VR3-Zb and the m_T^{min} distribution in VR3-Za, respectively.

8 Systematic uncertainties

Several sources of experimental and theoretical systematic uncertainty are considered in the SM background estimates and signal predictions. These uncertainties are included in the profile likelihood fit described in Sect. 9. The primary sources of systematic uncertainty are related to the jet energy scale (JES) and resolution (JER), theory uncertainties in the MC modelling, the reweighting procedure applied to simulation to match the distribution of the number of reconstructed vertices observed in data, the systematic uncertainty considered in the non-prompt background estimation and the theoretical cross-section uncertainties. The statistical uncertainty of the simulated event samples is taken into account as well. The effects of these uncertainties were evaluated for all signal samples and background processes. In the 2ℓ + 0jets and 3ℓ channels the normalizations of the MC predictions for the dominant background processes are extracted in dedicated control regions and the systematic uncertainties thus only affect the extrapolation to the signal regions in these cases.

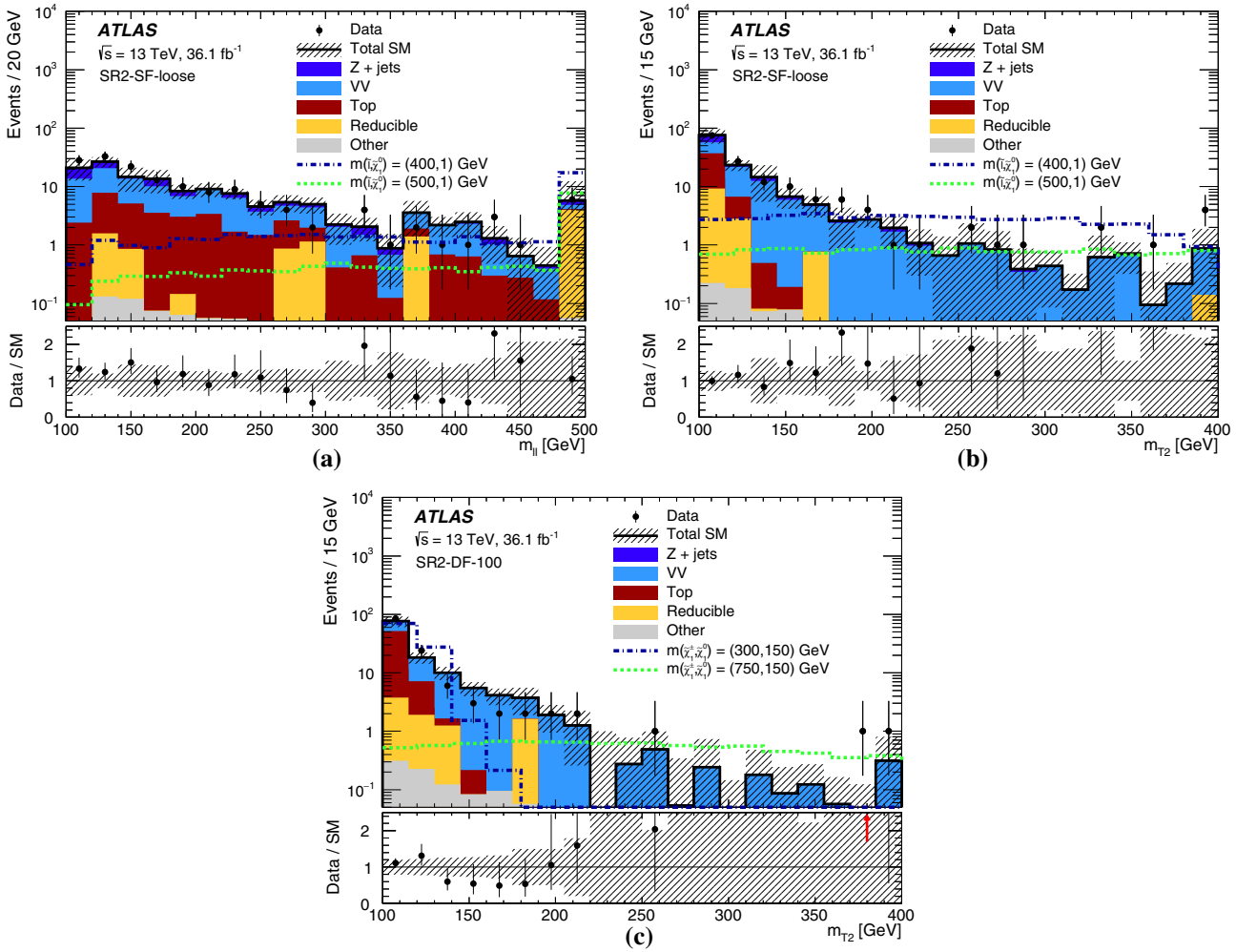

Fig. 4 The **a** $m_{\ell\ell}$ and **b** m_{T2} distributions for data and the estimated SM backgrounds in the $2\ell + 0$ jets channel for SR2-SF-loose and **c** the m_{T2} distribution for the SR2-DF-100 selection. The normalization factors extracted from the corresponding CRs are used to rescale the $t\bar{t}$ and VV contributions. The "top" background includes $t\bar{t}$ and Wt, and the "other" backgrounds include Higgs bosons, $t\bar{t}V$ and VVV. The "reducible" category corresponds to the data-driven matrix method's estimate. The uncertainty bands include all systematic and statistical contributions. Simulated signal models for sleptons (**a**, **b**) or charginos (**c**) pair production are overlayed for comparison. The final bin in each histogram also contains the events in the overflow bin. The vertical red arrows indicate bins where the ratio of data to SM background, minus the uncertainty on this quantity, is larger than the y-axis maximum

The JES and JER uncertainties are derived as a function of jet p_{T} and η, as well as of the pile-up conditions and the jet flavour composition of the selected jet sample. They are determined using a combination of data and simulation, through measurements of the jet response balance in dijet, Z + jets and γ+jets events [79,80].

The systematic uncertainties related to the $E_{\mathrm{T}}^{\mathrm{miss}}$ modelling in the simulation are estimated by propagating the uncertainties in the energy or momentum scale of each of the physics objects, as well as the uncertainties in the soft term's resolution and scale [95].

The remaining detector-related systematic uncertainties, such as those in the lepton reconstruction efficiency, energy scale and energy resolution, in the b-tagging efficiency and in the modelling of the trigger [73,75], are included but were found to be negligible in all channels.

The uncertainties coming from the modelling of diboson events in MC simulation are estimated by varying the renormalization, factorization and merging scales used to generate the samples, and the PDFs. In the $2\ell + 0$ jets channel the impact of these uncertainties in the modelling of Z + jets events is also considered, as well as uncertainties in the modelling of $t\bar{t}$ events due to parton shower simulation (by comparing samples generated with POWHEG + PYTHIA to POWHEG + Herwig++ [61]), ISR/FSR modelling (by comparing the predictions from an event sample generated by

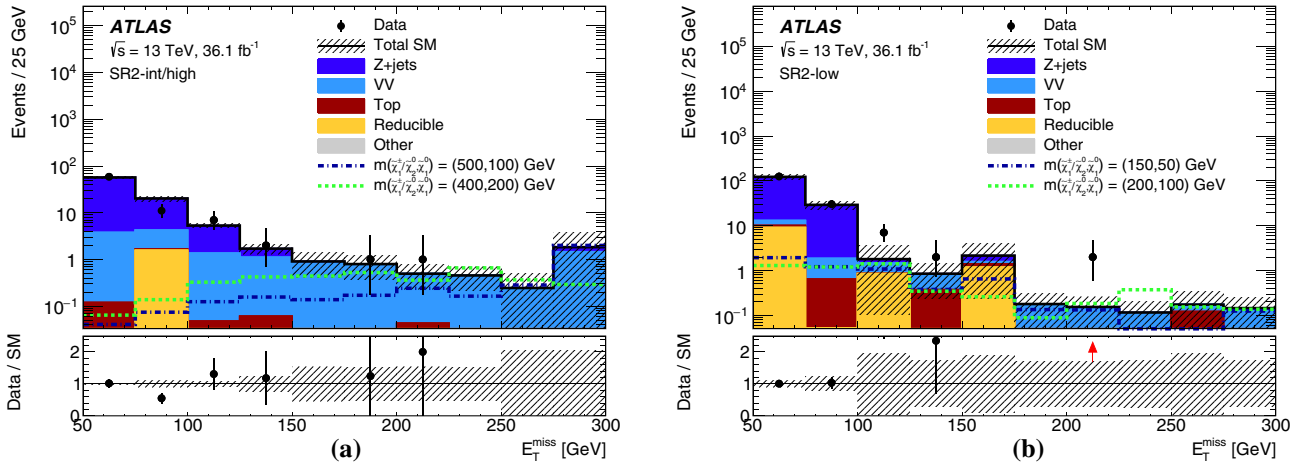

Fig. 5 Distributions of $E_{\mathrm{T}}^{\mathrm{miss}}$ for data and the expected SM backgrounds in the 2ℓ + jets channel for **a** SR2-int/high and **b** SR2-low, without the final $E_{\mathrm{T}}^{\mathrm{miss}}$ requirement applied. The "top" background includes $t\bar{t}$, Wt and $t\bar{t}V$, and the "other" backgrounds include Higgs bosons and VVV. The Z + jets contribution is evaluated using the data-driven γ + jet template method and the "reducible" category corresponds to the data-driven matrix method's estimate. The uncertainty bands include all systematic and statistical contributions. Simulated signal models for charginos/neutralinos production are overlayed for comparison. The final bin in each histogram also contains the events in the overflow bin. The vertical red arrows indicate bins where the ratio of data to SM background, minus the uncertainty on this quantity, is larger than the y-axis maximum

POWHEG + PYTHIA with those from two samples where the radiation settings are varied), and the PDF set.

In the 2ℓ + jets channel, uncertainties in the data-driven Z+jets estimate are calculated following the methodology used in Ref. [90]. An additional uncertainty is based on the difference between the expected background yield from the nominal method and a second method implemented as a cross-check, which extracts the dijet mass shape from data validation regions, normalizes the shape to the sideband regions of the SRs, and extrapolates the background into the W mass region.

For the matrix-method and fake-factor estimates of the FNP background, systematic uncertainties are assigned to account for differences in FNP lepton composition between the SR and the CR used to derive the fake rates and fake factors. An additional uncertainty is assigned to the MC subtraction of prompt leptons from this CR.

The exclusive SRs in the 2ℓ + 0 jets and 3ℓ channels are dominated by statistical uncertainties in the background estimates (which range from 10 to 70% in the higher mass regions in the 2ℓ + 0 jets channel and from 5 to 30% in the 3ℓ channel). The largest systematic uncertainties are those related to diboson modelling, the JES and JER uncertainties and those associated with the $E_{\mathrm{T}}^{\mathrm{miss}}$ modelling. In the 2ℓ + jets channel the dominant uncertainties are those associated with the data-driven estimate of the Z+jets background, which range from approximately 45 to 75%.

9 Results

The HistFitter framework [96] is used for the statistical interpretation of the results, with the CRs (for the 2ℓ + 0 jets and 3ℓ channels) and SRs both participating in a simultaneous likelihood fit. The likelihood is built as the product of a Poisson probability density function describing the observed number of events in each CR/SR and Gaussian distributions that constrain the nuisance parameters associated with the systematic uncertainties and whose widths correspond to the sizes of these uncertainties; Poisson distributions are used instead for MC statistical uncertainties. Correlations of a given nuisance parameter among the different background sources and the signal are taken into account when relevant.

In the 2ℓ + 0 jets and 3ℓ channels, a background-only fit which uses data in the CRs is performed to constrain the nuisance parameters of the likelihood function (these include the normalization factors for dominant backgrounds and the parameters associated with the systematic uncertainties). In all channels the background estimates are also used to evaluate how well the expected and observed numbers of events agree in the validation regions, and good agreement is found. In the 2ℓ + 0 jets, 2ℓ + jets, and 3ℓ channels, the number of considered VRs is 3, 8, and 6, respectively, and the most significant deviations observed are 0.4σ, 1.4σ, and 0.8σ, respectively. The precision of the expected background yields in the VRs is significantly better than in the corresponding SRs and the dominant sources of systematic uncertainty in the VRs and corresponding SRs are similar. For the 2ℓ + 0 jets channel, the results for the exclusive signal regions are shown

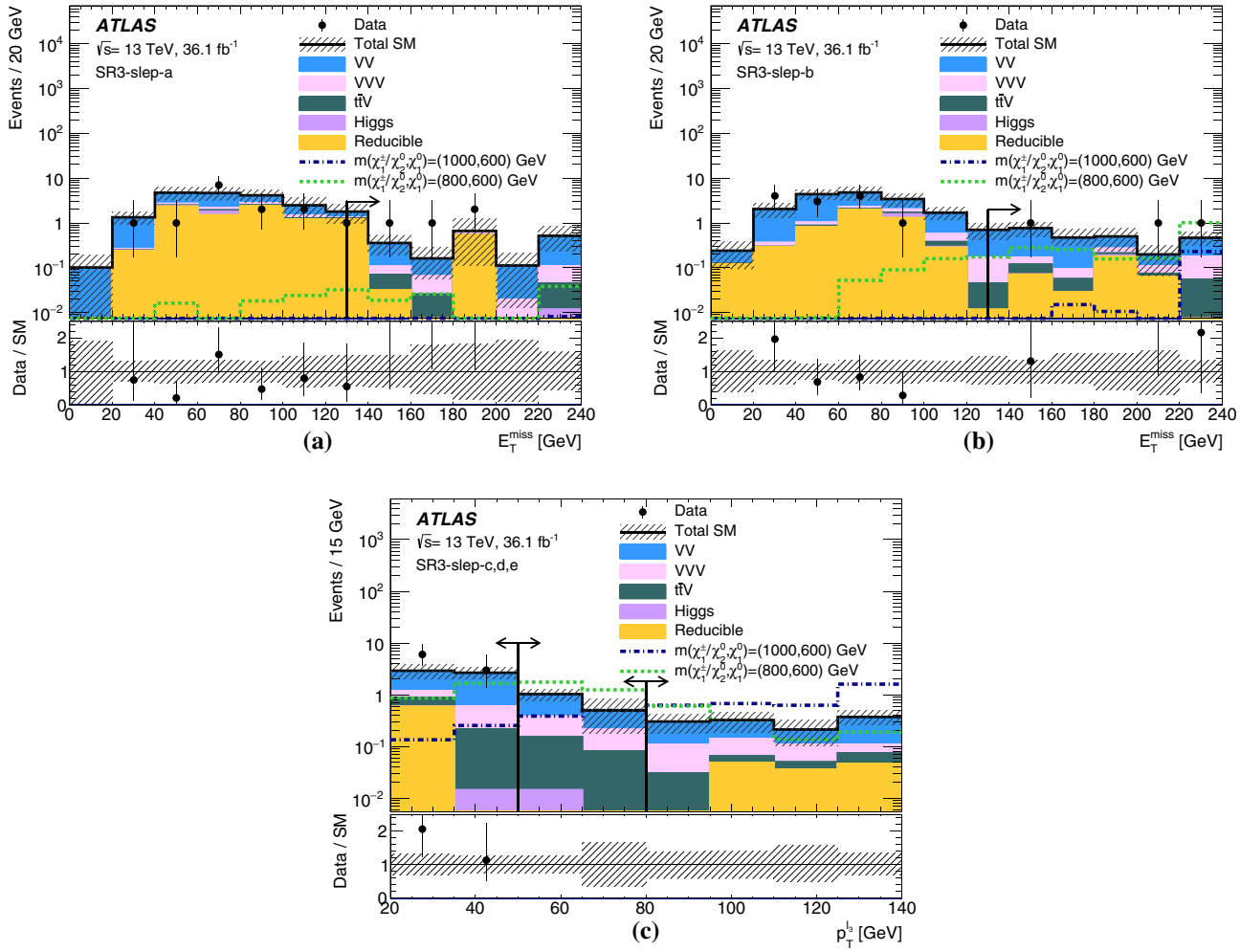

Fig. 6 Distributions of $E_{\mathrm{T}}^{\mathrm{miss}}$ for data and the estimated SM backgrounds in the 3ℓ channel for **a** SR3-slep-a and **b** SR3-slep-b and **c** distributions of the third leading lepton p_{T} in SR3-slep-c,d,e. The normalization factors extracted from the corresponding CRs are used to rescale the WZ background. The "reducible" category corresponds to the data-driven fake-factor estimate. The uncertainty bands include all systematic and statistical contributions. Simulated signal models for charginos/neutralinos production are overlayed for comparison. The final bin in each histogram also contains the events in the overflow bin

in Tables 8, 9 and 10 for SR2-SF-a to SR2-SF-g, SR2-SF-h to SR2-SF-m and SR2-DF-a to SR2-DF-d, respectively. The results for the 2ℓ + 0 jets inclusive signal regions are shown in Table 11, while Table 12 summarizes the expected SM background and observed events in the 2ℓ + jets SRs. For the 3ℓ channel, the results are shown in Table 13 for SR3-WZ-0Ja to SR3-WZ-0Jc and SR3-WZ-1Ja to SR3-WZ-1Jc (which target gauge-boson-mediated decays) and Table 14 for SR3-slep-a to SR3-slep-e. A summary of the observed and expected yields in all of the signal regions considered in this paper is provided in Fig. 3. No significant excess above the SM expectation is observed in any SR.

Figure 4 shows a selection of kinematic distributions for data and the estimated SM backgrounds with their associated statistical and systematic uncertainties for the loosest inclusive SRs in the 2ℓ + 0 jets channel: SR2-SF-loose and SR2-DF-100. The normalization factors extracted from the corresponding CRs are propagated to the VV and $t\bar{t}$ contributions. Figure 5 shows the $E_{\mathrm{T}}^{\mathrm{miss}}$ distribution in SR2-int and SR2-high, which differ only in the $E_{\mathrm{T}}^{\mathrm{miss}}$ requirement, and in SR2-low of the 2ℓ + jets channel. In the 3ℓ channel, distributions of $E_{\mathrm{T}}^{\mathrm{miss}}$ and the third leading lepton p_{T} are shown for the SR bins targeting $\tilde{\ell}$-mediated decays in Fig. 6 while Fig. 7 shows distributions of $E_{\mathrm{T}}^{\mathrm{miss}}$ in the bins targeting gauge-boson-mediated decays. Good agreement between data and expectations is observed in all distributions within the uncertainties.

In the absence of any significant excess, two types of exclusion limits for new physics scenarios are calculated using the $\mathrm{CL_s}$ prescription [97]. First, exclusion limits

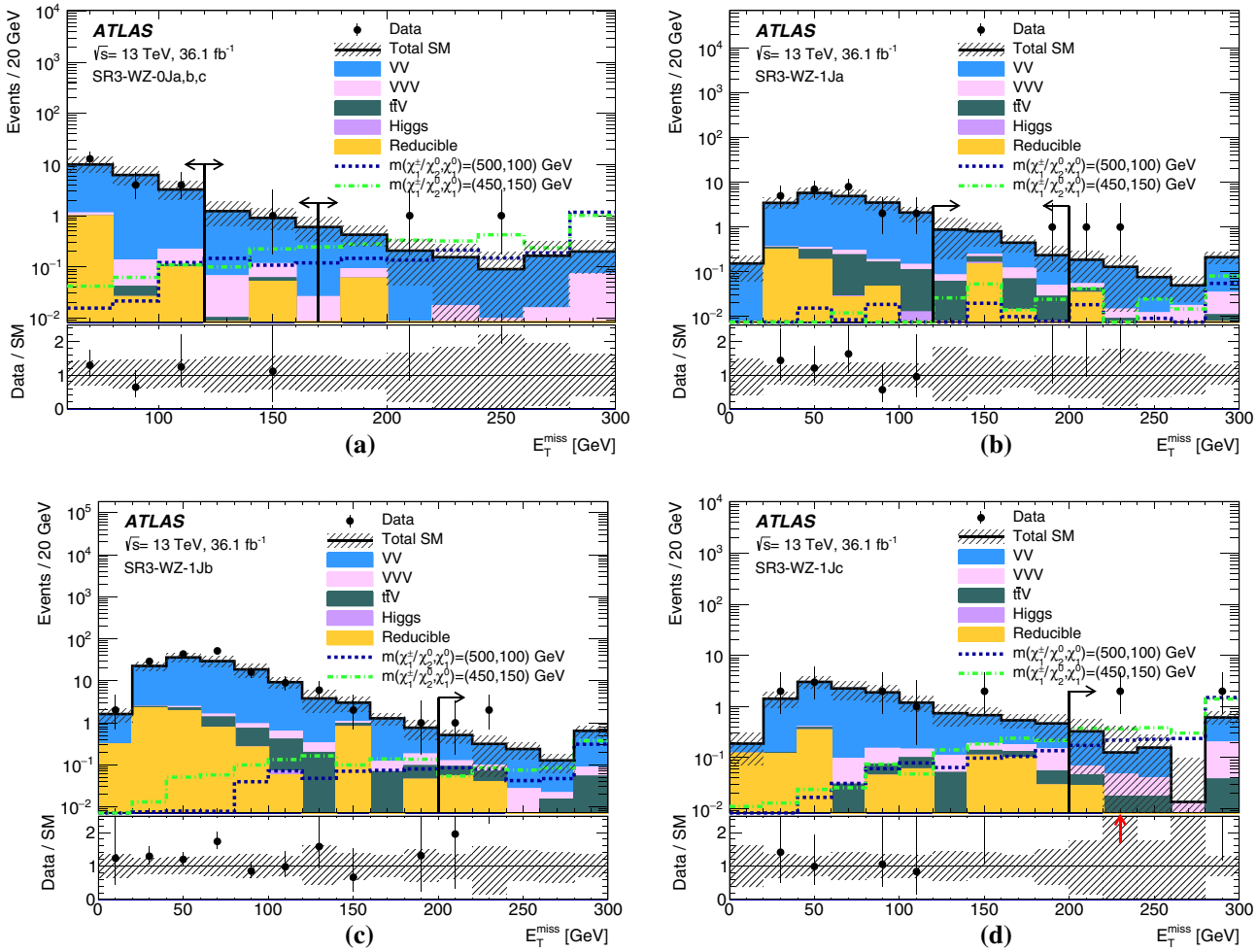

Fig. 7 Distributions of $E_{\mathrm{T}}^{\mathrm{miss}}$ for data and the estimated SM backgrounds in the 3ℓ channel for **a** SR3-WZ-0Ja,b,c, **b** SR3-WZ-1Ja, **c** SR3-WZ-1Jb and **d** SR3-WZ-1Jc. The normalization factors extracted from the corresponding CRs are used to rescale the 0-jet and $\geq$ 1-jet WZ background components. The "reducible" category corresponds to the data-driven fake-factor estimate. The uncertainty bands include all systematic and statistical contributions. Simulated signal models for charginos/neutralinos production are overlayed for comparison. The final bin in each histogram also contains the events in the overflow bin. The vertical red arrows indicate bins where the ratio of data to SM background, minus the uncertainty on this quantity, is larger than the y-axis maximum

are set on the masses of the charginos, neutralinos, and sleptons for the simplified models in Fig. 1, as shown in Fig. 8. Figure 8a, b show the limits in the 2ℓ + 0 jets channel in the models of direct chargino pair production with decays via sleptons and direct slepton pair production, respectively. Limits are calculated by statistically combining the mutually orthogonal exclusive SRs. For the chargino pair model, all SF and DF bins are used and chargino masses up to 750 GeV are excluded at 95% confidence level for a massless $\tilde{\chi}_1^0$ neutralino. In the region with large chargino mass, the observed limit is weaker than expected because the data exceeds the expected backgrounds in SF-e, SF-f, and SF-g. For the slepton pair model, which assumes mass-degenerate $\tilde{\ell}_{\mathrm{L}}$ and $\tilde{\ell}_{\mathrm{R}}$ states (where $\tilde{\ell} = \tilde{e}, \tilde{\mu}, \tilde{\tau}$), only SF bins are used and slepton masses up to 500 GeV are excluded for a massless $\tilde{\chi}_1^0$ neutralino.

Figure 8c shows the limits from the 3ℓ channel in the model of mass-degenerate chargino–neutralino pair production with decays via sleptons, calculated using a statistical combination of the five SR3-slep regions. In this model, chargino and neutralino masses up to 1100 GeV are excluded for $\tilde{\chi}_1^0$ neutralino masses less than 550 GeV.

Figure 8d shows the limits from the 3ℓ and 2ℓ + jets channels in the model of mass-degenerate chargino–neutralino pair production with decays via W/Z bosons. The 3ℓ limits are calculated using a statistical combination of the six SR3-WZ regions. Since the SRs in the 2ℓ + jets channel are not mutually exclusive, the observed $\mathrm{CL_s}$ value is taken from the signal region with the best expected $\mathrm{CL_s}$ value. The 3ℓ and 2ℓ

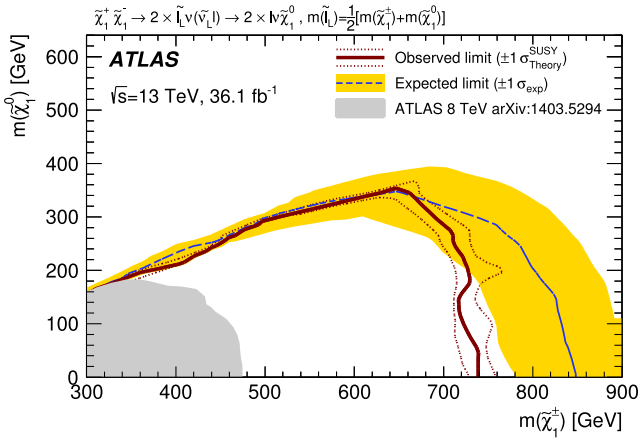

(a) 2ℓ+0jets channel: $\tilde{\chi}_1^+\tilde{\chi}_1^-$ production with $\tilde{\ell}$-mediated decays

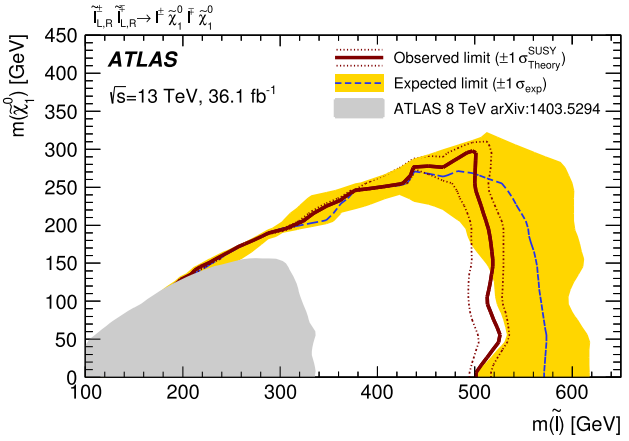

(b) 2ℓ+0jets channel: $\tilde{\ell}\tilde{\ell}$ production

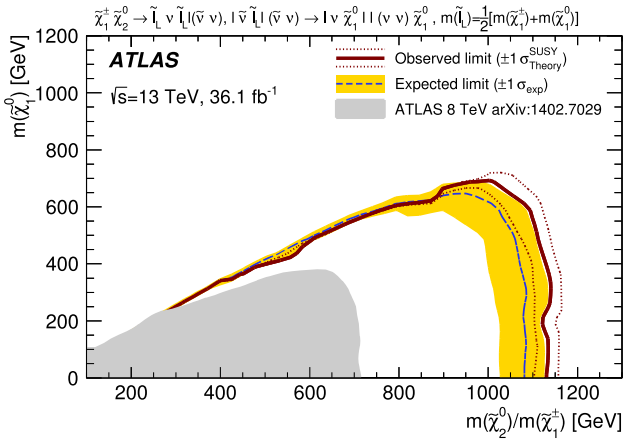

(c) 3ℓ channel: $\tilde{\chi}_1^\pm\tilde{\chi}_2^0$ production with $\tilde{\ell}$-mediated decays

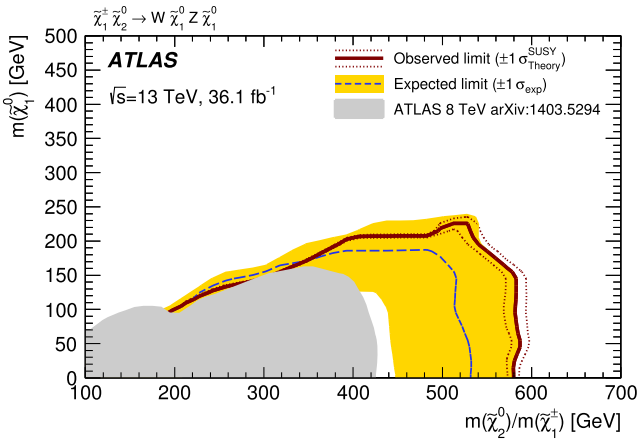

(d) 2ℓ+jets and 3ℓ channels: $\tilde{\chi}_1^\pm\tilde{\chi}_2^0$ production with decays via W/Z

Fig. 8 Observed and expected exclusion limits on SUSY simplified models for **a** chargino-pair production, **b** slepton-pair production, **c** chargino–neutralino production with slepton-mediated decays, and **d** chargino–neutralino production with decays via W/Z bosons. The observed (solid thick red line) and expected (thin dashed blue line) exclusion contours are indicated. The shaded band corresponds to the $\pm 1\sigma$ variations in the expected limit, including all uncertainties except theoretical uncertainties in the signal cross-section. The dotted lines around the observed limit illustrate the change in the observed limit as the nominal signal cross-section is scaled up and down by the theoretical uncertainty. All limits are computed at 95% confidence level. The observed limits obtained from ATLAS in Run 1 are also shown [23]

+ jets channels are then combined, using the channel with the best expected CL_s value for each point in the model parameter space. In this model, chargino and neutralino masses up to 580 GeV are excluded for a massless $\tilde{\chi}_1^0$ neutralino.

Second, model-independent upper limits are set on the visible signal cross-section ($\langle\epsilon\sigma\rangle_{\text{obs}}^{95}$) as well as on the observed (S_{obs}^{95}) and expected (S_{exp}^{95}) number of events from processes beyond-the-SM in the signal regions considered in this analysis. The p-value and the corresponding significance for the background-only hypothesis are also evaluated. For the 2ℓ + 0 jets channel the inclusive signal regions defined in Table 1 are considered whereas for the 3ℓ channel the calculation is performed for each bin separately. All the limits are at 95% confidence level. The results can be found in Table 15.

10 Conclusion

Searches for the electroweak production of neutralinos, charginos and sleptons decaying into final states with exactly two or three electrons or muons and missing transverse momentum are performed using 36.1 fb^{-1} of $\sqrt{s} = 13$ TeV proton–proton collisions recorded by the ATLAS detector at the Large Hadron Collider. Three different search channels

Table 15 Summary of results and model-independent limits in the inclusive $2\ell + 0$ jets, $2\ell +$ jets, and 3ℓ SRs. The observed (N_{obs}) and expected background (N_{exp}) yields in the signal regions are indicated. Signal model-independent upper limits at 95% confidence level on the visible signal cross-section ($\langle\epsilon\sigma\rangle^{95}_{\text{obs}}$), and the observed and expected upper limit on the number of BSM events (S^{95}_{obs} and S^{95}_{exp}, respectively) are also shown. The $\pm 1\sigma$ variations of the expected limit originate from the statistical and systematic uncertainties in the background prediction. The last two columns show the p value and the corresponding significance for the background-only hypothesis. For SRs where the data yield is smaller than expected, the p value is truncated at 0.5 and the significance is set to 0

Signal channel	Region	N_{obs}	N_{exp}	$\langle\epsilon\sigma\rangle^{95}_{\text{obs}}$[fb]	S^{95}_{obs}	S^{95}_{exp}	$p(s=0)$	Z
$2\ell + 0$ jets	DF-100	78	68 ± 7	0.88	32	27^{+11}_{-8}	0.22	0.77
	DF-150	11	11.5 ± 3.1	0.32	11.4	12^{+5}_{-4}	0.5	0
	DF-200	6	2.1 ± 1.9	0.33	12.0	$10.3^{+2.9}_{-1.9}$	0.06	1.5
	DF-300	2	0.6 ± 0.6	0.18	6.6	$5.6^{+1.1}_{-0.9}$	0.10	1.3
	SF-loose	153	133 ± 22	2.02	73	53^{+21}_{-16}	0.16	1.0
	SF-tight	9	9.8 ± 2.9	0.29	10.5	12^{+4}_{-3}	0.5	0
2ℓ + jets	SR2-int	2	$4.1^{+2.6}_{-1.8}$	0.13	4.5	$5.6^{+2.2}_{-1.4}$	0.5	0
	SR2-high	0	$1.6^{+1.6}_{-1.1}$	0.09	3.1	$3.1^{+1.4}_{-0.1}$	0.5	0
	SR2-low	11	$4.2^{+3.4}_{-1.6}$	0.43	15.7	12^{+4}_{-2}	0.06	1.6
3ℓ	WZ-0Ja	21	21.7 ± 2.9	0.35	12.8	14^{+3}_{-5}	0.5	0
	WZ-0Jb	1	2.7 ± 0.5	0.10	3.7	$4.6^{+2.1}_{-0.9}$	0.5	0
	WZ-0Jc	2	1.6 ± 0.3	0.13	4.8	$4.1^{+1.7}_{-0.7}$	0.28	0.57
	WZ-1Ja	1	2.2 ± 0.5	0.09	3.2	$4.5^{+1.6}_{-1.3}$	0.5	0
	WZ-1Jb	3	1.8 ± 0.3	0.16	5.6	$4.3^{+1.7}_{-0.9}$	0.18	0.91
	WZ-1Jc	4	1.3 ± 0.3	0.20	7.2	$4.2^{+1.7}_{-0.4}$	0.03	1.8
	slep-a	4	2.2 ± 0.8	0.19	6.8	$4.7^{+2.3}_{-0.5}$	0.23	0.72
	slep-b	3	2.8 ± 0.4	0.14	5.2	$5.1^{+1.9}_{-1.2}$	0.47	0.08
	slep-c	9	5.4 ± 0.9	0.29	10.5	$6.8^{+2.9}_{-1.3}$	0.09	1.4
	slep-d	0	1.4 ± 0.4	0.08	3.0	$3.6^{+1.2}_{-0.6}$	0.5	0
	slep-e	0	1.1 ± 0.2	0.09	3.3	$3.6^{+1.3}_{-0.5}$	0.5	0

are considered. The $2\ell + 0$ jets channel targets direct $\tilde{\chi}_1^+\tilde{\chi}_1^-$ production where each $\tilde{\chi}_1^\pm$ decays via an intermediate $\tilde{\ell}$, and direct $\tilde{\ell}\tilde{\ell}$ production. The 2ℓ + jets channel targets associated $\tilde{\chi}_1^\pm\tilde{\chi}_2^0$ production where each sparticle decays via an SM gauge boson giving a final state with two leptons consistent with a Z boson and two jets consistent with a W boson. Finally, the 3ℓ channel targets associated $\tilde{\chi}_1^\pm\tilde{\chi}_2^0$ production with decays via either intermediate $\tilde{\ell}$ or gauge bosons.

No significant excess above the SM expectation is observed in any of the signal regions considered across the three channels, and the results are used to calculate exclusion limits at 95% confidence level in several simplified model scenarios. For associated $\tilde{\chi}_1^\pm\tilde{\chi}_2^0$ production with $\tilde{\ell}$-mediated decays, masses up to 1100 GeV are excluded for $\tilde{\chi}_1^0$ neutralino masses less than 550 GeV. Both the 2ℓ + jets and 3ℓ channels place exclusion limits on associated $\tilde{\chi}_1^\pm\tilde{\chi}_2^0$ production with gauge-boson-mediated decays. For a massless $\tilde{\chi}_1^0$ neutralino, $\tilde{\chi}_1^\pm/\tilde{\chi}_2^0$ masses up to approximately 580 GeV are excluded. In the 2ℓ + 0 jets channel, for direct $\tilde{\chi}_1^+\tilde{\chi}_1^-$ production with decays via an intermediate $\tilde{\ell}$, masses up to 750 GeV are excluded for a massless $\tilde{\chi}_1^0$ neutralino. For $\tilde{\ell}\tilde{\ell}$ production, masses up to 500 GeV are excluded for a massless $\tilde{\chi}_1^0$ neutralino, assuming mass-degenerate $\tilde{\ell}_{\text{L}}$ and $\tilde{\ell}_{\text{R}}$ (where $\tilde{\ell} = \tilde{e}, \tilde{\mu}, \tilde{\tau}$). These results significantly improve upon previous exclusion limits based on Run 1 data.

Acknowledgements We thank CERN for the very successful operation of the LHC, as well as the support staff from our institutions without whom ATLAS could not be operated efficiently. We acknowledge the support of ANPCyT, Argentina; YerPhI, Armenia; ARC, Australia; BMWFW and FWF, Austria; ANAS, Azerbaijan; SSTC, Belarus; CNPq and FAPESP, Brazil; NSERC, NRC and CFI, Canada; CERN; CONICYT, Chile; CAS, MOST and NSFC, China; COLCIENCIAS, Colombia; MSMT CR, MPO CR and VSC CR, Czech Republic; DNRF and DNSRC, Denmark; IN2P3-CNRS, CEA-DRF/IRFU, France; SRNSFG, Georgia; BMBF, HGF, and MPG, Germany; GSRT, Greece; RGC, Hong Kong SAR, China; ISF and Benoziyo Center, Israel; INFN, Italy; MEXT and JSPS, Japan; CNRST, Morocco; NWO, Netherlands; RCN, Norway; MNiSW and NCN, Poland; FCT, Portugal; MNE/IFA, Romania; MES of Russia and NRC KI, Russian Federation; JINR; MESTD, Serbia; MSSR, Slovakia; ARRS and MIZŠ, Slovenia; DST/NRF, South Africa; MINECO, Spain; SRC and Wallenberg Foundation, Sweden; SERI, SNSF and Cantons of Bern and Geneva, Switzerland; MOST, Taiwan; TAEK, Turkey; STFC, United Kingdom; DOE and NSF, United States of America. In addition, individual groups and members have received support from BCKDF, the Canada Council, CANARIE, CRC, Compute Canada, FQRNT, and the Ontario Innovation Trust, Canada; EPLANET, ERC, ERDF, FP7, Horizon 2020 and Marie Skłodowska-Curie Actions, European Union; Investissements d'Avenir Labex and Idex, ANR, Région Auvergne and Fondation Partager le Savoir, France; DFG and AvH Foundation, Germany; Herakleitos, Thales and Aristeia programmes co-financed by EU-ESF and the Greek NSRF; BSF, GIF and Minerva, Israel; BRF, Norway; CERCA Programme Generalitat de Catalunya, Generalitat Valenciana, Spain; the Royal Society and Leverhulme Trust, United Kingdom. The crucial computing support from all WLCG partners is acknowledged gratefully, in particular from CERN, the ATLAS Tier-1 facilities at TRIUMF (Canada), NDGF (Denmark, Norway, Sweden), CC-IN2P3 (France),

KIT/GridKA (Germany), INFN-CNAF (Italy), NL-T1 (Netherlands), PIC (Spain), ASGC (Taiwan), RAL (UK) and BNL (USA), the Tier-2 facilities worldwide and large non-WLCG resource providers. Major contributors of computing resources are listed in Ref. [98].

Funded by SCOAP[3].

References

1. Yu. A. Golfand, E. P. Likhtman, Extension of the algebra of Poincare group generators and violation of p invariance. JETP Lett. **13**, 323 (1971). [Pisma Zh. Eksp. Teor. Fiz. **13**, 452 (1971)]
2. D.V. Volkov, V.P. Akulov, Is the neutrino a goldstone particle? Phys. Lett. B **46**, 109 (1973)
3. J. Wess, B. Zumino, Supergauge transformations in four-dimensions. Nucl. Phys. B **70**, 39 (1974)
4. J. Wess, B. Zumino, Supergauge invariant extension of quantum electrodynamics. Nucl. Phys. B **78**, 1 (1974)
5. S. Ferrara, B. Zumino, Supergauge Invariant Yang–Mills theories. Nucl. Phys. B **79**, 413 (1974)
6. A. Salam, J.A. Strathdee, Supersymmetry and nonabelian gauges. Phys. Lett. B **51**, 353 (1974)
7. S.P. Martin, A supersymmetry primer. Adv. Ser. Direct. High Energy Phys. **18**, 1 (1998). arXiv:hep-ph/9709356
8. P. Fayet, Supersymmetry and weak, electromagnetic and strong interactions. Phys. Lett. B **64**, 159 (1976)
9. P. Fayet, Spontaneously broken supersymmetric theories of weak, electromagnetic and strong interactions. Phys. Lett. B **69**, 489 (1977)
10. N. Sakai, Naturalness in supersymmetric guts. Z. Phys. C **11**, 153 (1981)
11. S. Dimopoulos, S. Raby, F. Wilczek, Supersymmetry and the scale of unification. Phys. Rev. D **24**, 1681 (1981)
12. L.E. Ibanez, G.G. Ross, Low-energy predictions in supersymmetric grand unified theories. Phys. Lett. B **105**, 439 (1981)
13. S. Dimopoulos, H. Georgi, Softly broken supersymmetry and SU(5). Nucl. Phys. B **193**, 150 (1981)
14. G.R. Farrar, P. Fayet, Phenomenology of the production, decay, and detection of new hadronic states associated with supersymmetry. Phys. Lett. B **76**, 575 (1978)
15. H. Goldberg, Constraint on the photino mass from cosmology. Phys. Rev. Lett. **50**, 1419 (1983). Erratum: Phys. Rev. Lett. **103**, 099905 (2009)
16. J.R. Ellis, J.S. Hagelin, D.V. Nanopoulos, K.A. Olive, M. Srednicki, Supersymmetric relics from the big bang. Nucl. Phys. B **238**, 453 (1984)
17. L. Evans, P. Bryant, LHC machine. JINST **3**, S08001 (2008)
18. ATLAS Collaboration, The ATLAS experiment at the CERN large hadron collider. JINST **3**, S08003 (2008)
19. CMS Collaboration, The CMS experiment at the CERN LHC. JINST **3**, S08004 (2008)
20. ATLAS Collaboration, Search for squarks and gluinos in final states with jets and missing transverse momentum using 36 fb^{-1} of $\sqrt{s} =$ 13 TeV pp collision data with the ATLAS detector. Phys. Rev. D **97**, 112001 (2018). https://doi.org/10.1103/PhysRevD.97.112001
21. CMS Collaboration, Search for supersymmetry in multijet events with missing transverse momentum in proton-proton collisions at 13 TeV. Phys. Rev. D **96**, 032003 (2017). arXiv:1704.07781 [hep-ex]
22. CMS Collaboration, Search for new phenomena with the MT2 variable in the all-hadronic final state produced in proton-proton collisions at $\sqrt{s} =$ 13 TeV. Eur. Phys. J. C **77**, 710 (2017). arXiv:1705.04650 [hep-ex]
23. ATLAS Collaboration, Search, for direct production of charginos, neutralinos and sleptons in final states with two leptons and missing transverse momentum in pp collisions at $\sqrt{s} =$ 8 TeV with the ATLAS detector. JHEP **05**, 071 (2014). arXiv:1403.5294 [hep-ex]
24. ATLAS Collaboration, Search for direct production of charginos and neutralinos in events with three leptons and missing transverse momentum in $\sqrt{s} =$ 8TeV pp collisions with the ATLAS detector. JHEP **04**, 169 (2014). arXiv:1402.7029 [hep-ex]
25. ATLAS collaboration, Search for the electroweak production of supersymmetric particles in $\sqrt{s} =$ 8 TeV pp collisions with the ATLAS detector. Phys. Rev. D **93**, 052002 (2016)
26. CMS Collaboration, Search for electroweak production of charginos and neutralinos in multilepton final states in proton-proton collisions at $\sqrt{s} =$ 13TeV. JHEP **03**, 166 (2018). https://doi.org/10.1007/JHEP03(2018)166
27. CMS Collaboration, Search for electroweak production of charginos and neutralinos using leptonic final states in pp collisions at $\sqrt{s} =$ 7TeV. JHEP **11**, 147 (2012). arXiv:1209.6620 [hep-ex]
28. CMS Collaboration, Searches for electroweak neutralino and chargino production in channels with Higgs, Z, and W bosons in pp collisions at 8 TeV. Phys. Rev. D **90**, 092007 (2014). arXiv:1409.3168 [hep-ex]
29. CMS collaboration, Searches for electroweak production of charginos, neutralinos, and sleptons decaying to leptons and W, Z, and Higgs bosons in pp collisions at 8 TeV. Eur. Phys. J. C **74**, 3036 (2014). arXiv:1405.7570 [hep-ex]
30. J. Alwall, P. Schuster, N. Toro, Simplified models for a first characterization of new physics at the LHC. Phys. Rev. D **79**, 075020 (2009). arXiv:0810.3921 [hep-ph]
31. ATLAS Collaboration, ATLAS Insertable B-Layer Technical Design Report, ATLAS-TDR-19 (2010). https://cds.cern.ch/record/1291633. ATLAS Insertable B-Layer Technical Design Report Addendum, ATLAS-TDR-19-ADD-1 (2012). https://cds.cern.ch/record/1451888
32. ATLAS Collaboration, Performance of the ATLAS trigger system in 2015. Eur. Phys. J. C **77**, 317 (2017). arXiv:1611.09661 [hep-ex]
33. ATLAS Collaboration, Luminosity determination in pp collisions at $\sqrt{s} =$ 8 TeV using the ATLAS detector at the LHC. Eur. Phys. J. C **76**, 653 (2016). arXiv:1608.03953 [hep-ex]
34. ATLAS Collaboration, The ATLAS simulation infrastructure. Eur. Phys. J. C **70**, 823 (2010). arXiv:1005.4568 [hep-ex]
35. S. Agostinelli, GEANT4: a simulation toolkit. Nucl. Instrum. Methods A **506**, 250 (2003)
36. ATLAS Collaboration, The simulation principle and performance of the ATLAS fast calorimeter simulation FastCaloSim. ATL-PHYS-PUB-2010-013 (2010). https://cds.cern.ch/record/1300517
37. T. Gleisberg, S. Höche, F. Krauss, M. Schönherr, S. Schumann et al., Event generation with SHERPA 1.1. JHEP **02**, 007 (2009). arXiv:0811.4622 [hep-ph]
38. ATLAS Collaboration, Multi-boson simulation for 13 TeV ATLAS analyses. ATL-PHYS-PUB- 2016-002 (2016). https://cds.cern.ch/record/2119986
39. J.M. Campbell, R.K. Ellis, An update on vector boson pair production at hadron colliders. Phys. Rev. D **60**, 113006 (1999). arXiv:hep-ph/9905386
40. J.M. Campbell, R.K. Ellis, C. Williams, Vector boson pair production at the LHC. JHEP **07**, 018 (2011). arXiv:1105.0020 [hep-ph]
41. T. Gleisberg, S. Höche, Comix, a new matrix element generator. JHEP **12**, 039 (2008). arXiv:0808.3674 [hep-ph]

42. F. Cascioli, P. Maierhofer, S. Pozzorini, Scattering amplitudes with open loops. Phys. Rev. Lett. **108**, 111601 (2012). arXiv:1111.5206 [hep-ph]
43. S. Schumann, F. Krauss, A parton shower algorithm based on Catani–Seymour dipole factorisation. JHEP **03**, 038 (2008). arXiv:0709.1027 [hep-ph]
44. S. Höche, F. Krauss, M. Schönherr, F. Siegert, QCD matrix elements + parton showers: the NLO case. JHEP **04**, 027 (2013). arXiv:1207.5030 [hep-ph]
45. R.D. Ball, Parton distributions for the LHC Run II. JHEP **04**, 040 (2015). arXiv:1410.8849 [hep-ph]
46. ATLAS Collaboration, Monte Carlo Generators for the Production of a W or Z/$\gamma*$ Boson in Association with Jets at ATLAS in Run 2. ATL-PHYS-PUB-2016-003 (2016). https://cds.cern.ch/record/2120133
47. R. Gavin, Y. Li, F. Petriello, S. Quackenbush, FEWZ, 2.0: a code for hadronic Z production at next-to-next-to-leading order. Comput. Phys. Commun. **182**, 2388 (2011). arXiv:1011.3540 [hep-ph]
48. E. Re, Single-top Wt-channel production matched with parton showers using the POWHEG method. Eur. Phys. J. C **71**, 1547 (2011). arXiv:1009.2450 [hep-ph]
49. S. Frixione, P. Nason, G. Ridolfi, A positive-weight next-to-leading-order Monte Carlo for heavy flavour hadroproduction. JHEP **09**, 126 (2007). arXiv:0707.3088 [hep-ph]
50. H.-L. Lai, New parton distributions for collider physics. Phys. Rev. D **82**, 074024 (2010). arXiv:1007.2241 [hep-ph]
51. ATLAS Collaboration, Simulation of top-quark production for the ATLAS experiment at $\sqrt{s}$ = 13TeV. ATL-PHYS-PUB-2016-004 (2016). https://cds.cern.ch/record/2120417
52. M. Czakon, A. Mitov, Top++: a program for the calculation of the top-pair cross-section at hadron colliders. Comput. Phys. Commun. **185**, 2930 (2014). arXiv:1112.5675 [hep-ph]
53. N. Kidonakis, Two-loop soft anomalous dimensions for single top quark associated production with a W^- or H^-. Phys. Rev. D **82**, 054018 (2010). arXiv:1005.4451 [hep-ph]
54. J. Alwall, The automated computation of tree-level and next-to-leading order differential cross sections, and their matching to parton shower simulations. JHEP **07**, 079 (2014). arXiv:1405.0301 [hep-ph]
55. T. Sjöstrand, S. Mrenna, P.Z. Skands, A brief introduction to PYTHIA 8.1. Comput. Phys. Commun. **178**, 852 (2008). arXiv:0710.3820 [hep-ph]
56. ATLAS Collaboration, Modelling of the $t\bar{t}$H and $t\bar{t}$V(V = W, Z) processes for $\sqrt{s}$ = 13TeV ATLAS analyses. ATL-PHYS-PUB-2016-005 (2016). https://cds.cern.ch/record/2120826
57. ATLAS Collaboration, ATLAS Pythia 8 tunes to 7 TeV data, ATL-PHYS-PUB-2014-021 (2014). https://cds.cern.ch/record/1966419
58. R.D. Ball et al., Parton distributions with LHC data. Nucl. Phys. B **867**, 244 (2013). arXiv:1207.1303 [hep-ph]
59. S. Alioli, P. Nason, C. Oleari, E. Re, A general framework for implementing NLO calculations in shower Monte Carlo programs: the POWHEG BOX. JHEP **06**, 043 (2010). arXiv:1002.2581 [hep-ph]
60. LHC Higgs Cross Section Working Group et al. Handbook of LHC Higgs Cross Sections: 4. Deciphering the Nature of the Higgs Sector. arXiv:1610.07922 [hep-ph]
61. M. Bahr, Herwig++ physics and manual. Eur. Phys. J. C **58**, 639 (2008). arXiv:0803.0883 [hep-ph]
62. L. Lönnblad, S. Prestel, Matching tree-level matrix elements with interleaved showers. JHEP **03**, 019 (2012). arXiv:1109.4829 [hep-ph]
63. W. Beenakker, R. Hopker, M. Spira, P. Zerwas, Squark and gluino production at hadron colliders. Nucl. Phys. B **492**, 51 (1997). arXiv:hep-ph/9610490
64. A. Kulesza, L. Motyka, Threshold resummation for squark-antisquark and gluino-pair production at the LHC. Phys. Rev. Lett. **102**, 111802 (2009). arXiv:0807.2405
65. A. Kulesza, L. Motyka, Soft gluon resummation for the production of gluino-gluino and squark-antisquark pairs at the LHC. Phys. Rev. D **80**, 095004 (2009). arXiv:0905.4749 [hep-ph]
66. W. Beenakker, S. Brensing, M. Kramer, A. Kulesza, E. Laenen, Soft-gluon resummation for squark and gluino hadroproduction. JHEP **12**, 041 (2009). arXiv:0909.4418 [hep-ph]
67. W. Beenakker, S. Brensing, M. Kramer, A. Kulesza, E. Laenen, Squark and gluino hadroproduction. Int. J. Mod. Phys. A **26**, 2637 (2011). arXiv:1105.1110 [hep-ph]
68. C. Borschensky, Squark and gluino production cross sections in pp collisions at $\sqrt{s}$ = 13, 14, 33 and 100 TeV. Eur. Phys. J. C **74**, 3174 (2014). arXiv:1407.5066 [hep-ph]
69. D.J. Lange, The EvtGen particle decay simulation package. Nucl. Instrum. Methods A **462**, 152 (2001)
70. ATLAS Collaboration, Summary of ATLAS Pythia 8 tunes. ATL-PHYS-PUB-2012-003 (2012). https://cds.cern.ch/record/1474107
71. A.D. Martin, W.J. Stirling, R.S. Thorne, G. Wat, Parton distributions for the LHC. Eur. Phys. J. C **63**, 189 (2009). arXiv:0901.0002 [hep-ph]
72. ATLAS Collaboration, Vertex Reconstruction Performance of the ATLAS Detector at $\sqrt{s}$ = 13TeV. ATL-PHYS-PUB-2015-026 (2015). https://cds.cern.ch/record/2037717
73. ATLAS Collaboration, Electron identification measurements in ATLAS using $\sqrt{s}$ = 13TeV data with 50 ns bunch spacing. ATL-PHYS-PUB-2015-041 (2015). https://cds.cern.ch/record/2048202
74. ATLAS Collaboration, Electron efficiency measurements with the ATLAS detector using LHC proton-proton collision data. Eur. Phys. J. C **77**, 195 (2012). arXiv:0710.3820 [hep-ph]
75. ATLAS Collaboration, Muon reconstruction performance of the ATLAS detector in proton-proton collision data at $\sqrt{s}$ = 13TeV. Eur. Phys. J. C **76**, 292 (2016). arXiv:1603.05598 [hep-ex]
76. M. Cacciari, G.P. Salam, G. Soyez, The anti-k_t jet clustering algorithm. JHEP **04**, 063 (2008). arXiv:0802.1189 [hep-ph]
77. M. Cacciari, G.P. Salam, G. Soyez, FastJet User Manual. Eur. Phys. J. C **72**, 1896 (2012). arXiv:1111.6097 [hep-ph]
78. ATLAS collaboration, Topological cell clustering in the ATLAS calorimeters and its performance in LHC Run 1. Eur. Phys. J. C **77**, 490 (2017). arXiv:1603.02934 [hep-ex]
79. ATLAS Collaboration, Jet Calibration and Systematic Uncertainties for Jets Reconstructed in the ATLAS Detector at $\sqrt{s}$ = 13TeV. ATL-PHYS-PUB-2015-015 (2015). https://cds.cern.ch/record/2037613
80. ATLAS collaboration, Jet energy scale measurements and their systematic uncertainties in proton-proton collisions at $\sqrt{s}$ = 13 TeV with the ATLAS detector. Phys. Rev. D **96**, 072002 (2017). arXiv:1703.09665 [hep-ex]
81. ATLAS Collaboration, Performance of pile-up mitigation techniques for jets in pp collisions at $\sqrt{s}$ = 8 TeV using the ATLAS detector. Eur. Phys. J. C **76**, 581 (2016). arXiv:1510.03823 [hep-ex]
82. M. Cacciari, G.P. Salam, G. Soyez, The catchment area of jets. JHEP **04**, 005 (2008). arXiv:0802.1188 [hep-ph]
83. ATLAS Collaboration, Optimisation of the ATLAS b-tagging performance for the 2016 LHC Run. ATL-PHYS-PUB-2016-012 (2016). https://cds.cern.ch/record/2160731
84. ATLAS Collaboration, Performance of b-jet identification in the ATLAS Experiment. JINST 11, P04008 (2016) . arXiv:1512.01094 [hep-ex]
85. ATLAS Collaboration, Measurement of the photon identification efficiencies with the ATLAS detector using LHC Run-1 data. Eur. Phys. J. C **76**, 666 (2016). arXiv:1606.01813 [hep-ex]
86. ATLAS Collaboration, Performance of missing transverse momentum reconstruction with the ATLAS detector in the first proton-

87. ATLAS Collaboration, Electron and photon energy calibration with the ATLAS detector using LHC Run 1 data. Eur. Phys. J. C **74**, 3071 (2014). arXiv:1407.5063 [hep-ex]
88. C.G. Lester, D.J. Summers, Measuring masses of semi-invisibly decaying particles pair produced at hadron colliders. Phys. Lett. B **463**, 99 (1999). arXiv:hep-ph/9906349
89. A. Barr, C. Lester, P. Stephens, A variable for measuring masses at hadron colliders when missing energy is expected; m(T2): the truth behind the glamour. J. Phys. G **29**, 2343 (2003). arXiv:hep-ph/0304226
90. ATLAS Collaboration, Search for new phenomena in events containing a same-flavour oppositesign dilepton pair, jets, and large missing transverse momentum in $\sqrt{s}$ = 13TeV pp collisions with the ATLAS detector. Eur. Phys. J. C **77**, 144 (2017). arXiv:1611.05791 [hep-ex]
91. CMS Collaboration, Search for physics beyond the standard model in events with a Z boson, jets, and missing transverse energy in pp collisions at $\sqrt{s}$ = 7TeV. Phys. Lett. B **716**, 260 (2012). arXiv:1204.3774 [hep-ex]
92. CMS Collaboration, Search for physics beyond the standard model in events with two leptons, jets, and missing transverse momentum in pp collisions at $\sqrt{s}$ = 8TeV. JHEP **04**, 124 (2015). arXiv:1502.06031 [hep-ex]
93. ATLAS Collaboration, Measurement of the top quark-pair production cross section with ATLAS in pp collisions at $\sqrt{s}$ = 7TeV. Eur. Phys. J. C **71**, 1577 (2011). arXiv:1012.1792 [hep-ex]
94. ATLAS Collaboration, Measurement of the $W^{\pm}$Z boson pair-production cross section in pp collisions at $\sqrt{s}$ = 13TeV with the ATLAS Detector. Phys. Lett. B **762**, 1 (2016). arXiv:1606.04017 [hep-ex]
95. ATLAS Collaboration, Expected performance of missing transverse momentum reconstruction for the ATLAS detector at $\sqrt{s}$ = 13TeV. ATL-PHYS-PUB-2015-023 (2015). https://cds.cern.ch/record/2037700
96. M. Baak et al., HistFitter software framework for statistical data analysis. Eur. Phys. J. C **75**, 153 (2015). arXiv:1410.1280 [hep-ex]
97. A.L. Read, Presentation of search results: the CL(s) technique. J. Phys. G **28**, 2693 (2002)
98. ATLAS Collaboration, ATLAS Computing Acknowledgements. ATL-GEN-PUB-2016-002. https://cds.cern.ch/record/2202407

ATLAS Collaboration

M. Aaboud[34d], G. Aad[99], B. Abbott[125], O. Abdinov[13,*], B. Abeloos[129], S. H. Abidi[165], O. S. AbouZeid[143], N. L. Abraham[153], H. Abramowicz[159], H. Abreu[158], R. Abreu[128], Y. Abulaiti[43a,43b], B. S. Acharya[64a,64b,p], S. Adachi[161], L. Adamczyk[81a], J. Adelman[119], M. Adersberger[112], T. Adye[141], A. A. Affolder[143], Y. Afik[158], T. Agatonovic-Jovin[16], C. Agheorghiesei[27c], J. A. Aguilar-Saavedra[137f,137a,aj], F. Ahmadov[77,ah], G. Aielli[71a,71b], S. Akatsuka[83], H. Akerstedt[43a,43b], T. P. A. Åkesson[94], E. Akilli[52], A. V. Akimov[108], G. L. Alberghi[23b,23a], J. Albert[174], P. Albicocco[49], M. J. Alconada Verzini[86], S. Alderweireldt[117], M. Aleksa[35], I. N. Aleksandrov[77], C. Alexa[27b], G. Alexander[159], T. Alexopoulos[10], M. Alhroob[125], B. Ali[139], G. Alimonti[66a], J. Alison[36], S. P. Alkire[38], B. M. M. Allbrooke[153], B. W. Allen[128], P. P. Allport[21], A. Aloisio[67a,67b], A. Alonso[39], F. Alonso[86], C. Alpigiani[145], A. A. Alshehri[55], M. I. Alstaty[99], B. Alvarez Gonzalez[35], D. Álvarez Piqueras[172], M. G. Alviggi[67a,67b], B. T. Amadio[18], Y. Amaral Coutinho[78b], C. Amelung[26], D. Amidei[103], S. P. Amor Dos Santos[137a,137c], S. Amoroso[35], G. Amundsen[26], C. Anastopoulos[146], L. S. Ancu[52], N. Andari[21], T. Andeen[11], C. F. Anders[59b], J. K. Anders[88], K. J. Anderson[36], A. Andreazza[66a,66b], V. Andrei[59a], S. Angelidakis[37], I. Angelozzi[118], A. Angerami[38], A. V. Anisenkov[120b,120a], N. Anjos[14], A. Annovi[69a], C. Antel[59a], M. Antonelli[49], A. Antonov[110,*], D. J. A. Antrim[169], F. Anulli[70a], M. Aoki[79], L. Aperio Bella[35], G. Arabidze[104], Y. Arai[79], J. P. Araque[137a], V. Araujo Ferraz[78b], A. T. H. Arce[47], R. E. Ardell[91], F. A. Arduh[86], J.-F. Arguin[107], S. Argyropoulos[75], M. Arik[12c], A. J. Armbruster[35], L. J. Armitage[90], O. Arnaez[165], H. Arnold[50], M. Arratia[31], O. Arslan[24], A. Artamonov[109,*], G. Artoni[132], S. Artz[97], S. Asai[161], N. Asbah[44], A. Ashkenazi[159], L. Asquith[153], K. Assamagan[29], R. Astalos[28a], M. Atkinson[171], N. B. Atlay[148], K. Augsten[139], G. Avolio[35], B. Axen[18], M. K. Ayoub[129], G. Azuelos[107,ax], A. E. Baas[59a], M. J. Baca[21], H. Bachacou[142], K. Bachas[65a,65b], M. Backes[132], P. Bagnaia[70a,70b], M. Bahmani[82], H. Bahrasemani[149], J. T. Baines[141], M. Bajic[39], O. K. Baker[181], E. M. Baldin[120b,120a], P. Balek[178], F. Balli[142], W. K. Balunas[134], E. Banas[82], A. Bandyopadhyay[24], S. Banerjee[179,m], A. A. E. Bannoura[180], L. Barak[159], E. L. Barberio[102], D. Barberis[53b,53a], M. Barbero[99], T. Barillari[113], M.-S. Barisits[35], J. Barkeloo[128], T. Barklow[150], N. Barlow[31], S. L. Barnes[58c], B. M. Barnett[141], R. M. Barnett[18], Z. Barnovska-Blenessy[58a], A. Baroncelli[72a], G. Barone[26], A. J. Barr[132], L. Barranco Navarro[172], F. Barreiro[96], J. Barreiro Guimarães da Costa[15a], R. Bartoldus[150], A. E. Barton[87], P. Bartos[28a], A. Basalaev[135], A. Bassalat[129], R. L. Bates[55], S. J. Batista[165], J. R. Batley[31], M. Battaglia[143], M. Bauce[70a,70b], F. Bauer[142], H. S. Bawa[150,n], J. B. Beacham[123], M. D. Beattie[87], T. Beau[133], P. H. Beauchemin[168], P. Bechtle[24], H. C. Beck[51], H. P. Beck[20,t], K. Becker[132], M. Becker[97], C. Becot[122], A. Beddall[12d], A. J. Beddall[12a], V. A. Bednyakov[77], M. Bedognetti[118], C. P. Bee[152], T. A. Beermann[35], M. Begalli[78b], M. Begel[29], J. K. Behr[44], A. S. Bell[92], G. Bella[159], L. Bellagamba[23b], A. Bellerive[33], M. Bellomo[158], K. Belotskiy[110], O. Beltramello[35], N. L. Belyaev[110], O. Benary[159,*], D. Benchekroun[34a], M. Bender[112], K. Bendtz[43a,43b], N. Benekos[10], Y. Benhammou[159], E. Benhar Noccioli[181], J. Benitez[75], D. P. Benjamin[47], M. Benoit[52], J. R. Bensinger[26], S. Bentvelsen[118], L. Beresford[132], M. Beretta[49], D. Berge[118], E. Bergeaas Kuutmann[170], N. Berger[5], J. Beringer[18], S. Berlendis[56], N. R. Bernard[100], G. Bernardi[133], C. Bernius[150], F. U. Bernlochner[24], T. Berry[91], P. Berta[97], C. Bertella[15a], G. Bertoli[43a,43b],

F. Bertolucci[69a,69b], I. A. Bertram[87], C. Bertsche[44], D. Bertsche[125], G. J. Besjes[39], O. Bessidskaia Bylund[43a,43b], M. Bessner[44], N. Besson[142], A. Bethani[98], S. Bethke[113], A. J. Bevan[90], J. Beyer[113], R. M. Bianchi[136], O. Biebel[112], D. Biedermann[19], R. Bielski[98], K. Bierwagen[97], N. V. Biesuz[69a,69b], M. Biglietti[72a], T. R. V. Billoud[107], H. Bilokon[49], M. Bindi[51], A. Bingul[12d], C. Bini[70a,70b], S. Biondi[23b,23a], T. Bisanz[51], C. Bittrich[46], D. M. Bjergaard[47], J. E. Black[150], K. M. Black[25], R. E. Blair[6], T. Blazek[28a], I. Bloch[44], C. Blocker[26], A. Blue[55], W. Blum[97,*], U. Blumenschein[90], Dr. Blunier[144a], G. J. Bobbink[118], V. S. Bobrovnikov[120b,120a], S. S. Bocchetta[94], A. Bocci[47], C. Bock[112], M. Boehler[50], D. Boerner[180], D. Bogavac[112], A. G. Bogdanchikov[120b,120a], C. Bohm[43a], V. Boisvert[91], P. Bokan[170], T. Bold[81a], A. S. Boldyrev[111], A. E. Bolz[59b], M. Bomben[133], M. Bona[90], M. Boonekamp[142], A. Borisov[121], G. Borissov[87], J. Bortfeldt[35], D. Bortoletto[132], V. Bortolotto[61a,61b,61c], D. Boscherini[23b], M. Bosman[14], J. D. Bossio Sola[30], J. Boudreau[136], J. Bouffard[2], E. V. Bouhova-Thacker[87], D. Boumediene[37], C. Bourdarios[129], S. K. Boutle[55], A. Boveia[123], J. Boyd[35], I. R. Boyko[77], A. J. Bozson[91], J. Bracinik[21], A. Brandt[8], G. Brandt[51], O. Brandt[59a], U. Bratzler[162], B. Brau[100], J. E. Brau[128], W. D. Breaden Madden[55], K. Brendlinger[44], A. J. Brennan[102], L. Brenner[118], R. Brenner[170], S. Bressler[178], D. L. Briglin[21], T. M. Bristow[48], D. Britton[55], D. Britzger[44], I. Brock[24], R. Brock[104], G. Brooijmans[38], T. Brooks[91], W. K. Brooks[144b], J. Brosamer[18], E. Brost[119], J. H Broughton[21], P. A. Bruckman de Renstrom[82], D. Bruncko[28b], A. Bruni[23b], G. Bruni[23b], L. S. Bruni[118], S. Bruno[71a,71b], B.H. Brunt[31], M. Bruschi[23b], N. Bruscino[24], P. Bryant[36], L. Bryngemark[44], T. Buanes[17], Q. Buat[149], P. Buchholz[148], A. G. Buckley[55], I. A. Budagov[77], M. K. Bugge[131], F. Bührer[50], O. Bulekov[110], D. Bullock[8], T. J. Burch[119], S. Burdin[88], C. D. Burgard[50], A. M. Burger[5], B. Burghgrave[119], K. Burka[82], S. Burke[141], I. Burmeister[45], J. T. P. Burr[132], E. Busato[37], D. Büscher[50], V. Büscher[97], P. Bussey[55], J. M. Butler[25], C. M. Buttar[55], J. M. Butterworth[92], P. Butti[35], W. Buttinger[29], A. Buzatu[155], A. R. Buzykaev[120b,120a], S. Cabrera Urbán[172], D. Caforio[139], V. M. M. Cairo[40b,40a], O. Cakir[4a], N. Calace[52], P. Calafiura[18], A. Calandri[99], G. Calderini[133], P. Calfayan[63], G. Callea[40b,40a], L. P. Caloba[78b], S. Calvente Lopez[96], D. Calvet[37], S. Calvet[37], T. P. Calvet[99], R. Camacho Toro[36], S. Camarda[35], P. Camarri[71a,71b], D. Cameron[131], R. Caminal Armadans[171], C. Camincher[56], S. Campana[35], M. Campanelli[92], A. Camplani[66a,66b], A. Campoverde[148], V. Canale[67a,67b], M. Cano Bret[58c], J. Cantero[126], T. Cao[159], M. D. M. Capeans Garrido[35], I. Caprini[27b], M. Caprini[27b], M. Capua[40b,40a], R. M. Carbone[38], R. Cardarelli[71a], F. C. Cardillo[50], I. Carli[140], T. Carli[35], G. Carlino[67a], B. T. Carlson[136], L. Carminati[66a,66b], R. M. D. Carney[43a,43b], S. Caron[117], E. Carquin[144b], S. Carrá[66a,66b], G. D. Carrillo-Montoya[35], D. Casadei[21], M. P. Casado[14,g], M. Casolino[14], D. W. Casper[169], R. Castelijn[118], V. Castillo Gimenez[172], N. F. Castro[137a], A. Catinaccio[35], J. R. Catmore[131], A. Cattai[35], J. Caudron[24], V. Cavaliere[171], E. Cavallaro[14], D. Cavalli[66a], M. Cavalli-Sforza[14], V. Cavasinni[69a,69b], E. Celebi[12b], F. Ceradini[72a,72b], L. Cerda Alberich[172], A. S. Cerqueira[78a], A. Cerri[153], L. Cerrito[71a,71b], F. Cerutti[18], A. Cervelli[20], S. A. Cetin[12b], A. Chafaq[34a], D. Chakraborty[119], S. K. Chan[57], W. S. Chan[118], Y. L. Chan[61a], P. Chang[171], J. D. Chapman[31], D. G. Charlton[21], C. C. Chau[33], C. A. Chavez Barajas[153], S. Che[123], S. Cheatham[64a,64c], A. Chegwidden[104], S. Chekanov[6], S. V. Chekulaev[166a], G. A. Chelkov[77,aw], M. A. Chelstowska[35], C. Chen[58a], C. H. Chen[76], H. Chen[29], J. Chen[58a], S. Chen[161], S. J. Chen[15c], X. Chen[15b,av], Y. Chen[80], H. C. Cheng[103], H. J. Cheng[15d], A. Cheplakov[77], E. Cheremushkina[121], R. Cherkaoui El Moursli[34e], E. Cheu[7], K. Cheung[62], L. Chevalier[142], V. Chiarella[49], G. Chiarelli[69a], G. Chiodini[65a], A. S. Chisholm[35], A. Chitan[27b], Y. H. Chiu[174], M. V. Chizhov[77], K. Choi[63], A. R. Chomont[37], S. Chouridou[160], Y. S. Chow[61], V. Christodoulou[92], M. C. Chu[61a], J. Chudoba[138], A. J. Chuinard[101], J. J. Chwastowski[82], L. Chytka[127], A. K. Ciftci[4a], D. Cinca[45], V. Cindro[89], I. A. Cioară[24], C. Ciocca[23b,23a], A. Ciocio[18], F. Cirotto[67a,67b], Z. H. Citron[178], M. Citterio[66a], M. Ciubancan[27b], A. Clark[52], B. L. Clark[57], M. R. Clark[38], P. J. Clark[48], R. N. Clarke[18], C. Clement[43a,43b], Y. Coadou[99], M. Cobal[64a,64c], A. Coccaro[52], J. Cochran[76], L. Colasurdo[117], B. Cole[38], A. P. Colijn[118], J. Collot[56], T. Colombo[169], P. Conde Muiño[137a,j], E. Coniavitis[50], S. H. Connell[32b], I. A. Connelly[98], S. Constantinescu[27b], G. Conti[35], F. Conventi[67a,ay], M. Cooke[18], A. M. Cooper-Sarkar[132], F. Cormier[173], K. J. R. Cormier[165], M. Corradi[70a,70b], F. Corriveau[101,af], A. Cortes-Gonzalez[35], G. Cortiana[113], G. Costa[66a], M. J. Costa[172], D. Costanzo[146], G. Cottin[31], G. Cowan[91], B. E. Cox[98], K. Cranmer[122], S. J. Crawley[55], R. A. Creager[134], G. Cree[33], S. Crépé-Renaudin[56], F. Crescioli[133], W. A. Cribbs[43a,43b], M. Cristinziani[24], V. Croft[122], G. Crosetti[40b,40a], A. Cueto[96], T. Cuhadar Donszelmann[146], A. R. Cukierman[150], J. Cummings[181], M. Curatolo[49], J. Cúth[97], S. Czekierda[82], P. Czodrowski[35], M. J. Da Cunha Sargedas De Sousa[137a,137b], C. Da Via[98], W. Dabrowski[81a], T. Dado[28a,z], T. Dai[103], O. Dale[17], F. Dallaire[107], C. Dallapiccola[100], M. Dam[39], G. D'amen[23b,23a], J. R. Dandoy[134], M. F. Daneri[30], N. P. Dang[179,m], A. C. Daniells[21], N. D. Dann[98], M. Danninger[173], M. Dano Hoffmann[142], V. Dao[152], G. Darbo[53b], S. Darmora[8], J. Dassoulas[3], A. Dattagupta[128], T. Daubney[44], S. D'Auria[55], W. Davey[24], C. David[44], T. Davidek[140], D. R. Davis[47], P. Davison[92], E. Dawe[102], I. Dawson[146], K. De[8], R. De Asmundis[67a], A. De Benedetti[125], S. De Castro[23b,23a], S. De Cecco[133], N. De Groot[117], P. de Jong[118], H. De la Torre[104], F. De Lorenzi[76], A. De Maria[51,v], D. De Pedis[70a], A. De Salvo[70a], U. De Sanctis[71a,71b], A. De Santo[153], K. De Vasconcelos Corga[99], J. B. De Vivie De Regie[129], R. Debbe[29], C. Debenedetti[143], D. V. Dedovich[77], N. Dehghanian[3], I. Deigaard[118], M. Del Gaudio[40b,40a], J. Del Peso[96],

D. Delgove[129], F. Deliot[142], C. M. Delitzsch[7], M. Della Pietra[67a,67b], D. Della Volpe[52], A. Dell'Acqua[35], L. Dell'Asta[25], M. Dell'Orso[69a,69b], M. Delmastro[5], C. Delporte[129], P. A. Delsart[56], D. A. DeMarco[165], S. Demers[181], M. Demichev[77], A. Demilly[133], S. P. Denisov[121], D. Denysiuk[142], L. D'Eramo[133], D. Derendarz[82], J. E. Derkaoui[34d], F. Derue[133], P. Dervan[88], K. Desch[24], C. Deterre[44], K. Dette[165], M. R. Devesa[30], P. O. Deviveiros[35], A. Dewhurst[141], S. Dhaliwal[26], F. A. Di Bello[52], A. Di Ciaccio[71a,71b], L. Di Ciaccio[5], W. K. Di Clemente[134], C. Di Donato[67a,67b], A. Di Girolamo[35], B. Di Girolamo[35], B. Di Micco[72a,72b], R. Di Nardo[35], K. F. Di Petrillo[57], A. Di Simone[50], R. Di Sipio[165], D. Di Valentino[33], C. Diaconu[99], M. Diamond[165], F. A. Dias[39], M. A. Diaz[144a], E. B. Diehl[103], J. Dietrich[19], S. Díez Cornell[44], A. Dimitrievska[16], J. Dingfelder[24], P. Dita[27b], S. Dita[27b], F. Dittus[35], F. Djama[99], T. Djobava[157b], J. I. Djuvsland[59a], M. A. B. Do Vale[78c], D. Dobos[35], M. Dobre[27b], C. Doglioni[94], J. Dolejsi[140], Z. Dolezal[140], M. Donadelli[78d], S. Donati[69a,69b], P. Dondero[68a,68b], J. Donini[37], M. D'Onofrio[88], J. Dopke[141], A. Doria[67a], M. T. Dova[86], A. T. Doyle[55], E. Drechsler[51], M. Dris[10], Y. Du[58b], J. Duarte-Campderros[159], A. Dubreuil[52], E. Duchovni[178], G. Duckeck[112], A. Ducourthial[133], O. A. Ducu[107,y], D. Duda[118], A. Dudarev[35], A. C. Dudder[97], E. M. Duffield[18], L. Duflot[129], M. Dührssen[35], C. Dülsen[180], M. Dumancic[178], A. E. Dumitriu[27b,e], A. K. Duncan[55], M. Dunford[59a], H. DuranYildiz[4a], M. Düren[54], A. Durglishvili[157b], D. Duschinger[46], B. Dutta[44], D. Duvnjak[1], M. Dyndal[44], B. S. Dziedzic[82], C. Eckardt[44], K. M. Ecker[113], R. C. Edgar[103], T. Eifert[35], G. Eigen[17], K. Einsweiler[18], T. Ekelof[170], M. El Kacimi[34c], R. El Kosseifi[99], V. Ellajosyula[99], M. Ellert[170], S. Elles[5], F. Ellinghaus[180], A. A. Elliot[174], N. Ellis[35], J. Elmsheuser[29], M. Elsing[35], D. Emeliyanov[141], Y. Enari[161], O. C. Endner[97], J. S. Ennis[176], J. Erdmann[45], A. Ereditato[20], M. Ernst[29], S. Errede[171], M. Escalier[129], C. Escobar[172], B. Esposito[49], O. Estrada Pastor[172], A. I. Etienvre[142], E. Etzion[159], H. Evans[63], A. Ezhilov[135], M. Ezzi[34e], F. Fabbri[23b,23a], L. Fabbri[23b,23a], V. Fabiani[117], G. Facini[92], R. M. Fakhrutdinov[121], S. Falciano[70a], R. J. Falla[92], J. Faltova[35], Y. Fang[15a], M. Fanti[66a,66b], A. Farbin[8], A. Farilla[72a], C. Farina[136], E. M. Farina[68a,68b], T. Farooque[104], S. Farrell[18], S. M. Farrington[176], P. Farthouat[35], F. Fassi[34e], P. Fassnacht[35], D. Fassouliotis[9], M. Faucci Giannelli[48], A. Favareto[53b,53a], W. J. Fawcett[132], L. Fayard[129], O. L. Fedin[135,r], W. Fedorko[173], S. Feigl[131], L. Feligioni[99], C. Feng[58b], E. J. Feng[35], H. Feng[103], M. J. Fenton[55], A. B. Fenyuk[121], L. Feremenga[8], P. Fernandez Martinez[172], S. Fernandez Perez[14], J. Ferrando[44], A. Ferrari[170], P. Ferrari[118], R. Ferrari[68a], D. E. Ferreira de Lima[59b], A. Ferrer[172], D. Ferrere[52], C. Ferretti[103], F. Fiedler[97], M. Filipuzzi[44], A. Filipčič[89], F. Filthaut[117], M. Fincke-Keeler[174], K. D. Finelli[154], M. C. N. Fiolhais[137a,137c,b], L. Fiorini[172], A. Fischer[2], C. Fischer[14], J. Fischer[180], W. C. Fisher[104], N. Flaschel[44], I. Fleck[148], P. Fleischmann[103], R. R. M. Fletcher[134], T. Flick[180], B. M. Flierl[112], L. R. Flores Castillo[61a], M. J. Flowerdew[113], G. T. Forcolin[98], A. Formica[142], F. A. Förster[14], A. C. Forti[98], A. G. Foster[21], D. Fournier[129], H. Fox[87], S. Fracchia[146], P. Francavilla[133], M. Franchini[23b,23a], S. Franchino[59a], D. Francis[35], L. Franconi[131], M. Franklin[57], M. Frate[169], M. Fraternali[68a,68b], D. Freeborn[92], S. M. Fressard-Batraneanu[35], B. Freund[107], D. Froidevaux[35], J. A. Frost[132], C. Fukunaga[162], T. Fusayasu[114], J. Fuster[172], C. Gabaldon[56], O. Gabizon[158], A. Gabrielli[23b,23a], A. Gabrielli[18], G. P. Gach[81a], S. Gadatsch[35], S. Gadomski[52], G. Gagliardi[53b,53a], L. G. Gagnon[107], C. Galea[117], B. Galhardo[137a,137c], E. J. Gallas[132], B. J. Gallop[141], P. Gallus[139], G. Galster[39], K. K. Gan[123], S. Ganguly[37], Y. Gao[88], Y. S. Gao[150,n], C. García[172], J. E. García Navarro[172], J. A. García Pascual[15a], M. Garcia-Sciveres[18], R. W. Gardner[36], N. Garelli[150], V. Garonne[131], A. Gascon Bravo[44], K. Gasnikova[44], C. Gatti[49], A. Gaudiello[53b,53a], G. Gaudio[68a], I. L. Gavrilenko[108], C. Gay[173], G. Gaycken[24], E. N. Gazis[10], C. N. P. Gee[141], J. Geisen[51], M. Geisen[97], M. P. Geisler[59a], K. Gellerstedt[43a,43b], C. Gemme[53b], M. H. Genest[56], C. Geng[103], S. Gentile[70a,70b], C. Gentsos[160], S. George[91], D. Gerbaudo[14], A. Gershon[159], G. Gessner[45], S. Ghasemi[148], M. Ghneimat[24], B. Giacobbe[23b], S. Giagu[70a,70b], N. Giangiacomi[23b,23a], P. Giannetti[69a], S. M. Gibson[91], M. Gignac[173], M. Gilchriese[18], D. Gillberg[33], G. Gilles[180], D. M. Gingrich[3,ax], M. P. Giordani[64a,64c], F. M. Giorgi[23b], P. F. Giraud[142], P. Giromini[57], G. Giugliarelli[64a,64c], D. Giugni[66a], F. Giuli[132], C. Giuliani[113], M. Giulini[59b], B. K. Gjelsten[131], S. Gkaitatzis[160], I. Gkialas[9,l], E. L. Gkougkousis[14], P. Gkountoumis[10], L. K. Gladilin[111], C. Glasman[96], J. Glatzer[14], P. C. F. Glaysher[44], A. Glazov[44], M. Goblirsch-Kolb[26], J. Godlewski[82], S. Goldfarb[102], T. Golling[52], D. Golubkov[121], A. Gomes[137a,137b], R. Goncalves Gama[78b], J. Goncalves Pinto Firmino Da Costa[142], R. Gonçalo[137a], G. Gonella[50], L. Gonella[21], A. Gongadze[77], S. González de la Hoz[172], S. Gonzalez-Sevilla[52], L. Goossens[35], P. A. Gorbounov[109], H. A. Gordon[29], I. Gorelov[116], B. Gorini[35], E. Gorini[65a,65b], A. Gorišek[89], A. T. Goshaw[47], C. Gössling[45], M. I. Gostkin[77], C. A. Gottardo[24], C. R. Goudet[129], D. Goujdami[34c], A. G. Goussiou[145], N. Govender[32b,c], E. Gozani[158], L. Graber[51], I. Grabowska-Bold[81a], P. O. J. Gradin[170], J. Gramling[169], E. Gramstad[131], S. Grancagnolo[19], V. Gratchev[135], P. M. Gravila[27f], C. Gray[55], H. M. Gray[18], Z. D. Greenwood[93,al], C. Grefe[24], K. Gregersen[92], I. M. Gregor[44], P. Grenier[150], K. Grevtsov[5], J. Griffiths[8], A. A. Grillo[143], K. Grimm[87], S. Grinstein[14,aa], Ph. Gris[37], J.-F. Grivaz[129], S. Groh[97], E. Gross[178], J. Grosse-Knetter[51], G. C. Grossi[93], Z. J. Grout[92], A. Grummer[116], L. Guan[103], W. Guan[179], J. Guenther[74], F. Guescini[166a], D. Guest[169], O. Gueta[159], B. Gui[123], E. Guido[53b,53a], T. Guillemin[5], S. Guindon[35], U. Gul[55], C. Gumpert[35], J. Guo[58c], W. Guo[103], Y. Guo[58a,u], R. Gupta[41], S. Gupta[132], G. Gustavino[125], B. J. Gutelman[158], P. Gutierrez[125], N. G. Gutierrez Ortiz[92], C. Gutschow[92], C. Guyot[142], M. P. Guzik[81a],

C. Gwenlan[132], C. B. Gwilliam[88], A. Haas[122], C. Haber[18], H. K. Hadavand[8], N. Haddad[34e], A. Hadef[99], S. Hageböck[24], M. Hagihara[167], H. Hakobyan[182,*], M. Haleem[44], J. Haley[126], G. Halladjian[104], G. D. Hallewell[99], K. Hamacher[180], P. Hamal[127], K. Hamano[174], A. Hamilton[32a], G. N. Hamity[146], P. G. Hamnett[44], L. Han[58a], S. Han[15d], K. Hanagaki[79,x], K. Hanawa[161], M. Hance[143], B. Haney[134], P. Hanke[59a], J. B. Hansen[39], J. D. Hansen[39], M. C. Hansen[24], P. H. Hansen[39], K. Hara[167], A. S. Hard[179], T. Harenberg[180], F. Hariri[129], S. Harkusha[105], P. F. Harrison[176], N. M. Hartmann[112], Y. Hasegawa[147], A. Hasib[48], S. Hassani[142], S. Haug[20], R. Hauser[104], L. Hauswald[46], L. B. Havener[38], M. Havranek[139], C. M. Hawkes[21], R. J. Hawkings[35], D. Hayakawa[163], D. Hayden[104], C. P. Hays[132], J. M. Hays[90], H. S. Hayward[88], S. J. Haywood[141], S. J. Head[21], T. Heck[97], V. Hedberg[94], L. Heelan[8], S. Heer[24], K. K. Heidegger[50], S. Heim[44], T. Heim[18], B. Heinemann[44,as], J. J. Heinrich[112], L. Heinrich[122], C. Heinz[54], J. Hejbal[138], L. Helary[35], A. Held[173], S. Hellman[43a,43b], C. Helsens[35], R. C. W. Henderson[87], Y. Heng[179], S. Henkelmann[173], A. M. Henriques Correia[35], S. Henrot-Versille[129], G. H. Herbert[19], H. Herde[26], V. Herget[175], Y. Hernández Jiménez[32c], H. Herr[97], G. Herten[50], R. Hertenberger[112], L. Hervas[35], T. C. Herwig[134], G. G. Hesketh[92], N. P. Hessey[166a], J. W. Hetherly[41], S. Higashino[79], E. Higón-Rodriguez[172], K. Hildebrand[36], E. Hill[174], J. C. Hill[31], K. H. Hiller[44], S. J. Hillier[21], M. Hils[46], I. Hinchliffe[18], M. Hirose[50], D. Hirschbuehl[180], B. Hiti[89], O. Hladik[138], X. Hoad[48], J. Hobbs[152], N. Hod[166a], M. C. Hodgkinson[146], P. Hodgson[146], A. Hoecker[35], M. R. Hoeferkamp[116], F. Hoenig[112], D. Hohn[24], T. R. Holmes[36], M. Homann[45], S. Honda[167], T. Honda[79], T. M. Hong[136], B. H. Hooberman[171], W. H. Hopkins[128], Y. Horii[115], A. J. Horton[149], J.-Y. Hostachy[56], A. Hostiuc[145], S. Hou[155], A. Hoummada[34a], J. Howarth[98], J. Hoya[86], M. Hrabovsky[127], J. Hrdinka[35], I. Hristova[19], J. Hrivnac[129], A. Hrynevich[106], T. Hryn'ova[5], P. J. Hsu[62], S.-C. Hsu[145], Q. Hu[58a], S. Hu[58c], Y. Huang[15a], Z. Hubacek[139], F. Hubaut[99], F. Huegging[24], T. B. Huffman[132], E. W. Hughes[38], G. Hughes[87], M. Huhtinen[35], P. Huo[152], N. Huseynov[77,ah], J. Huston[104], J. Huth[57], G. Iacobucci[52], G. Iakovidis[29], I. Ibragimov[148], L. Iconomidou-Fayard[129], Z. Idrissi[34e], P. Iengo[35], O. Igonkina[118,ad], T. Iizawa[177], Y. Ikegami[79], M. Ikeno[79], Y. Ilchenko[11], D. Iliadis[160], N. Ilic[150], G. Introzzi[68a,68b], P. Ioannou[9,*], M. Iodice[72a], K. Iordanidou[38], V. Ippolito[57], M. F. Isacson[170], N. Ishijima[130], M. Ishino[161], M. Ishitsuka[163], C. Issever[132], S. Istin[12c], F. Ito[167], J. M. Iturbe Ponce[61a], R. Iuppa[73a,73b], H. Iwasaki[79], J. M. Izen[42], V. Izzo[67a], S. Jabbar[3], P. Jackson[1], R. M. Jacobs[24], V. Jain[2], K. B. Jakobi[97], K. Jakobs[50], S. Jakobsen[74], T. Jakoubek[138], D. O. Jamin[126], D. K. Jana[93], R. Jansky[52], J. Janssen[24], M. Janus[51], P. A. Janus[81a], G. Jarlskog[94], N. Javadov[77,ah], T. Javůrek[50], M. Javurkova[50], F. Jeanneau[142], L. Jeanty[18], J. Jejelava[157a,ai], A. Jelinskas[176], P. Jenni[50,d], C. Jeske[176], S. Jézéquel[5], H. Ji[179], J. Jia[152], H. Jiang[76], Y. Jiang[58a], Z. Jiang[150,s], S. Jiggins[92], J. Jimenez Pena[172], S. Jin[15a], A. Jinaru[27b], O. Jinnouchi[163], H. Jivan[32c], P. Johansson[146], K. A. Johns[7], C. A. Johnson[63], W. J. Johnson[145], K. Jon-And[43a,43b], R. W. L. Jones[87], S. D. Jones[153], S. Jones[7], T. J. Jones[88], J. Jongmanns[59a], P. M. Jorge[137a,137b], J. Jovicevic[166a], X. Ju[179], A. Juste Rozas[14,aa], A. Kaczmarska[82], M. Kado[129], H. Kagan[123], M. Kagan[150], S. J. Kahn[99], T. Kaji[177], E. Kajomovitz[47], C. W. Kalderon[94], A. Kaluza[97], S. Kama[41], A. Kamenshchikov[121], N. Kanaya[161], L. Kanjir[89], V. A. Kantserov[110], J. Kanzaki[79], B. Kaplan[122], L. S. Kaplan[179], D. Kar[32c], K. Karakostas[10], N. Karastathis[10], M. J. Kareem[51], E. Karentzos[10], S. N. Karpov[77], Z. M. Karpova[77], K. Karthik[122], V. Kartvelishvili[87], A. N. Karyukhin[121], K. Kasahara[167], L. Kashif[179], R. D. Kass[123], A. Kastanas[151], Y. Kataoka[161], C. Kato[161], A. Katre[52], J. Katzy[44], K. Kawade[80], K. Kawagoe[85], T. Kawamoto[161], G. Kawamura[51], E. F. Kay[88], V. F. Kazanin[120b,120a], R. Keeler[174], R. Kehoe[41], J. S. Keller[33], E. Kellermann[94], J. J. Kempster[91], J Kendrick[21], H. Keoshkerian[165], O. Kepka[138], S. Kersten[180], B. P. Kerševan[89], R. A. Keyes[101], M. Khader[171], F. Khalil-Zada[13], A. Khanov[126], A. G. Kharlamov[120b,120a], T. Kharlamova[120b,120a], A. Khodinov[164], T. J. Khoo[52], V. Khovanskiy[109,*], E. Khramov[77], J. Khubua[157b], S. Kido[80], C. R. Kilby[91], H. Y. Kim[8], S. H. Kim[167], Y. K. Kim[36], N. Kimura[160], O. M. Kind[19], B. T. King[88], D. Kirchmeier[46], J. Kirk[141], A. E. Kiryunin[113], T. Kishimoto[161], D. Kisielewska[81a], V. Kitali[44], O. Kivernyk[5], E. Kladiva[28b,*], T. Klapdor-Kleingrothaus[50], M. H. Klein[103], M. Klein[88], U. Klein[88], K. Kleinknecht[97], P. Klimek[119], A. Klimentov[29], R. Klingenberg[45,*], T. Klingl[24], T. Klioutchnikova[35], P. Kluit[118], S. Kluth[113], E. Kneringer[74], E. B. F. G. Knoops[99], A. Knue[113], A. Kobayashi[161], D. Kobayashi[163], T. Kobayashi[161], M. Kobel[46], M. Kocian[150], P. Kodys[140], T. Koffas[33], E. Koffeman[118], M. K. Köhler[178], N. M. Köhler[113], T. Koi[150], M. Kolb[59b], I. Koletsou[5], A. A. Komar[108,*], T. Kondo[79], N. Kondrashova[58c], K. Köneke[50], A. C. König[117], T. Kono[79,ar], R. Konoplich[122,an], N. Konstantinidis[92], R. Kopeliansky[63], S. Koperny[81a], A. K. Kopp[50], K. Korcyl[82], K. Kordas[160], A. Korn[92], A. A. Korol[120b,120a,aq], I. Korolkov[14], E. V. Korolkova[146], O. Kortner[113], S. Kortner[113], T. Kosek[140], V. V. Kostyukhin[24], A. Kotwal[47], A. Koulouris[10], A. Kourkoumeli-Charalampidi[68a,68b], C. Kourkoumelis[9], E. Kourlitis[146], V. Kouskoura[29], A. B. Kowalewska[82], R. Kowalewski[174], T. Z. Kowalski[81a], C. Kozakai[161], W. Kozanecki[142], A. S. Kozhin[121], V. A. Kramarenko[111], G. Kramberger[89], D. Krasnopevtsev[110], M. W. Krasny[133], A. Krasznahorkay[35], D. Krauss[113], J. A. Kremer[81a], J. Kretzschmar[88], K. Kreutzfeldt[54], P. Krieger[165], K. Krizka[18], K. Kroeninger[45], H. Kroha[113], J. Kroll[138], J. Kroll[134], J. Kroseberg[24], J. Krstic[16], U. Kruchonak[77], H. Krüger[24], N. Krumnack[76], M. C. Kruse[47], T. Kubota[102], H. Kucuk[92], S. Kuday[4b], J. T. Kuechler[180], S. Kuehn[35], A. Kugel[59a], F. Kuger[175], T. Kuhl[44], V. Kukhtin[77], R. Kukla[99], Y. Kulchitsky[105], S. Kuleshov[144b], Y. P. Kulinich[171], M. Kuna[70a,70b],

T. Kunigo[83], A. Kupco[138], T. Kupfer[45], O. Kuprash[159], H. Kurashige[80], L. L. Kurchaninov[166a], Y. A. Kurochkin[105], M. G. Kurth[15d], V. Kus[138], E. S. Kuwertz[174], M. Kuze[163], J. Kvita[127], T. Kwan[174], D. Kyriazopoulos[146], A. La Rosa[113], J. L. La Rosa Navarro[78d], L. La Rotonda[40b,40a], F. La Ruffa[40b,40a], C. Lacasta[172], F. Lacava[70a,70b], J. Lacey[44], D. P. J. Lack[98], H. Lacker[19], D. Lacour[133], E. Ladygin[77], R. Lafaye[5], B. Laforge[133], S. Lai[51], S. Lammers[63], W. Lampl[7], E. Lançon[29], U. Landgraf[50], M. P. J. Landon[90], M. C. Lanfermann[52], V. S. Lang[44], J. C. Lange[14], R. J. Langenberg[35], A. J. Lankford[169], F. Lanni[29], K. Lantzsch[24], A. Lanza[68a], A. Lapertosa[53b,53a], S. Laplace[133], J. F. Laporte[142], T. Lari[66a], F. Lasagni Manghi[23b,23a], M. Lassnig[35], T. S. Lau[61a], P. Laurelli[49], W. Lavrijsen[18], A. T. Law[143], P. Laycock[88], T. Lazovich[57], M. Lazzaroni[66a,66b], B. Le[102], O. Le Dortz[133], E. Le Guirriec[99], E. P. Le Quilleuc[142], M. LeBlanc[174], T. LeCompte[6], F. Ledroit-Guillon[56], C. A. Lee[29], G. R. Lee[141,i], L. Lee[57], S. C. Lee[155], B. Lefebvre[101], G. Lefebvre[133], M. Lefebvre[174], F. Legger[112], C. Leggett[18], G. Lehmann Miotto[35], X. Lei[7], W. A. Leight[44], M. A. L. Leite[78d], R. Leitner[140], D. Lellouch[178], B. Lemmer[51], K. J. C. Leney[92], T. Lenz[24], B. Lenzi[35], R. Leone[7], S. Leone[69a], C. Leonidopoulos[48], G. Lerner[153], C. Leroy[107], A. A. J. Lesage[142], C. G. Lester[31], M. Levchenko[135], J. Levêque[5], D. Levin[103], L. J. Levinson[178], M. Levy[21], D. Lewis[90], B. Li[58a,u], C.-Q. Li[58a,am], H. Li[152], L. Li[58c], Q. Li[15d], Q. Y. Li[58a], S. Li[47], X. Li[58c], Y. Li[148], Z. Liang[15a], B. Liberti[71a], A. Liblong[165], K. Lie[61c], J. Liebal[24], W. Liebig[17], A. Limosani[154], S. C. Lin[156], T. H. Lin[97], R. A. Linck[63], B. E. Lindquist[152], A. L. Lionti[52], E. Lipeles[134], A. Lipniacka[17], M. Lisovyi[59b], T. M. Liss[171,au], A. Lister[173], A. M. Litke[143], B. Liu[76], H. B. Liu[29], H. Liu[103], J. B. Liu[58a], J. K. K. Liu[132], J. Liu[58b], K. Liu[99], L. Liu[171], M. Liu[58a], Y. L. Liu[58a], Y. W. Liu[58a], M. Livan[68a,68b], A. Lleres[56], J. Llorente Merino[15a], S. L. Lloyd[90], C. Y. Lo[61b], F. Lo Sterzo[155], E. M. Lobodzinska[44], P. Loch[7], F. K. Loebinger[98], K. M. Loew[26], A. Loginov[181,*], T. Lohse[19], K. Lohwasser[146], M. Lokajicek[138], B. A. Long[25], J. D. Long[171], R. E. Long[87], L. Longo[65a,65b], K. A. Looper[123], J. A. Lopez[144b], D. Lopez Mateos[57], I. Lopez Paz[14], A. Lopez Solis[133], J. Lorenz[112], N. Lorenzo Martinez[5], M. Losada[22], P. J. Lösel[112], A. Lösle[50], X. Lou[15a], A. Lounis[129], J. Love[6], P. A. Love[87], H. Lu[61a], N. Lu[103], Y. J. Lu[62], H. J. Lubatti[145], C. Luci[70a,70b], A. Lucotte[56], C. Luedtke[50], F. Luehring[63], W. Lukas[74], L. Luminari[70a], O. Lundberg[43a,43b], B. Lund-Jensen[151], M. S. Lutz[100], P. M. Luzi[133], D. Lynn[29], R. Lysak[138], E. Lytken[94], F. Lyu[15a], V. Lyubushkin[77], H. Ma[29], L. L. Ma[58b], Y. Ma[58b], G. Maccarrone[49], A. Macchiolo[113], C. M. Macdonald[146], J. Machado Miguens[134,137b], D. Madaffari[172], R. Madar[37], W. F. Mader[46], A. Madsen[44], J. Maeda[80], S. Maeland[17], T. Maeno[29], A. S. Maevskiy[111], V. Magerl[50], J. Mahlstedt[118], C. Maiani[129], C. Maidantchik[78b], A. A. Maier[113], T. Maier[112], A. Maio[137a,137b,137d], O. Majersky[28a], S. Majewski[128], Y. Makida[79], N. Makovec[129], B. Malaescu[133], Pa. Malecki[82], V. P. Maleev[135], F. Malek[56], U. Mallik[75], D. Malon[6], C. Malone[31], S. Maltezos[10], S. Malyukov[35], J. Mamuzic[172], G. Mancini[49], I. Mandić[89], J. Maneira[137a,137b], L. Manhaes de Andrade Filho[78a], J. Manjarres Ramos[46], K. H. Mankinen[94], A. Mann[112], A. Manousos[35], B. Mansoulie[142], J. D. Mansour[15a], R. Mantifel[101], M. Mantoani[51], S. Manzoni[66a,66b], L. Mapelli[35], G. Marceca[30], L. March[52], L. Marchese[132], G. Marchiori[133], M. Marcisovsky[138], C. A. Marin Tobon[35], M. Marjanovic[37], D. E. Marley[103], F. Marroquim[78b], S. P. Marsden[98], Z. Marshall[18], M. U. F Martensson[170], S. Marti-Garcia[172], C. B. Martin[123], T. A. Martin[176], V. J. Martin[48], B. Martin dit Latour[17], M. Martinez[14,aa], V. I. Martinez Outschoorn[171], S. Martin-Haugh[141], V. S. Martoiu[27b], A. C. Martyniuk[92], A. Marzin[35], L. Masetti[97], T. Mashimo[161], R. Mashinistov[108], J. Masik[98], A. L. Maslennikov[120b,120a], L. Massa[71a,71b], P. Mastrandrea[5], A. Mastroberardino[40b,40a], T. Masubuchi[161], P. Mättig[180], J. Maurer[27b], B. Maček[89], S. J. Maxfield[88], D. A. Maximov[120b,120a], R. Mazini[155], I. Maznas[160], S. M. Mazza[66a,66b], N. C. Mc Fadden[116], G. Mc Goldrick[165], S. P. Mc Kee[103], A. McCarn[103], R. L. McCarthy[152], T. G. McCarthy[113], L. I. McClymont[92], E. F. McDonald[102], J. A. Mcfayden[35], G. Mchedlidze[51], S. J. McMahon[141], P. C. McNamara[102], C. J. McNicol[176], R. A. McPherson[174,af], S. Meehan[145], T. M. Megy[50], S. Mehlhase[112], A. Mehta[88], T. Meideck[56], B. Meirose[42], D. Melini[172,h], B. R. Mellado Garcia[32c], J. D. Mellenthin[51], M. Melo[28a], F. Meloni[20], A. Melzer[24], S. B. Menary[98], L. Meng[88], X. T. Meng[103], A. Mengarelli[23b,23a], S. Menke[113], E. Meoni[40b,40a], S. Mergelmeyer[19], C. Merlassino[20], P. Mermod[52], L. Merola[67a,67b], C. Meroni[66a], F. S. Merritt[36], A. Messina[70a,70b], J. Metcalfe[6], A. S. Mete[169], C. Meyer[134], J. Meyer[118], J.-P. Meyer[142], H. Meyer Zu Theenhausen[59a], F. Miano[153], R. P. Middleton[141], S. Miglioranzi[53b,53a], L. Mijović[48], G. Mikenberg[178], M. Mikestikova[138], M. Mikuž[89], M. Milesi[102], A. Milic[165], D. A. Millar[90], D. W. Miller[36], C. Mills[48], A. Milov[178], D. A. Milstead[43a,43b], A. A. Minaenko[121], Y. Minami[161], I. A. Minashvili[157b], A. I. Mincer[122], B. Mindur[81a], M. Mineev[77], Y. Minegishi[161], Y. Ming[179], L. M. Mir[14], K. P. Mistry[134], T. Mitani[177], J. Mitrevski[112], V. A. Mitsou[172], A. Miucci[20], P. S. Miyagawa[146], A. Mizukami[79], J. U. Mjörnmark[94], T. Mkrtchyan[182], M. Mlynarikova[140], T. Moa[43a,43b], K. Mochizuki[107], P. Mogg[50], S. Mohapatra[38], S. Molander[43a,43b], R. Moles-Valls[24], M. C. Mondragon[104], K. Mönig[44], J. Monk[39], E. Monnier[99], A. Montalbano[152], J. Montejo Berlingen[35], F. Monticelli[86], S. Monzani[66a], R. W. Moore[3], N. Morange[129], D. Moreno[22], M. Moreno Llácer[35], P. Morettini[53b], S. Morgenstern[35], D. Mori[149], T. Mori[161], M. Morii[57], M. Morinaga[177], V. Morisbak[131], A. K. Morley[35], G. Mornacchi[35], J. D. Morris[90], L. Morvaj[152], P. Moschovakos[10], M. Mosidze[157b], H. J. Moss[146], J. Moss[150,o], K. Motohashi[163], R. Mount[150], E. Mountricha[29], E. J. W. Moyse[100], S. Muanza[99], F. Mueller[113], J. Mueller[136],

R. S. P. Mueller[112], D. Muenstermann[87], P. Mullen[55], G. A. Mullier[20], F. J. Munoz Sanchez[98], W. J. Murray[176,141], H. Musheghyan[35], M. Muškinja[89], A. G. Myagkov[121,ao], M. Myska[139], B. P. Nachman[18], O. Nackenhorst[52], K. Nagai[132], R. Nagai[79,ar], K. Nagano[79], Y. Nagasaka[60], K. Nagata[167], M. Nagel[50], E. Nagy[99], A. M. Nairz[35], Y. Nakahama[115], K. Nakamura[79], T. Nakamura[161], I. Nakano[124], R. F. Naranjo Garcia[44], R. Narayan[11], D. I. Narrias Villar[59a], I. Naryshkin[135], T. Naumann[44], G. Navarro[22], R. Nayyar[7], H. A. Neal[103,*], P. Y. Nechaeva[108], T. J. Neep[142], A. Negri[68a,68b], M. Negrini[23b], S. Nektarijevic[117], C. Nellist[129], A. Nelson[169], M. E. Nelson[132], S. Nemecek[138], P. Nemethy[122], M. Nessi[35,f], M. S. Neubauer[171], M. Neumann[180], P. R. Newman[21], T. Y. Ng[61c], T. Nguyen Manh[107], R. B. Nickerson[132], R. Nicolaidou[142], J. Nielsen[143], V. Nikolaenko[121,ao], I. Nikolic-Audit[133], K. Nikolopoulos[21], J. K. Nilsen[131], P. Nilsson[29], Y. Ninomiya[161], A. Nisati[70a], N. Nishu[58c], R. Nisius[113], I. Nitsche[45], T. Nitta[177], T. Nobe[161], Y. Noguchi[83], M. Nomachi[130], I. Nomidis[33], M. A. Nomura[29], T. Nooney[90], M. Nordberg[35], N. Norjoharuddeen[132], O. Novgorodova[46], M. Nozaki[79], L. Nozka[127], K. Ntekas[169], E. Nurse[92], F. Nuti[102], F. G. Oakham[33,ax], H. Oberlack[113], T. Obermann[24], J. Ocariz[133], A. Ochi[80], I. Ochoa[38], J. P. Ochoa-Ricoux[144a], K. O'Connor[26], S. Oda[85], S. Odaka[79], A. Oh[98], S. H. Oh[47], C. C. Ohm[18], H. Ohman[170], H. Oide[53b,53a], H. Okawa[167], Y. Okumura[161], T. Okuyama[79], A. Olariu[27b], L. F. Oleiro Seabra[137a], S. A. Olivares Pino[144a], D. Oliveira Damazio[29], A. Olszewski[82], J. Olszowska[82], D. C. O'Neil[149], A. Onofre[137a,137e], K. Onogi[115], P. U. E. Onyisi[11], H. Oppen[131], M. J. Oreglia[36], Y. Oren[159], D. Orestano[72a,72b], N. Orlando[61b], A. A. O'Rourke[44], R. S. Orr[165], B. Osculati[53b,53a,*], V. O'Shea[55], R. Ospanov[58a], G. Otero y Garzon[30], H. Otono[85], M. Ouchrif[34d], F. Ould-Saada[131], A. Ouraou[142], K. P. Oussoren[118], Q. Ouyang[15a], M. Owen[55], R. E. Owen[21], V. E. Ozcan[12c], N. Ozturk[8], H. A. Pacey[31], K. Pachal[149], A. Pacheco Pages[14], L. Pacheco Rodriguez[142], C. Padilla Aranda[14], S. Pagan Griso[18], M. Paganini[181], F. Paige[29,*], G. Palacino[63], S. Palazzo[40b,40a], S. Palestini[35], M. Palka[81b], D. Pallin[37], E. St. Panagiotopoulou[10], I. Panagoulias[10], C. E. Pandini[69a,69b], J. G. Panduro Vazquez[91], P. Pani[35], S. Panitkin[29], D. Pantea[27b], L. Paolozzi[52], T. D. Papadopoulou[10], K. Papageorgiou[9,l], A. Paramonov[6], D. Paredes Hernandez[181], A. J. Parker[87], K. A. Parker[44], M. A. Parker[31], F. Parodi[53b,53a], J. A. Parsons[38], U. Parzefall[50], V. R. Pascuzzi[165], J. M. P. Pasner[143], E. Pasqualucci[70a], S. Passaggio[53b], F. Pastore[91], S. Pataraia[97], J. R. Pater[98], T. Pauly[35], B. Pearson[113], S. Pedraza Lopez[172], R. Pedro[137a,137b], S. V. Peleganchuk[120b,120a], O. Penc[138], C. Peng[15d], H. Peng[58a], J. Penwell[63], B. S. Peralva[78a], M. M. Perego[142], D. V. Perepelitsa[29], F. Peri[19], L. Perini[66a,66b], H. Pernegger[35], S. Perrella[67a,67b], R. Peschke[44], V. D. Peshekhonov[77,*], K. Peters[44], R. F. Y. Peters[98], B. A. Petersen[35], T. C. Petersen[39], E. Petit[56], A. Petridis[1], C. Petridou[160], P. Petroff[129], E. Petrolo[70a], M. Petrov[132], F. Petrucci[72a,72b], N. E. Pettersson[100], A. Peyaud[142], R. Pezoa[144b], F. H. Phillips[104], P. W. Phillips[141], G. Piacquadio[152], E. Pianori[176], A. Picazio[100], E. Piccaro[90], M. A. Pickering[132], R. Piegaia[30], J. E. Pilcher[36], A. D. Pilkington[98], A. W. J. Pin[98], M. Pinamonti[71a,71b], J. L. Pinfold[3], H. Pirumov[44], M. Pitt[178], L. Plazak[28a], M.-A. Pleier[29], V. Pleskot[97], E. Plotnikova[77], D. Pluth[76], P. Podberezko[120b,120a], R. Poettgen[94], R. Poggi[68a,68b], L. Poggioli[129], I. Pogrebnyak[104], D. Pohl[24], G. Polesello[68a], A. Poley[44], A. Policicchio[40b,40a], R. Polifka[35], A. Polini[23b], C. S. Pollard[55], V. Polychronakos[29], K. Pommès[35], D. Ponomarenko[110], L. Pontecorvo[70a], G. A. Popeneciu[27d], D. M. Portillo Quintero[133], S. Pospisil[139], K. Potamianos[18], I. N. Potrap[77], C. J. Potter[31], H. Potti[11], T. Poulsen[94], J. Poveda[35], M. E. Pozo Astigarraga[35], P. Pralavorio[99], A. Pranko[18], S. Prell[76], D. Price[98], M. Primavera[65a], S. Prince[101], N. Proklova[110], K. Prokofiev[61c], F. Prokoshin[144b], S. Protopopescu[29], J. Proudfoot[6], M. Przybycien[81a], A. Puri[171], P. Puzo[129], J. Qian[103], G. Qin[55], Y. Qin[98], A. Quadt[51], M. Queitsch-Maitland[44], D. Quilty[55], S. Raddum[131], V. Radeka[29], V. Radescu[132], S. K. Radhakrishnan[152], P. Radloff[128], P. Rados[102], F. Ragusa[66a,66b], G. Rahal[95], J. A. Raine[98], S. Rajagopalan[29], C. Rangel-Smith[170], T. Rashid[129], S. Raspopov[5], M. G. Ratti[66a,66b], D. M. Rauch[44], F. Rauscher[112], S. Rave[97], I. Ravinovich[178], J. H. Rawling[98], M. Raymond[35], A. L. Read[131], N. P. Readioff[56], M. Reale[65a,65b], D. M. Rebuzzi[68a,68b], A. Redelbach[175], G. Redlinger[29], R. Reece[143], R. G. Reed[32c], K. Reeves[42], L. Rehnisch[19], J. Reichert[134], A. Reiss[97], C. Rembser[35], H. Ren[15d], M. Rescigno[70a], S. Resconi[66a], E. D. Resseguie[134], S. Rettie[173], E. Reynolds[21], O. L. Rezanova[120b,120a], P. Reznicek[140], R. Rezvani[107], R. Richter[113], S. Richter[92], E. Richter-Was[81b], O. Ricken[24], M. Ridel[133], P. Rieck[113], C. J. Riegel[180], J. Rieger[51], O. Rifki[125], M. Rijssenbeek[152], A. Rimoldi[68a,68b], M. Rimoldi[20], L. Rinaldi[23b], G. Ripellino[151], B. Ristić[35], E. Ritsch[35], I. Riu[14], F. Rizatdinova[126], E. Rizvi[90], C. Rizzi[14], R. T. Roberts[98], S. H. Robertson[101,af], A. Robichaud-Veronneau[101], D. Robinson[31], J. E. M. Robinson[44], A. Robson[55], E. Rocco[97], C. Roda[69a,69b], Y. Rodina[99,ab], S. Rodriguez Bosca[172], A. Rodriguez Perez[14], D. Rodriguez Rodriguez[172], S. Roe[35], C. S. Rogan[57], O. Røhne[131], J. Roloff[57], A. Romaniouk[110], M. Romano[23b,23a], S. M. Romano Saez[37], E. Romero Adam[172], N. Rompotis[88], M. Ronzani[50], L. Roos[133], S. Rosati[70a], K. Rosbach[50], P. Rose[143], N.-A. Rosien[51], E. Rossi[67a,67b], L. P. Rossi[53b], J. H. N. Rosten[31], R. Rosten[145], M. Rotaru[27b], J. Rothberg[145], D. Rousseau[129], A. Rozanov[99], Y. Rozen[158], X. Ruan[32c], F. Rubbo[150], F. Rühr[50], A. Ruiz-Martinez[33], Z. Rurikova[50], N. A. Rusakovich[77], H. L. Russell[101], J. P. Rutherfoord[7], N. Ruthmann[35], Y. F. Ryabov[135], M. Rybar[171], G. Rybkin[129], S. Ryu[6], A. Ryzhov[121], G. F. Rzehorz[51], A. F. Saavedra[154], G. Sabato[118], S. Sacerdoti[30], H. F.-W. Sadrozinski[143], R. Sadykov[77], F. Safai Tehrani[70a], P. Saha[119], M. Sahinsoy[59a], M. Saimpert[44], M. Saito[161], T. Saito[161], H. Sakamoto[161],

Y. Sakurai[177], G. Salamanna[72a,72b], J. E. Salazar Loyola[144b], D. Salek[118], P. H. Sales De Bruin[170], D. Salihagic[113], A. Salnikov[150], J. Salt[172], D. Salvatore[40b,40a], F. Salvatore[153], A. Salvucci[61a,61b,61c], A. Salzburger[35], D. Sammel[50], D. Sampsonidis[160], D. Sampsonidou[160], J. Sánchez[172], V. Sanchez Martinez[172], A. Sanchez Pineda[64a,64c], H. Sandaker[131], R. L. Sandbach[90], C. O. Sander[44], M. Sandhoff[180], C. Sandoval[22], D. P. C. Sankey[141], M. Sannino[53b,53a], Y. Sano[115], A. Sansoni[49], C. Santoni[37], H. Santos[137a], I. Santoyo Castillo[153], A. Sapronov[77], J. G. Saraiva[137a,137d], B. Sarrazin[24], O. Sasaki[79], K. Sato[167], E. Sauvan[5], G. Savage[91], P. Savard[165,ax], N. Savic[113], C. Sawyer[141], L. Sawyer[93,al], J. Saxon[36], C. Sbarra[23b], A. Sbrizzi[23a], T. Scanlon[92], D. A. Scannicchio[169], J. Schaarschmidt[145], P. Schacht[113], B. M. Schachtner[112], D. Schaefer[35], L. Schaefer[134], R. Schaefer[44], J. Schaeffer[97], S. Schaepe[24], S. Schaetzel[59b], U. Schäfer[97], A. C. Schaffer[129], D. Schaile[112], R. D. Schamberger[152], V. A. Schegelsky[135], D. Scheirich[140], M. Schernau[169], C. Schiavi[53b,53a], S. Schier[143], L. K. Schildgen[24], C. Schillo[50], M. Schioppa[40b,40a], S. Schlenker[35], K. R. Schmidt-Sommerfeld[113], K. Schmieden[35], C. Schmitt[97], S. Schmitt[44], S. Schmitz[97], U. Schnoor[50], L. Schoeffel[142], A. Schoening[59b], B. D. Schoenrock[104], E. Schopf[24], M. Schott[97], J. F. P. Schouwenberg[117], J. Schovancova[35], S. Schramm[52], N. Schuh[97], A. Schulte[97], M. J. Schultens[24], H.-C. Schultz-Coulon[59a], H. Schulz[19], M. Schumacher[50], B. A. Schumm[143], Ph. Schune[142], A. Schwartzman[150], T. A. Schwarz[103], H. Schweiger[98], Ph. Schwemling[142], R. Schwienhorst[104], A. Sciandra[24], G. Sciolla[26], M. Scornajenghi[40b,40a], F. Scuri[69a], F. Scutti[102], J. Searcy[103], P. Seema[24], S. C. Seidel[116], A. Seiden[143], J. M. Seixas[78b], G. Sekhniaidze[67a], K. Sekhon[103], S. J. Sekula[41], N. Semprini-Cesari[23b,23a], S. Senkin[37], C. Serfon[131], L. Serin[129], L. Serkin[64a,64b], M. Sessa[72a,72b], R. Seuster[174], H. Severini[125], T. Šfiligoj[89], F. Sforza[168], A. Sfyrla[52], E. Shabalina[51], N. W. Shaikh[43a,43b], L. Y. Shan[15a], R. Shang[171], J. T. Shank[25], M. Shapiro[18], A. S. Sharma[1], P. B. Shatalov[109], K. Shaw[64a,64b], S. M. Shaw[98], A. Shcherbakova[43a,43b], C. Y. Shehu[153], Y. Shen[125], N. Sherafati[33], P. Sherwood[92], L. Shi[155,at], S. Shimizu[80], C. O. Shimmin[181], M. Shimojima[114], I. P. J. Shipsey[132], S. Shirabe[85], M. Shiyakova[77], J. Shlomi[178], A. Shmeleva[108], D. Shoaleh Saadi[107], M. J. Shochet[36], S. Shojaii[102], D. R. Shope[125], S. Shrestha[123], E. Shulga[110], M. A. Shupe[7], P. Sicho[138], A. M. Sickles[171], P. E. Sidebo[151], E. Sideras Haddad[32c], O. Sidiropoulou[175], A. Sidoti[23b,23a], F. Siegert[46], Dj. Sijacki[16], J. Silva[137a,137d], S. B. Silverstein[43a], V. Simak[139], L. Simic[16], S. Simion[129], E. Simioni[97], B. Simmons[92], M. Simon[97], P. Sinervo[165], N. B. Sinev[128], M. Sioli[23b,23a], G. Siragusa[175], I. Siral[103], S. Yu. Sivoklokov[111], J. Sjölin[43a,43b], M. B. Skinner[87], P. Skubic[125], M. Slater[21], T. Slavicek[139], M. Slawinska[82], K. Sliwa[168], R. Slovak[140], V. Smakhtin[178], B. H. Smart[5], J. Smiesko[28a], N. Smirnov[110], S. Yu. Smirnov[110], Y. Smirnov[110], L. N. Smirnova[111], O. Smirnova[94], J. W. Smith[51], M. N. K. Smith[38], R. W. Smith[38], M. Smizanska[87], K. Smolek[139], A. A. Snesarev[108], I. M. Snyder[128], S. Snyder[29], R. Sobie[174,af], F. Socher[46], A. Soffer[159], A. Søgaard[48], D. A. Soh[155], G. Sokhrannyi[89], C. A. Solans Sanchez[35], M. Solar[139], E. Yu. Soldatov[110], U. Soldevila[172], A. A. Solodkov[121], A. Soloshenko[77], O. V. Solovyanov[121], V. Solovyev[135], P. Sommer[50], H. Son[168], A. Sopczak[139], D. Sosa[59b], C. L. Sotiropoulou[69a,69b], R. Soualah[64a,64c,k], A. M. Soukharev[120b,120a], D. South[44], B. C. Sowden[91], S. Spagnolo[65a,65b], M. Spalla[69a,69b], M. Spangenberg[176], F. Spanò[91], D. Sperlich[19], F. Spettel[113], T. M. Spieker[59a], R. Spighi[23b], G. Spigo[35], L. A. Spiller[102], M. Spousta[140], R. D. St. Denis[55,*], A. Stabile[66a,66b], R. Stamen[59a], S. Stamm[19], E. Stanecka[82], R. W. Stanek[6], C. Stanescu[72a], M. M. Stanitzki[44], B. Stapf[118], S. Stapnes[131], E. A. Starchenko[121], G. H. Stark[36], J. Stark[56], S. H. Stark[39], P. Staroba[138], P. Starovoitov[59a], S. Stärz[35], R. Staszewski[82], M. Stegler[44], P. Steinberg[29], B. Stelzer[149], H. J. Stelzer[35], O. Stelzer-Chilton[166a], H. Stenzel[54], G. A. Stewart[55], M. C. Stockton[128], M. Stoebe[101], G. Stoicea[27b], P. Stolte[51], S. Stonjek[113], A. R. Stradling[8], A. Straessner[46], M. E. Stramaglia[20], J. Strandberg[151], S. Strandberg[43a,43b], M. Strauss[125], P. Strizenec[28b], R. Ströhmer[175], D. M. Strom[128], R. Stroynowski[41], A. Strubig[48], S. A. Stucci[29], B. Stugu[17], N. A. Styles[44], D. Su[150], J. Su[136], S. Suchek[59a], Y. Sugaya[130], M. Suk[139], V. V. Sulin[108], D. M. S. Sultan[73a,73b], S. Sultansoy[4c], T. Sumida[83], S. Sun[57], X. Sun[3], K. Suruliz[153], C. J. E. Suster[154], M. R. Sutton[153], S. Suzuki[79], M. Svatos[138], M. Swiatlowski[36], S. P. Swift[2], I. Sykora[28a], T. Sykora[140], D. Ta[50], K. Tackmann[44,ac], J. Taenzer[159], A. Taffard[169], R. Tafirout[166a], E. Tahirovic[90], N. Taiblum[159], H. Takai[29], R. Takashima[84], E. H. Takasugi[113], T. Takeshita[147], Y. Takubo[79], M. Talby[99], A. A. Talyshev[120b,120a], J. Tanaka[161], M. Tanaka[163], R. Tanaka[129], S. Tanaka[79], R. Tanioka[80], B. B. Tannenwald[123], S. Tapia Araya[144b], S. Tapprogge[97], S. Tarem[158], G. F. Tartarelli[66a], P. Tas[140], M. Tasevsky[138], T. Tashiro[83], E. Tassi[40b,40a], A. Tavares Delgado[137a,137b], Y. Tayalati[34e], A. C. Taylor[116], A. J. Taylor[48], G. N. Taylor[102], P. T. E. Taylor[102], W. Taylor[166b], P. Teixeira-Dias[91], D. Temple[149], H. Ten Kate[35], P. K. Teng[155], J. J. Teoh[130], F. Tepel[180], S. Terada[79], K. Terashi[161], J. Terron[96], S. Terzo[14], M. Testa[49], R. J. Teuscher[165,af], T. Theveneaux-Pelzer[99], F. Thiele[39], J. P. Thomas[21], J. Thomas-Wilsker[91], A. S. Thompson[55], P. D. Thompson[21], L. A. Thomsen[181], E. Thomson[134], M. J. Tibbetts[18], R. E. Ticse Torres[99], V. O. Tikhomirov[108,ap], Yu. A. Tikhonov[120b,120a], S. Timoshenko[110], P. Tipton[181], S. Tisserant[99], K. Todome[163], S. Todorova-Nova[5], S. Todt[46], J. Tojo[85], S. Tokár[28a], K. Tokushuku[79], E. Tolley[123], L. Tomlinson[98], M. Tomoto[115], L. Tompkins[150,s], K. Toms[116], B. Tong[57], P. Tornambe[50], E. Torrence[128], H. Torres[46], E. Torró Pastor[145], J. Toth[99,ae], F. Touchard[99], D. R. Tovey[146], C. J. Treado[122], T. Trefzger[175], F. Tresoldi[153], A. Tricoli[29], I. M. Trigger[166a], S. Trincaz-Duvoid[133], M. F. Tripiana[14], W. Trischuk[165], B. Trocmé[56], A. Trofymov[44], C. Troncon[66a],

M. Trottier-McDonald[18], M. Trovatelli[174], L. Truong[32b], M. Trzebinski[82], A. Trzupek[82], K. W. Tsang[61a], J. C.-L. Tseng[132], P. V. Tsiareshka[105], G. Tsipolitis[10], N. Tsirintanis[9], S. Tsiskaridze[14], V. Tsiskaridze[50], E. G. Tskhadadze[157a], K. M. Tsui[61a], I. I. Tsukerman[109], V. Tsulaia[18], S. Tsuno[79], D. Tsybychev[152], Y. Tu[61b], A. Tudorache[27b], V. Tudorache[27b], T. T. Tulbure[27a], A. N. Tuna[57], S. A. Tupputi[23b,23a], S. Turchikhin[77], D. Turgeman[178], I. Turk Cakir[4b,w], R. Turra[66a], P. M. Tuts[38], G. Ucchielli[23b,23a], I. Ueda[79], M. Ughetto[43a,43b], F. Ukegawa[167], G. Unal[35], A. Undrus[29], G. Unel[169], F. C. Ungaro[102], Y. Unno[79], C. Unverdorben[112], J. Urban[28b], P. Urquijo[102], P. Urrejola[97], G. Usai[8], J. Usui[79], L. Vacavant[99], V. Vacek[139], B. Vachon[101], K. O. H. Vadla[131], A. Vaidya[92], C. Valderanis[112], E. Valdes Santurio[43a,43b], M. Valente[52], S. Valentinetti[23b,23a], A. Valero[172], L. Valéry[14], S. Valkar[140], A. Vallier[5], J. A. Valls Ferrer[172], W. Van Den Wollenberg[118], H. Van der Graaf[118], P. Van Gemmeren[6], J. Van Nieuwkoop[149], I. Van Vulpen[118], M. C. van Woerden[118], M. Vanadia[71a,71b], W. Vandelli[35], A. Vaniachine[164], P. Vankov[118], G. Vardanyan[182], R. Vari[70a], E. W. Varnes[7], C. Varni[53b,53a], T. Varol[41], D. Varouchas[129], A. Vartapetian[8], K. E. Varvell[154], G. A. Vasquez[144b], J. G. Vasquez[181], F. Vazeille[37], D. Vazquez Furelos[14], T. Vazquez Schroeder[101], J. Veatch[51], V. Veeraraghavan[7], L. M. Veloce[165], F. Veloso[137a,137c], S. Veneziano[70a], A. Ventura[65a,65b], M. Venturi[174], N. Venturi[35], A. Venturini[26], V. Vercesi[68a], M. Verducci[72a,72b], W. Verkerke[118], A. T. Vermeulen[118], J. C. Vermeulen[118], M. C. Vetterli[149,ax], N. Viaux Maira[144b], O. Viazlo[94], I. Vichou[171,*], T. Vickey[146], O. E. Vickey Boeriu[146], G. H. A. Viehhauser[132], S. Viel[18], L. Vigani[132], M. Villa[23b,23a], M. Villaplana Perez[66a,66b], E. Vilucchi[49], M. G. Vincter[33], V. B. Vinogradov[77], A. Vishwakarma[44], C. Vittori[23b,23a], I. Vivarelli[153], S. Vlachos[10], M. Vogel[180], P. Vokac[139], G. Volpi[14], H. von der Schmitt[113], E. Von Toerne[24], V. Vorobel[140], K. Vorobev[110], M. Vos[172], R. Voss[35], J. H. Vossebeld[88], N. Vranjes[16], M. Vranjes Milosavljevic[16], V. Vrba[139], M. Vreeswijk[118], R. Vuillermet[35], I. Vukotic[36], P. Wagner[24], W. Wagner[180], J. Wagner-Kuhr[112], H. Wahlberg[86], S. Wahrmund[46], J. Walder[87], R. Walker[112], W. Walkowiak[148], V. Wallangen[43a,43b], C. Wang[15c], C. Wang[58b,e], F. Wang[179], H. Wang[18], H. Wang[3], J. Wang[154], J. Wang[44], Q. Wang[125], R. Wang[6], S. M. Wang[155], T. Wang[38], W. Wang[155,q], W. X. Wang[58a,ag], Z. Wang[58c], C. Wanotayaroj[128], A. Warburton[101], C. P. Ward[31], D. R. Wardrope[92], A. Washbrook[48], P. M. Watkins[21], A. T. Watson[21], M. F. Watson[21], G. Watts[145], S. Watts[98], B. M. Waugh[92], A. F. Webb[11], S. Webb[97], M. S. Weber[20], S. A. Weber[33], S. W. Weber[175], J. S. Webster[6], A. R. Weidberg[132], B. Weinert[63], J. Weingarten[51], M. Weirich[97], C. Weiser[50], H. Weits[118], P. S. Wells[35], T. Wenaus[29], T. Wengler[35], S. Wenig[35], N. Wermes[24], M. D. Werner[76], P. Werner[35], M. Wessels[59a], T. D. Weston[20], K. Whalen[128], N. L. Whallon[145], A. M. Wharton[87], A. S. White[103], A. White[8], M. J. White[1], R. White[144b], D. Whiteson[169], B. W. Whitmore[87], F. J. Wickens[141], W. Wiedenmann[179], M. Wielers[141], C. Wiglesworth[39], L. A. M. Wiik-Fuchs[50], A. Wildauer[113], F. Wilk[98], H. G. Wilkens[35], H. H. Williams[134], S. Williams[31], C. Willis[104], S. Willocq[100], J. A. Wilson[21], I. Wingerter-Seez[5], E. Winkels[153], F. Winklmeier[128], O. J. Winston[153], B. T. Winter[24], M. Wittgen[150], M. Wobisch[93], T. M. H. Wolf[118], R. Wolff[99], M. W. Wolter[82], H. Wolters[137a,137c], V. W. S. Wong[173], S. D. Worm[21], B. K. Wosiek[82], J. Wotschack[35], K. W. Woźniak[82], M. Wu[36], S. L. Wu[179], X. Wu[52], Y. Wu[103], T. R. Wyatt[98], B. M. Wynne[48], S. Xella[39], Z. Xi[103], L. Xia[15b], D. Xu[15a], L. Xu[29], T. Xu[142], B. Yabsley[154], S. Yacoob[32a], D. Yamaguchi[163], Y. Yamaguchi[163], A. Yamamoto[79], S. Yamamoto[161], T. Yamanaka[161], F. Yamane[80], M. Yamatani[161], Y. Yamazaki[80], Z. Yan[25], H. J. Yang[58c,58d], H. T. Yang[18], Y. Yang[155], Z. Yang[17], W.-M. Yao[18], Y. C. Yap[133], Y. Yasu[79], E. Yatsenko[5], K. H. Yau Wong[24], J. Ye[41], S. Ye[29], I. Yeletskikh[77], E. Yigitbasi[25], E. Yildirim[97], K. Yorita[177], K. Yoshihara[134], C. J. S. Young[35], C. Young[150], J. Yu[8], J. Yu[76], S. P. Y. Yuen[24], I. Yusuff[31,a], B. Zabinski[82], G. Zacharis[10], R. Zaidan[14], A. M. Zaitsev[121,ao], N. Zakharchuk[44], J. Zalieckas[17], A. Zaman[152], S. Zambito[57], D. Zanzi[102], C. Zeitnitz[180], G. Zemaityte[132], A. Zemla[81a], J. C. Zeng[171], Q. Zeng[150], O. Zenin[121], T. Ženiš[28a], D. Zerwas[129], D. Zhang[103], F. Zhang[179], G. Zhang[58a,ag], H. Zhang[129], J. Zhang[6], L. Zhang[50], L. Zhang[58a], M. Zhang[171], P. Zhang[15c], R. Zhang[58a,e], R. Zhang[24], X. Zhang[58b], Y. Zhang[15d], Z. Zhang[129], X. Zhao[41], Y. Zhao[58b,129,ak], Z. Zhao[58a], A. Zhemchugov[77], B. Zhou[103], C. Zhou[179], L. Zhou[41], M. S. Zhou[15d], M. Zhou[152], N. Zhou[15b], C. G. Zhu[58b], H. Zhu[15a], J. Zhu[103], Y. Zhu[58a], X. Zhuang[15a], K. Zhukov[108], A. Zibell[175], D. Zieminska[63], N. I. Zimine[77], C. Zimmermann[97], S. Zimmermann[50], Z. Zinonos[113], M. Zinser[97], M. Ziolkowski[148], L. Živković[16], G. Zobernig[179], A. Zoccoli[23b,23a], R. Zou[36], M. Zur Nedden[19], L. Zwalinski[35]

[1] Department of Physics, University of Adelaide, Adelaide, Australia
[2] Physics Department, SUNY Albany, Albany, NY, USA
[3] Department of Physics, University of Alberta, Edmonton, AB, Canada
[4] [(a)]Department of Physics, Ankara University, Ankara, Turkey; [(b)]Istanbul Aydin University, Istanbul, Turkey; [(c)]Division of Physics, TOBB University of Economics and Technology, Ankara, Turkey
[5] LAPP, Université Grenoble Alpes, Université Savoie Mont Blanc, CNRS/IN2P3, Annecy, France
[6] High Energy Physics Division, Argonne National Laboratory, Argonne, IL, USA
[7] Department of Physics, University of Arizona, Tucson, AZ, USA

[8] Department of Physics, University of Texas at Arlington, Arlington, TX, USA
[9] Physics Department, National and Kapodistrian University of Athens, Athens, Greece
[10] Physics Department, National Technical University of Athens, Zografou, Greece
[11] Department of Physics, University of Texas at Austin, Austin, TX, USA
[12] [(a)]Faculty of Engineering and Natural Sciences, Bahcesehir University, Istanbul, Turkey; [(b)]Faculty of Engineering and Natural Sciences, Istanbul Bilgi University, Istanbul, Turkey; [(c)]Department of Physics, Bogazici University, Istanbul, Turkey; [(d)]Department of Physics Engineering, Gaziantep University, Gaziantep, Turkey
[13] Institute of Physics, Azerbaijan Academy of Sciences, Baku, Azerbaijan
[14] Institut de Física d'Altes Energies (IFAE), Barcelona Institute of Science and Technology, Barcelona, Spain
[15] [(a)]Institute of High Energy Physics, Chinese Academy of Sciences, Beijing, China; [(b)]Physics Department, Tsinghua University, Beijing, China; [(c)]Department of Physics, Nanjing University, Nanjing, China; [(d)]University of Chinese Academy of Science (UCAS), Beijing, China
[16] Institute of Physics, University of Belgrade, Belgrade, Serbia
[17] Department for Physics and Technology, University of Bergen, Bergen, Norway
[18] Physics Division, Lawrence Berkeley National Laboratory and University of California, Berkeley, CA, USA
[19] Institut für Physik, Humboldt Universität zu Berlin, Berlin, Germany
[20] Albert Einstein Center for Fundamental Physics and Laboratory for High Energy Physics, University of Bern, Bern, Switzerland
[21] School of Physics and Astronomy, University of Birmingham, Birmingham, UK
[22] Centro de Investigaciónes, Universidad Antonio Nariño, Bogotá, Colombia
[23] [(a)]Dipartimento di Fisica e Astronomia, Università di Bologna, Bologna, Italy; [(b)]INFN Sezione di Bologna, Bologna, Italy
[24] Physikalisches Institut, Universität Bonn, Bonn, Germany
[25] Department of Physics, Boston University, Boston, MA, USA
[26] Department of Physics, Brandeis University, Waltham, MA, USA
[27] [(a)]Transilvania University of Brasov, Brasov, Romania; [(b)]Horia Hulubei National Institute of Physics and Nuclear Engineering, Bucharest, Romania; [(c)]Department of Physics, Alexandru Ioan Cuza University of Iasi, Iasi, Romania; [(d)]Physics Department, National Institute for Research and Development of Isotopic and Molecular Technologies, Cluj-Napoca, Romania; [(e)]University Politehnica Bucharest, Bucharest, Romania; [(f)]West University in Timisoara, Timisoara, Romania
[28] [(a)]Faculty of Mathematics, Physics and Informatics, Comenius University, Bratislava, Slovak Republic; [(b)]Department of Subnuclear Physics, Institute of Experimental Physics of the Slovak Academy of Sciences, Kosice, Slovak Republic
[29] Physics Department, Brookhaven National Laboratory, Upton, NY, USA
[30] Departamento de Física, Universidad de Buenos Aires, Buenos Aires, Argentina
[31] Cavendish Laboratory, University of Cambridge, Cambridge, UK
[32] [(a)]Department of Physics, University of Cape Town, Cape Town, South Africa; [(b)]Department of Mechanical Engineering Science, University of Johannesburg, Johannesburg, South Africa; [(c)]School of Physics, University of the Witwatersrand, Johannesburg, South Africa
[33] Department of Physics, Carleton University, Ottawa, ON, Canada
[34] [(a)]Faculté des Sciences Ain Chock, Réseau Universitaire de Physique des Hautes Energies-Université Hassan II, Casablanca, Morocco; [(b)]Centre National de l'Energie des Sciences Techniques Nucleaires (CNESTEN), Rabat, Morocco; [(c)]Faculté des Sciences Semlalia, Université Cadi Ayyad, LPHEA-Marrakech, Marrakech, Morocco; [(d)]Faculté des Sciences, Université Mohamed Premier and LPTPM, Oujda, Morocco; [(e)]Faculté des sciences, Université Mohammed V, Rabat, Morocco
[35] CERN, Geneva, Switzerland
[36] Enrico Fermi Institute, University of Chicago, Chicago, IL, USA
[37] LPC, Université Clermont Auvergne, CNRS/IN2P3, Clermont-Ferrand, France
[38] Nevis Laboratory, Columbia University, Irvington, NY, USA
[39] Niels Bohr Institute, University of Copenhagen, Copenhagen, Denmark
[40] [(a)]Dipartimento di Fisica, Università della Calabria, Rende, Italy; [(b)]INFN Gruppo Collegato di Cosenza, Laboratori Nazionali di Frascati, Frascati, Italy
[41] Physics Department, Southern Methodist University, Dallas, TX, USA
[42] Physics Department, University of Texas at Dallas, Richardson, TX, USA

[43] [(a)]Department of Physics, Stockholm University, Stockholm, Sweden; [(b)]Oskar Klein Centre, Stockholm, Sweden
[44] Deutsches Elektronen-Synchrotron DESY, Hamburg and Zeuthen, Germany
[45] Lehrstuhl für Experimentelle Physik IV, Technische Universität Dortmund, Dortmund, Germany
[46] Institut für Kern- und Teilchenphysik, Technische Universität Dresden, Dresden, Germany
[47] Department of Physics, Duke University, Durham, NC, USA
[48] SUPA-School of Physics and Astronomy, University of Edinburgh, Edinburgh, UK
[49] INFN e Laboratori Nazionali di Frascati, Frascati, Italy
[50] Physikalisches Institut, Albert-Ludwigs-Universität Freiburg, Freiburg, Germany
[51] II Physikalisches Institut, Georg-August-Universität Göttingen, Göttingen, Germany
[52] Département de Physique Nucléaire et Corpusculaire, Université de Genève, Geneva, Switzerland
[53] [(a)]Dipartimento di Fisica, Università di Genova, Genoa, Italy; [(b)]INFN Sezione di Genova, Genoa, Italy
[54] II. Physikalisches Institut, Justus-Liebig-Universität Giessen, Giessen, Germany
[55] SUPA-School of Physics and Astronomy, University of Glasgow, Glasgow, UK
[56] LPSC, Université Grenoble Alpes, CNRS/IN2P3, Grenoble INP, Grenoble, France
[57] Laboratory for Particle Physics and Cosmology, Harvard University, Cambridge, MA, USA
[58] [(a)]Department of Modern Physics and State Key Laboratory of Particle Detection and Electronics, University of Science and Technology of China, Hefei, China; [(b)]Institute of Frontier and Interdisciplinary Science and Key Laboratory of Particle Physics and Particle Irradiation (MOE), Shandong University, Qingdao, China; [(c)]School of Physics and Astronomy, Shanghai Jiao Tong University, KLPPAC-MoE, SKLPPC, Shanghai, China; [(d)]Tsung-Dao Lee Institute, Shanghai, China
[59] [(a)]Kirchhoff-Institut für Physik, Ruprecht-Karls-Universität Heidelberg, Heidelberg, Germany; [(b)]Physikalisches Institut, Ruprecht-Karls-Universität Heidelberg, Heidelberg, Germany
[60] Faculty of Applied Information Science, Hiroshima Institute of Technology, Hiroshima, Japan
[61] [(a)]Department of Physics, Chinese University of Hong Kong, Shatin, N.T., Hong Kong; [(b)]Department of Physics, University of Hong Kong, Hong Kong, China; [(c)]Department of Physics and Institute for Advanced Study, Hong Kong University of Science and Technology, Clear Water Bay, Kowloon, Hong Kong, China
[62] Department of Physics, National Tsing Hua University, Hsinchu, Taiwan
[63] Department of Physics, Indiana University, Bloomington, IN, USA
[64] [(a)]INFN Gruppo Collegato di Udine, Sezione di Trieste, Udine, Italy; [(b)]ICTP, Trieste, Italy; [(c)]Dipartimento di Chimica, Fisica e Ambiente, Università di Udine, Udine, Italy
[65] [(a)]INFN Sezione di Lecce, Lecce, Italy; [(b)]Dipartimento di Matematica e Fisica, Università del Salento, Lecce, Italy
[66] [(a)]INFN Sezione di Milano, Milan, Italy; [(b)]Dipartimento di Fisica, Università di Milano, Milan, Italy
[67] [(a)]INFN Sezione di Napoli, Naples, Italy; [(b)]Dipartimento di Fisica, Università di Napoli, Naples, Italy
[68] [(a)]INFN Sezione di Pavia, Pavia, Italy; [(b)]Dipartimento di Fisica, Università di Pavia, Pavia, Italy
[69] [(a)]INFN Sezione di Pisa, Pisa, Italy; [(b)]Dipartimento di Fisica E. Fermi, Università di Pisa, Pisa, Italy
[70] [(a)]INFN Sezione di Roma, Rome, Italy; [(b)]Dipartimento di Fisica, Sapienza Università di Roma, Rome, Italy
[71] [(a)]INFN Sezione di Roma Tor Vergata, Rome, Italy; [(b)]Dipartimento di Fisica, Università di Roma Tor Vergata, Rome, Italy
[72] [(a)]INFN Sezione di Roma Tre, Rome, Italy; [(b)]Dipartimento di Matematica e Fisica, Università Roma Tre, Rome, Italy
[73] [(a)]INFN-TIFPA, Trento, Italy; [(b)]Università degli Studi di Trento, Trento, Italy
[74] Institut für Astro- und Teilchenphysik, Leopold-Franzens-Universität, Innsbruck, Austria
[75] University of Iowa, Iowa City, IA, USA
[76] Department of Physics and Astronomy, Iowa State University, Ames, IA, USA
[77] Joint Institute for Nuclear Research, Dubna, Russia
[78] [(a)]Departamento de Engenharia Elétrica, Universidade Federal de Juiz de Fora (UFJF), Juiz de Fora, Brazil; [(b)]Universidade Federal do Rio De Janeiro COPPE/EE/IF, Rio de Janeiro, Brazil; [(c)]Universidade Federal de São João del Rei (UFSJ), São João del Rei, Brazil; [(d)]Instituto de Física, Universidade de São Paulo, São Paulo, Brazil
[79] KEK, High Energy Accelerator Research Organization, Tsukuba, Japan
[80] Graduate School of Science, Kobe University, Kobe, Japan
[81] [(a)]Faculty of Physics and Applied Computer Science, AGH University of Science and Technology, Kraków, Poland; [(b)]Marian Smoluchowski Institute of Physics, Jagiellonian University, Kraków, Poland
[82] Institute of Nuclear Physics Polish Academy of Sciences, Kraków, Poland
[83] Faculty of Science, Kyoto University, Kyoto, Japan

[84] Kyoto University of Education, Kyoto, Japan
[85] Research Center for Advanced Particle Physics and Department of Physics, Kyushu University, Fukuoka, Japan
[86] Instituto de Física La Plata, Universidad Nacional de La Plata and CONICET, La Plata, Argentina
[87] Physics Department, Lancaster University, Lancaster, UK
[88] Oliver Lodge Laboratory, University of Liverpool, Liverpool, UK
[89] Department of Experimental Particle Physics, Jožef Stefan Institute and Department of Physics, University of Ljubljana, Ljubljana, Slovenia
[90] School of Physics and Astronomy, Queen Mary University of London, London, UK
[91] Department of Physics, Royal Holloway University of London, Egham, UK
[92] Department of Physics and Astronomy, University College London, London, UK
[93] Louisiana Tech University, Ruston, LA, USA
[94] Fysiska institutionen, Lunds Universitet, Lund, Sweden
[95] Centre de Calcul de l'Institut National de Physique Nucléaire et de Physique des Particules (IN2P3), Villeurbanne, France
[96] Departamento de Física Teorica C-15 and CIAFF, Universidad Autónoma de Madrid, Madrid, Spain
[97] Institut für Physik, Universität Mainz, Mainz, Germany
[98] School of Physics and Astronomy, University of Manchester, Manchester, UK
[99] CPPM, Aix-Marseille Université, CNRS/IN2P3, Marseille, France
[100] Department of Physics, University of Massachusetts, Amherst, MA, USA
[101] Department of Physics, McGill University, Montreal, QC, Canada
[102] School of Physics, University of Melbourne, Victoria, Australia
[103] Department of Physics, University of Michigan, Ann Arbor, MI, USA
[104] Department of Physics and Astronomy, Michigan State University, East Lansing, MI, USA
[105] B.I. Stepanov Institute of Physics, National Academy of Sciences of Belarus, Minsk, Belarus
[106] Research Institute for Nuclear Problems of Byelorussian State University, Minsk, Belarus
[107] Group of Particle Physics, University of Montreal, Montreal, QC, Canada
[108] P.N. Lebedev Physical Institute of the Russian Academy of Sciences, Moscow, Russia
[109] Institute for Theoretical and Experimental Physics (ITEP), Moscow, Russia
[110] National Research Nuclear University MEPhI, Moscow, Russia
[111] D.V. Skobeltsyn Institute of Nuclear Physics, M.V. Lomonosov Moscow State University, Moscow, Russia
[112] Fakultät für Physik, Ludwig-Maximilians-Universität München, Munich, Germany
[113] Max-Planck-Institut für Physik (Werner-Heisenberg-Institut), Munich, Germany
[114] Nagasaki Institute of Applied Science, Nagasaki, Japan
[115] Graduate School of Science and Kobayashi-Maskawa Institute, Nagoya University, Nagoya, Japan
[116] Department of Physics and Astronomy, University of New Mexico, Albuquerque, NM, USA
[117] Institute for Mathematics, Astrophysics and Particle Physics, Radboud University Nijmegen/Nikhef, Nijmegen, The Netherlands
[118] Nikhef National Institute for Subatomic Physics, University of Amsterdam, Amsterdam, The Netherlands
[119] Department of Physics, Northern Illinois University, DeKalb, IL, USA
[120] [(a)]Budker Institute of Nuclear Physics and NSU, SB RAS, Novosibirsk, Russia; [(b)]Novosibirsk State University, Novosibirsk, Russia
[121] Institute for High Energy Physics of the National Research Centre Kurchatov Institute, Protvino, Russia
[122] Department of Physics, New York University, New York, NY, USA
[123] Ohio State University, Columbus, OH, USA
[124] Faculty of Science, Okayama University, Okayama, Japan
[125] Homer L. Dodge Department of Physics and Astronomy, University of Oklahoma, Norman, OK, USA
[126] Department of Physics, Oklahoma State University, Stillwater, OK, USA
[127] Palacký University, RCPTM, Joint Laboratory of Optics, Olomouc, Czech Republic
[128] Center for High Energy Physics, University of Oregon, Eugene, OR, USA
[129] LAL, Université Paris-Sud, CNRS/IN2P3, Université Paris-Saclay, Orsay, France
[130] Graduate School of Science, Osaka University, Osaka, Japan
[131] Department of Physics, University of Oslo, Oslo, Norway
[132] Department of Physics, Oxford University, Oxford, UK

[133] LPNHE, Sorbonne Université, Paris Diderot Sorbonne Paris Cité, CNRS/IN2P3 Paris, France
[134] Department of Physics, University of Pennsylvania, Philadelphia, PA, USA
[135] Konstantinov Nuclear Physics Institute of National Research Centre "Kurchatov Institute", PNPI, St. Petersburg, Russia
[136] Department of Physics and Astronomy, University of Pittsburgh, Pittsburgh, PA, USA
[137] [(a)]Laboratório de Instrumentação e Física Experimental de Partículas-LIP, Lisbon, Portugal; [(b)]Departamento de Física, Faculdade de Ciências, Universidade de Lisboa, Lisbon, Portugal; [(c)]Departamento de Física, Universidade de Coimbra, Coimbra, Portugal; [(d)]Centro de Física Nuclear da Universidade de Lisboa, Lisbon, Portugal; [(e)]Departamento de Física, Universidade do Minho, Braga, Portugal; [(f)]Departamento de Física Teorica y del Cosmos, Universidad de Granada, Granada, Spain; [(g)]Dep Física and CEFITEC of Faculdade de Ciências e Tecnologia, Universidade Nova de Lisboa, Caparica, Portugal
[138] Institute of Physics, Academy of Sciences of the Czech Republic, Prague, Czech Republic
[139] Czech Technical University in Prague, Prague, Czech Republic
[140] Faculty of Mathematics and Physics, Charles University, Prague, Czech Republic
[141] Particle Physics Department, Rutherford Appleton Laboratory, Didcot, UK
[142] IRFU, CEA, Université Paris-Saclay, Gif-sur-Yvette, France
[143] Santa Cruz Institute for Particle Physics, University of California Santa Cruz, Santa Cruz, CA, USA
[144] [(a)]Departamento de Física, Pontificia Universidad Católica de Chile, Santiago, Chile; [(b)]Departamento de Física, Universidad Técnica Federico Santa María, Valparaiso, Chile
[145] Department of Physics, University of Washington, Seattle, WA, USA
[146] Department of Physics and Astronomy, University of Sheffield, Sheffield, UK
[147] Department of Physics, Shinshu University, Nagano, Japan
[148] Department Physik, Universität Siegen, Siegen, Germany
[149] Department of Physics, Simon Fraser University, Burnaby, BC, Canada
[150] SLAC National Accelerator Laboratory, Stanford, CA, USA
[151] Physics Department, Royal Institute of Technology, Stockholm, Sweden
[152] Departments of Physics and Astronomy, Stony Brook University, Stony Brook, NY, USA
[153] Department of Physics and Astronomy, University of Sussex, Brighton, UK
[154] School of Physics, University of Sydney, Sydney, Australia
[155] Institute of Physics, Academia Sinica, Taipei, Taiwan
[156] Academia Sinica Grid Computing, Institute of Physics, Academia Sinica, Taipei, Taiwan
[157] [(a)]E. Andronikashvili Institute of Physics, Iv. Javakhishvili Tbilisi State University, Tbilisi, Georgia; [(b)]High Energy Physics Institute, Tbilisi State University, Tbilisi, Georgia
[158] Department of Physics, Technion, Israel Institute of Technology, Haifa, Israel
[159] Raymond and Beverly Sackler School of Physics and Astronomy, Tel Aviv University, Tel Aviv, Israel
[160] Department of Physics, Aristotle University of Thessaloniki, Thessaloniki, Greece
[161] International Center for Elementary Particle Physics and Department of Physics, University of Tokyo, Tokyo, Japan
[162] Graduate School of Science and Technology, Tokyo Metropolitan University, Tokyo, Japan
[163] Department of Physics, Tokyo Institute of Technology, Tokyo, Japan
[164] Tomsk State University, Tomsk, Russia
[165] Department of Physics, University of Toronto, Toronto, ON, Canada
[166] [(a)]TRIUMF, Vancouver, BC, Canada; [(b)]Department of Physics and Astronomy, York University, Toronto, ON, Canada
[167] Division of Physics and Tomonaga Center for the History of the Universe, Faculty of Pure and Applied Sciences, University of Tsukuba, Tsukuba, Japan
[168] Department of Physics and Astronomy, Tufts University, Medford, MA, USA
[169] Department of Physics and Astronomy, University of California Irvine, Irvine, CA, USA
[170] Department of Physics and Astronomy, University of Uppsala, Uppsala, Sweden
[171] Department of Physics, University of Illinois, Urbana, IL, USA
[172] Instituto de Física Corpuscular (IFIC), Centro Mixto Universidad de Valencia - CSIC, Valencia, Spain
[173] Department of Physics, University of British Columbia, Vancouver, BC, Canada
[174] Department of Physics and Astronomy, University of Victoria, Victoria, BC, Canada
[175] Fakultät für Physik und Astronomie, Julius-Maximilians-Universität Würzburg, Würzburg, Germany
[176] Department of Physics, University of Warwick, Coventry, UK
[177] Waseda University, Tokyo, Japan

[178] Department of Particle Physics, Weizmann Institute of Science, Rehovot, Israel
[179] Department of Physics, University of Wisconsin, Madison, WI, USA
[180] Fakultät für Mathematik und Naturwissenschaften, Fachgruppe Physik, Bergische Universität Wuppertal, Wuppertal, Germany
[181] Department of Physics, Yale University, New Haven, CT, USA
[182] Yerevan Physics Institute, Yerevan, Armenia

[a] Also at Department of Physics, University of Malaya, Kuala Lumpur, Malaysia
[b] Also at Borough of Manhattan Community College, City University of New York, NY, USA
[c] Also at Centre for High Performance Computing, CSIR Campus, Rosebank, Cape Town, South Africa.
[d] Also at CERN, Geneva, Switzerland
[e] Also at CPPM, Aix-Marseille Université, CNRS/IN2P3, Marseille, France
[f] Also at Département de Physique Nucléaire et Corpusculaire, Université de Genève, Geneva, Switzerland
[g] Also at Departament de Fisica de la Universitat Autonoma de Barcelona, Barcelona, Spain
[h] Also at Departamento de Física Teorica y del Cosmos, Universidad de Granada, Granada (Spain), Spain
[i] Also at Departamento de Física, Pontificia Universidad Católica de Chile, Santiago, Chile
[j] Also at Departamento de Física, Instituto Superior Técnico, Universidade de Lisboa, Lisbon, Portugal
[k] Also at Department of Applied Physics and Astronomy, University of Sharjah, Sharjah, United Arab Emirates
[l] Also at Department of Financial and Management Engineering, University of the Aegean, Chios, Greece
[m] Also at Department of Physics and Astronomy, University of Louisville, Louisville, KY, USA
[n] Also at Department of Physics, California State University, Fresno CA, USA
[o] Also at Department of Physics, California State University, Sacramento CA, USA
[p] Also at Department of Physics, King's College London, London, UK
[q] Also at Department of Physics, Nanjing University, Nanjing, China
[r] Also at Department of Physics, St Petersburg State Polytechnical University, St. Petersburg, Russia
[s] Also at Department of Physics, Stanford University, USA
[t] Also at Department of Physics, University of Fribourg, Fribourg, Switzerland
[u] Also at Department of Physics, University of Michigan, Ann Arbor MI, USA
[v] Also at Dipartimento di Fisica E Fermi, Università di Pisa, Pisa, Italy
[w] Also at Giresun University, Faculty of Engineering, Giresun, Turkey
[x] Also at Graduate School of Science, Osaka University, Osaka, Japan
[y] Also at Horia Hulubei National Institute of Physics and Nuclear Engineering, Bucharest, Romania
[z] Also at II Physikalisches Institut, Georg-August-Universität Göttingen, Göttingen, Germany
[aa] Also at Institucio Catalana de Recerca i Estudis Avancats, ICREA, Barcelona, Spain
[ab] Also at Institut de Física d'Altes Energies (IFAE), Barcelona Institute of Science and Technology, Barcelona, Spain
[ac] Also at Institut für Experimentalphysik, Universität Hamburg, Hamburg, Germany
[ad] Also at Institute for Mathematics, Astrophysics and Particle Physics, Radboud University Nijmegen/Nikhef, Nijmegen, The Netherlands
[ae] Also at Institute for Particle and Nuclear Physics, Wigner Research Centre for Physics, Budapest, Hungary
[af] Also at Institute of Particle Physics (IPP), Canada
[ag] Also at Institute of Physics, Academia Sinica, Taipei, Taiwan
[ah] Also at Institute of Physics, Azerbaijan Academy of Sciences, Baku, Azerbaijan
[ai] Also at Institute of Theoretical Physics, Ilia State University, Tbilisi, Georgia
[aj] Instituto de Fíca Teórica de la Universidad Autónoma de Madrid, Spain
[ak] Also at LAL, Université Paris-Sud, CNRS/IN2P3, Université Paris-Saclay, Orsay, France
[al] Also at Louisiana Tech University, Ruston LA, USA
[am] Also at LPNHE, Sorbonne Université, Paris Diderot Sorbonne Paris Cité, CNRS/IN2P3, Paris, France
[an] Also at Manhattan College, New York NY, USA
[ao] Also at Moscow Institute of Physics and Technology State University, Dolgoprudny, Russia
[ap] Also at National Research Nuclear University MEPhI, Moscow, Russia
[aq] Also at Novosibirsk State University, Novosibirsk, Russia
[ar] Also at Ochadai Academic Production, Ochanomizu University, Tokyo, Japan
[as] Also at Physikalisches Institut, Albert-Ludwigs-Universität Freiburg, Freiburg, Germany

[at] Also at School of Physics, Sun Yat-sen University, Guangzhou, China
[au] Also at The City College of New York, New York NY, USA
[av] Also at The Collaborative Innovation Center of Quantum Matter (CICQM), Beijing, China
[aw] Also at Tomsk State University, Tomsk, and Moscow Institute of Physics and Technology State University, Dolgoprudny, Russia
[ax] Also at TRIUMF, Vancouver BC, Canada
[ay] Also at Universita di Napoli Parthenope, Naples, Italy
*Deceased